**Supplementary Information For:**

# Synthesis, self-assembly and immunological activity of α-galactose functionalized dendron-lipid amphiphiles

John F. Trant,[a] Namrata Jain,[a] Delfina M. Mazzuca,[b] James T. McIntosh,[a] Bo Fan,[c] S.M. Mansour Haeryfar,[b] Sebastien Lecommandoux,[d] and Elizabeth R. Gillies*[a,c]

[a] Department of Chemistry and Centre for Advanced Materials and Biomaterials Research, The University of Western Ontario, 1151 Richmond Street, London, Canada, N6A 5B7; E-mail: egillie@uwo.ca
[b] Department of Microbiology and Immunology, Department of Medicine, Centre for Human Immunology, Schulich School of Medicine and Dentistry, The University of Western Ontario, 1151 Richmond Street, London, Canada, N6A 5C1.
[c] Department of Chemical and Biochemical Engineering, The University of Western Ontario, 1151 Richmond St., London, Canada, N6A 5B9.
[d] Univ. Bordeaux; Bordeaux-INP ENSCBP; CNRS, Laboratoire de Chimie des Polymères Organique (LCPO), UMR 5629, 16 avenue Pey Berland, F-33600, Pessac, France.

**Table of Contents**

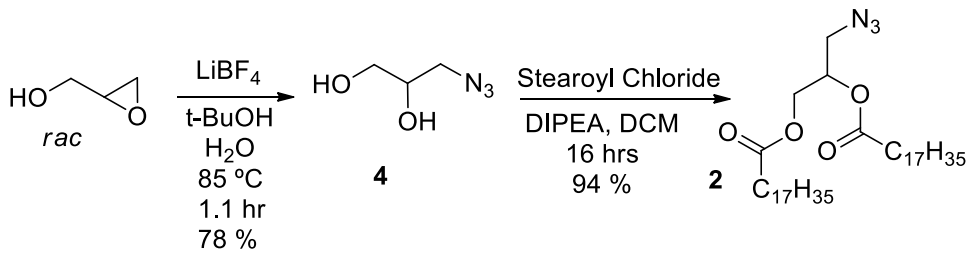


**Scheme S1**. Synthesis of azido diglyceride **2**.

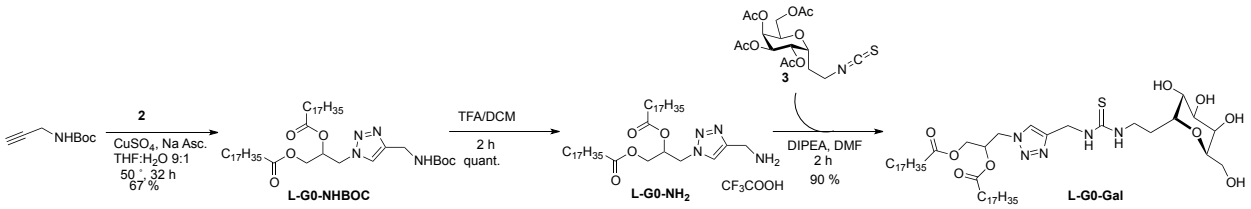


**Scheme S2**. Synthesis of L-G0-Gal.

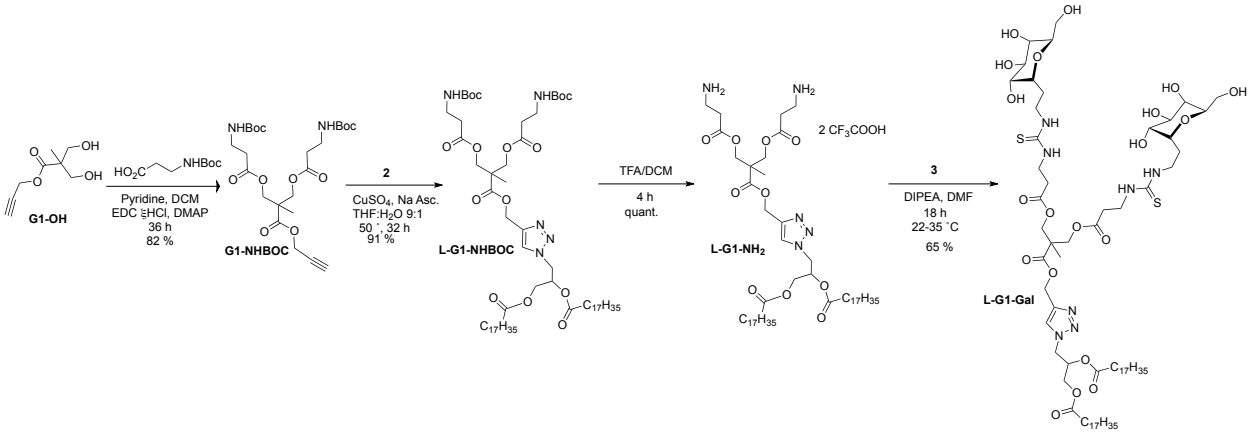


**Scheme S3**. Synthesis of L-G1-Gal.

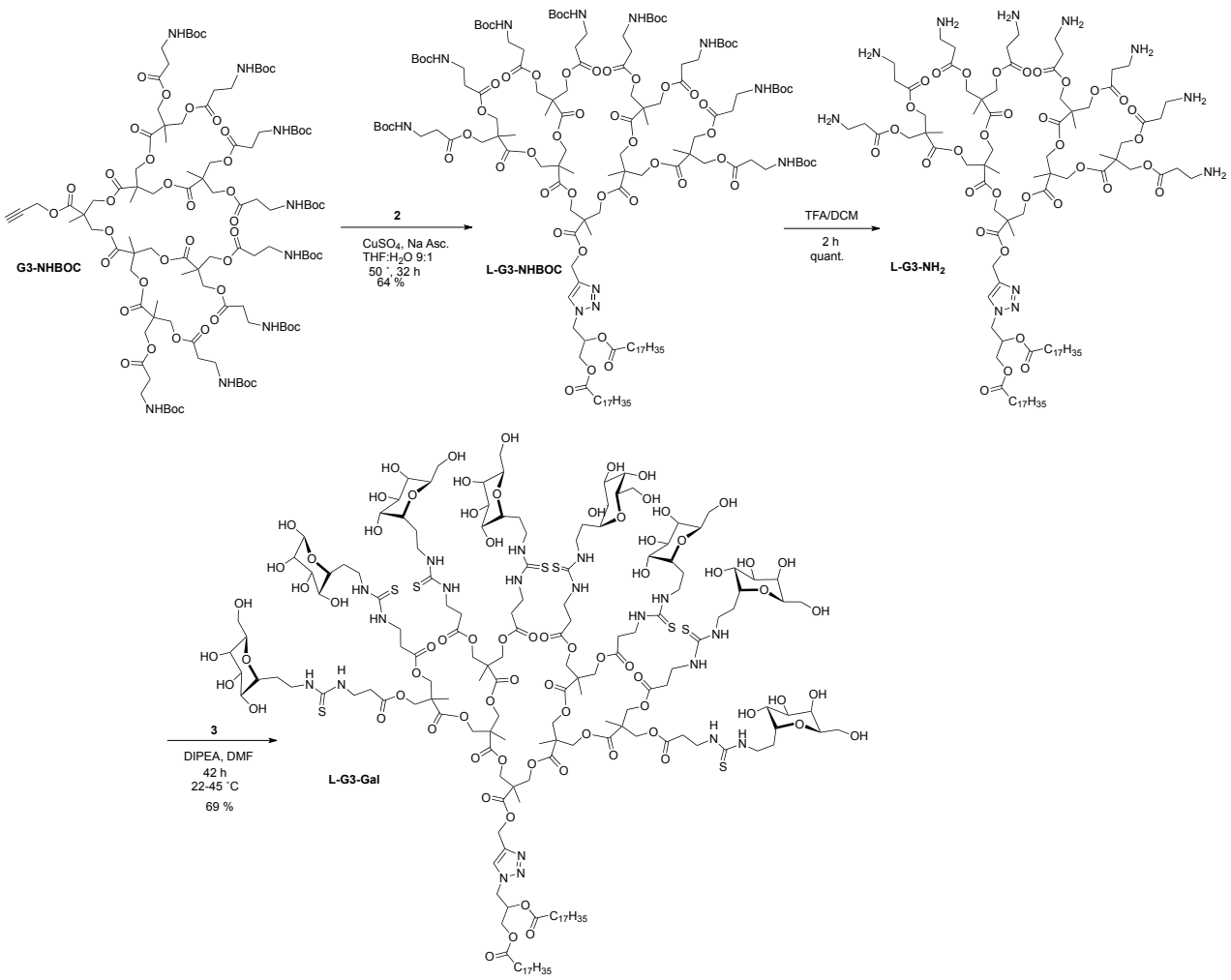


**Scheme S4**. Synthesis of L-G3-Gal.

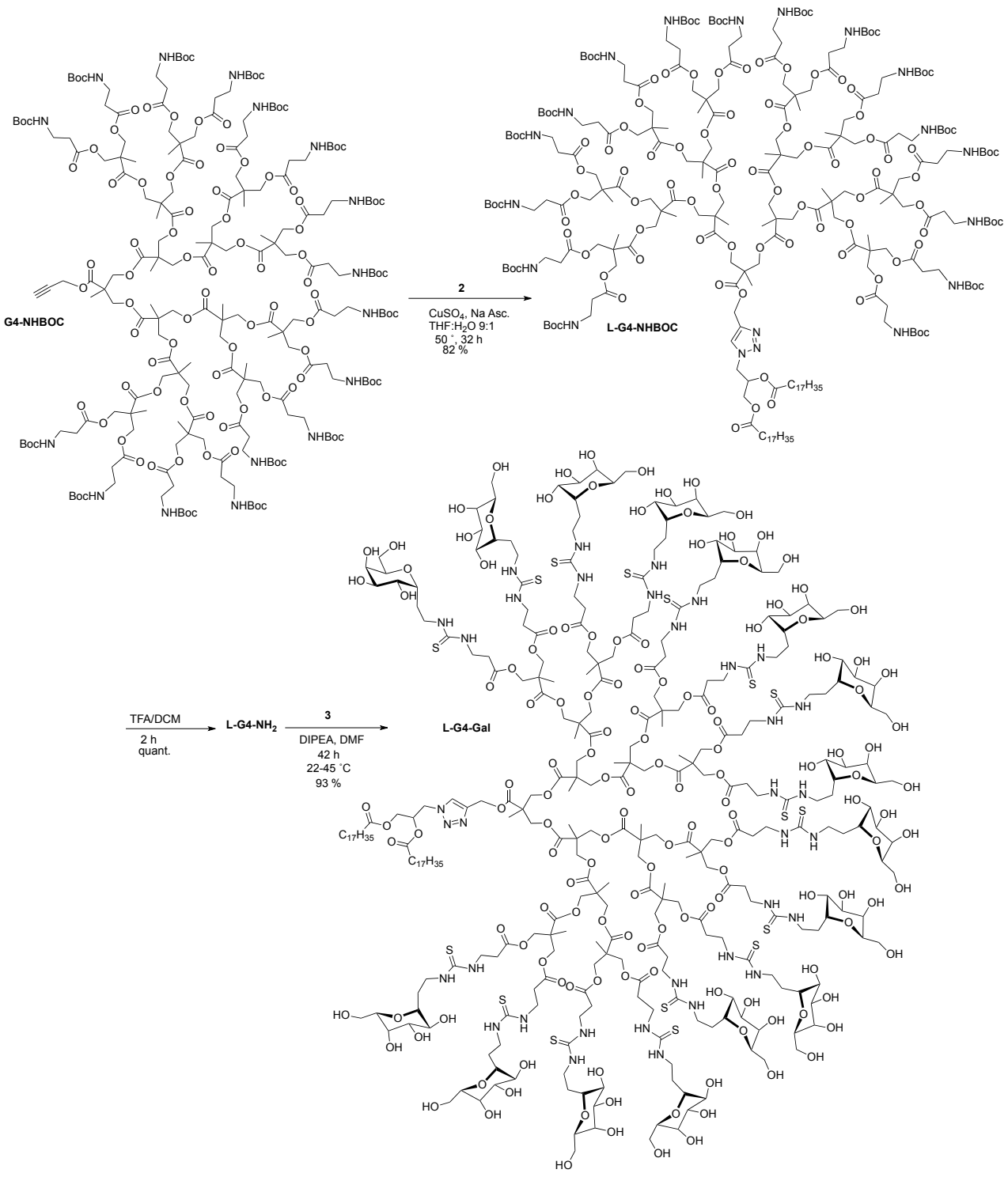


**Scheme S5**. Synthesis of L-G4-Gal.

**General materials and procedures**

Solvents were purchased from Caledon Labs (Caledon, Ontario). All other chemicals were purchased from Sigma-Aldrich, AK Scientific, Chem-Impex, Oakwood Chemicals, Alfa Aesar or Acros Chemicals and were used without further purification unless otherwise noted. Anhydrous toluene, tetrahydrofuran (THF), diethyl ether and *N*,*N*-dimethylformamide (DMF) were obtained from an Innovative Technology (Newburyport, USA) solvent purification system based on aluminium oxide columns. $CH_2Cl_2$, pyridine, *N*,*N*-diisopropylethylamine (DIPEA) and $NEt_3$ were freshly distilled from $CaH_2$ prior to use. Purified water was obtained from a Millipore deionization system. Thin layer chromatography (TLC) was performed using EMD aluminium-backed silica 60 F254-coated plates. Dialysis was performed using Spectrum Laboratories (Rancho Dominguez, CA, USA) dialysis tubing with a molecular weigh cut-off (MWCO) of 1 kg/mol or 2 kg/mol. $^1$H NMR spectra were obtained at 400 MHz or 600 MHz, and $^{13}$C NMR spectra were obtained at 100 or 150 MHz on Varian Inova instruments. NMR chemical shifts (δ) are reported in ppm and are calibrated against residual solvent signals of $CHCl_3$ (δ 7.26), $(CD_3)SO(CD_2H)$ (δ 2.50), $(CD_3)CO(CD_2H)$ (δ 2.05), or $CD_2HOD$ (δ 3.31). Mass spectrometry was performed using either a Bruker microTOF 11 for electrospray ionization (ESI), or an AB Sciex 5800 TOF/TOF mass spectrometer for matrix assisted laser desorption ionization (MALDI). The matrix for MALDI was 2,5-dihydroxybenzoic acid (DHB) in all cases except L-G3-OH, where it was *trans*-indole-3-acrylic acid, and all measurements were performed in reflective mode. Other details for mass spectrometry acquisition are included with copies of the individual spectra below. Differential scanning calorimetry (DSC) was performed on a TA Q20 DSC instrument. For DSC, the heating/cooling rate was 10 °C/min between -120 to +150 °C. Glass transition temperatures ($T_g$) were obtained from the second heating cycle. Thermal data was interpreted using Universal Analyses 2000 (TA Instruments). Thermogravimetric analysis (data not shown) was performed using a TA Q600 SDT instrument prior to DSC analysis to ensure thermal stability prior to DSC measurements. Dynamic light scattering (DLS) data were obtained using a Zetasizer Nano ZS instrument from Malvern Instruments, equipped with a 633 nm laser. TEM images were acquired on a Phillips CM10 microscope operating at 90 kV with a 40 μm aperture. For TEM sample preparation, 5 μL of a ~0.2 mg/mL polymer assembly suspension was dropped directly on a TEM grid (Formvar/carbon film, 400 mesh, copper, Electron Microscopy Sciences, Hatfield, PA, USA) and allowed to evaporate to dryness over 16

hrs before image acquisition. No staining was performed. Fluorescence spectra were obtained using a QM-4 SE spectrometer from Photon Technology International (PTI) equipped with double excitation and emission monochromators.

***rac*-3-azido-propan-1,2-diol** (**4**). This compound was prepared by a modified version of previously published procedure.[1] Glycolic acid (5.0 g, 4.5 mL, 68 mmol) was dissolved in *tert*-butanol (195 mL) and water (6.5 mL) along with lithium tetrafluoroborate (1.3 g, 14 mmol) and sodium azide (8.8 g, 140 mmol) in a two-necked round-bottom flask equipped with a water-cooled condenser under a nitrogen atmosphere with magnetic stirring. The reaction mixture was heated at ~ 85 ºC for 70 minutes. The reaction was then cooled to ambient temperature, and concentrated to dryness under reduced pressure. The resulting solid was then redissolved in 50 mL of water, and extracted seven times with ethyl acetate (100 mL each). The combined organic phases were then dried with $MgSO_4$, filtered and concentrated under reduced pressure. The residue was then purified by column chromatography (ethyl acetate to 95:5 ethyl acetate:methanol) to provide 6.1 g of the product in 78 % yield. Yellow oil. Rf = 0.5, ethyl acetate. $^1$H NMR (400 MHz, *CDCl$_3$*) $\delta_{ppm}$: 3.89-3.82 (m, 1H), 3.67 (dd, *J* = 11.5, 3.5 Hz, 1H), 3.57 (dd, *J* = 11.5, 6.3 Hz, 1H), 3.37-3.35 (m, 2H); $^{13}$C NMR (125 MHz, *CDCl$_3$*): $\delta_{ppm}$ 70.9, 64.0, 53.4. Spectral data are consistent with previously published spectra.[1]

**Azido diglyceride** (**2**). 3-Azidopropane-1,2-diol (**4**, 1.57 g, 13.4 mmol) was dissolved in $CH_2Cl_2$ (25 mL) and cooled to 0 ºC. DIPEA (9.6 mL, 55 mmol) was added to the solution followed by stearoyl chloride (18.1 mL, 16.3 g, 53.7 mmol) and the reaction was stirred for 16 hours. TLC showed consumption of the glycerol, and the reaction was quenched with 1 M HCl, diluted with $CH_2Cl_2$, and the phases were partitioned. The organic phase was washed sequentially with saturated sodium bicarbonate and brine, and then was dried with $MgSO_4$, filtered and concentrated. The crude NMR spectrum showed complete conversion, and the material was purified twice by column chromatography (2:98 diethyl ether:hexanes to 10:90 ethyl acetate:hexanes), to provide 6.1 g of the product as a clear oil in 94% yield. Spectral data is consistent with previously published data.[2] $^1$H NMR (400 MHz, *CDCl$_3$*) $\delta_{ppm}$: 5.17 (ddd, *J*= 4.7, 5.9, 9.2 Hz, 1H), 4.28 (dd, *J* = 11.9, 4.5 Hz, 1H), 4.16 (dd, *J* = 11.9, 5.7 Hz, 1H), 3.47 (dd, *J* = 12.2, 3.7 Hz, 1H), 3.45 (dd, *J* = 12.1, 4.8 Hz, 1H), 2.33 (dt, *J* = 13.9, 7.5 Hz, 4H), 1.66-1.56 (m,

4H), 1.34-1.20 (m, 56H), 0.88 (t, $J$ = 6.8, 1.3 Hz, 6H); $^{13}$C NMR (150 MHz, *CDCl$_3$*): $\delta_{ppm}$ 173.2, 172.8, 69.8, 62.3, 50.9, 34.2, 34.0, 31.9, 29.69, 29.65, 29.61, 29.46, 29.35, 29.25, 29.10, 29.06, 24.85, 24.80, 22.7, 14.1; MS Calculated for $C_{39}H_{75}N_3O_4Na$ $[M+Na]^+$: 672.5655: Found (ESI): 672.5661.

**Standard protocol for copper-assisted azide-alkyne cycloaddition**

Azido diglyceride **2** and the appropriate alkyne were dissolved in THF (obtained from the solvent purification system) and then 10 % v/v of distilled water was added. The flask was then purged with nitrogen. Copper (II) sulfate (50 mol % relative to azide) and sodium ascorbate (100 mol % relative to azide) were added, and the flask was sealed with a septum under a nitrogen balloon and warmed to 50 ºC. The mixture was stirred for 32 hours. It was then diluted with ethyl acetate and filtered through a celite plug. The filtrate was then further diluted with ethyl acetate and washed sequentially with saturated ammonium chloride, saturated sodium bicarbonate and brine. Finally it was dried with $MgSO_4$, filtered, and concentrated *in vacuo* to provide the crude material which was then purified as described for each specific example below.

**L-G0-NHBOC**. Following the standard protocol, **2** (265 mg, 0.41 mmol), *N*-(*tert*-butylcarboxy)-propargylamine (94 mg, 0.61 mmol), copper (II) sulfate (51 mg, 0.21 mmol) and sodium ascorbate (81 mg, 0.41 mmol) were dissolved in THF (1.5 mL) and water (150 µL). Following work-up, the residue was purified by column chromatography (8:2 to 1:1 hexanes:ethyl acetate) to provide 220 mg of material in 67 % yield as an amorphous white solid. Rf = 0.3 (1:1 hexanes:ethyl acetate); $^1$H NMR (400 MHz, *CDCl$_3$*): $\delta_{ppm}$ 7.55 (s, 1H), 5.36 (qd, $J$ = 6.3, 4.9 Hz, 1H), 5.14-5.08 (m, 1H), 4.60 (dd, $J$ = 14.6, 4.8 Hz, 1H), 4.55 (dd, $J$ = 14.4, 6.3 Hz, 1H), 4.37 (d, $J$ = 6.0 Hz, 2H), 4.30 (dd, $J$ = 12.1, 4.5 Hz, 1H), 4.05 (dd, $J$ = 12.1, 5.2 Hz, 1H), 2.37-2.25 (m, 4H), 1.66-1.50 (m, 4H), 1.43 (s, 9H), 1.32-1.20 (m, 56H), 0.87 (t, $J$ = 6.9 Hz, 6H); $^{13}$C NMR (150 MHz, *CDCl$_3$*): $\delta_{ppm}$ 173.1, 172.5, 155.8, 145.7, 122.8, 79.7, 69.3, 61.9, 50.1, 36.0, 34.01, 33.97, 31.9, 29.7, 29.7, 29.5, 29.3, 29.3, 29.2, 29.1, 29.0, 28.3, 24.8, 24.7, 22.7, 14.1; ESI (MS): Calculated for $C_{47}H_{88}N_4O_6$: 804.6704. MS Calculated for $C_{47}H_{88}N_4O_6Na$ $[M+Na]^+$: 827.6602; Found (ESI): 827.6622.

**L-G0-NH$_2$.** **L-G0-NHBOC** (110 mg, 0.14 mmol) was dissolved in 1.5 mL of $CH_2Cl_2$ and 1.5 mL of trifluoroacetic acid. The mixture was stirred for 2 hours, and then evaporated to dryness *in vacuo* to provide 110 mg of the product as a white solid in quantitative yield. $^1$H NMR (400 MHz, 1:1 *$CD_3OD$:$CDCl_3$*): $\delta_{ppm}$ 8.05 (s, 1H), 5.47-5.39 (m, 1H), 4.71 (dd, *J* = 14.6, 4.6 Hz, 1H), 4.66 (dd, *J* = 14.6, 7.1 Hz, 1H), 4.39 (dd, *J* = 12.2, 3.6 Hz, 1H), 4.21 (s, 2H), 4.07 (dd, *J* = 12.2, 6.0 Hz, 1H), 2.33 (dd, *J* = 7.5, 7.5 Hz, 2H), 2.27 (ddd, *J* = 7.3, 7.2, 1.6 Hz, 2H), 1.80-1.49 (m, 4H), 1.35-1.14 (m, 56H), 0.86 (t, *J* = 6.8 Hz, 6H); $^{13}$C NMR (100 MHz, 1:1 *$CD_3OD$:$CDCl_3$*): $\delta_{ppm}$ 174.5, 174.0, 140.9, 126.1, 87.9, 70.5, 63.1, 51.1, 34.7, 32.8, 30.5 30.5, 30.3, 30.2, 30.1, 29.9, 29.8, 27.8, 25.7, 25.5, 23.4, 14.4; MS Calculated for $C_{42}H_{81}N_4O_4$ $[M+H]^+$: 705.6258. Found (ESI): 705.6275.

**L-G0-Gal**. **L-G0-NH$_2$** (60 mg, 0.07 mmol) was dissolved in anhydrous DMF (2 mL) to which was added DIPEA (64 μL, 0.36 mmol) and isothiocyanate-activated α-*C*-galactoside **3**[3] (51 mg, 0.20 mmol). The reaction mixture was stirred at ambient temperature for 8 hours, then at 35 ºC for an additional 10 hours. The solution was then concentrated to dryness *in vacuo* and the mixture was then purified by preparative TLC (15:85 methanol:ethyl acetate) to provide 63 mg of material as a white solid in 90 % yield. Rf = 0.58 (15:85 methanol:ethyl acetate); $T_m$ = 56 ºC; $^1$H NMR (400 MHz, *$CDCl_3$*): $\delta_{ppm}$ 8.01 (br s, 0.2H), 7.77 (br s, 0.5H), 7.67-7.50 (m, 0.3H), 5.38 (br s, 1H), 4.85-4.44 (m, 4H), 4.42-4.24 (m, 2H), 4.13-3.85 (m, 3H), 3.78-3.56 (m, 3H), 3.51-3.29 (m, 3H), 2.43-2.20 (m, 4H), 1.90-1.71 (m, 1H), 1.65-1.47 (m, 5H), 1.35-1.10 (m, 56H), 0.86 (t, *J* = 6.5, 6.5 Hz, 6H); Peaks corresponding to the sugar integrate low in $CDCl_3$ due to poor solubility of the sugar in this solvent. Addition of $(CD_3)_2SO$ improves the solubility of the sugar but is not as favorable for seeing the peaks corresponding to the triazole and thiourea peaks. $^1$H NMR (400 MHz, 1:1 *$CDCl_3$:$(CD_3)_2SO$*): $\delta_{ppm}$ 8.68 (s, 0.1H), 7.97-7.68 (m, 0.6H), 5.28 (s, 1H), 4.76-4.28 (m, 4H), 4.28-4.12 (m, 1H), 4.04-3.78 (m, 2H), 3.78-3.58 (m, 2H), 3.58-3.31 (m, 3H), 2.23-2.09 (m, 4H), 1.95-1.63 (m, 2H), 1.50-1.33 (m, 4H), 1.25-1.08 (m, 56H), 0.77 (t, *J* = 6.8 Hz, 6H);$^{13}$C NMR (100 MHz, 1:1 *$CD_3OD$:$CDCl_3$*): $\delta_{ppm}$ 172.1, 171.6, 131.1, 127.6, 71.4, 71.2, 69.9, 68.5, 68.2, 67.4, 61.2, 60.8, 41.2, 33.1, 33.0, 30.9, 28.7, 28.5, 28.34, 28.31, 28.1, 28.0, 24.6, 23.9, 23.8, 21.7, 13.3. MS Calculated. for $C_{51}H_{96}N_5O_9$ $[M-S+H]^+$: 922.7208. Found (ESI): 922.7231.

**G1-NHBOC. G1-OH**[4] (2.00 g, 11.6 mmol, 1 equiv.) and Boc-protected β-alanine (8.75 g, 46 mmol, 4 equiv.), were dissolved in distilled pyridine (4.6 mL, 5 equiv.) under a nitrogen atmosphere. EDC·HCl (7.18 g, 46 mmol, 4 equiv.) and DMAP (5.64 g, 69 mmol, 4 equiv.) were then added to the reaction mixture. 40 mL of anhydrous $CH_2Cl_2$ was then added and the solution was stirred at room temperature for 36 hours. The reaction mixture was then diluted with 100 mL of $CH_2Cl_2$, and washed sequentially with $H_2O$ (1 x 50 mL), 1M HCl (3 x 50 mL), 1M $Na_2CO_3$ (2x 50 mL), and brine (1x 50 mL). The organic phase was then dried, filtered, and concentrated in the usual manner. The residue was further purified by column chromatography (2:1 hexanes:ethyl acetate) to give 4.9 g (82%) of **G1-NHBOC** as a clear oil. $^1$H NMR (400 MHz, *CDCl₃*): $\delta_{ppm}$ 5.19 (br s, 2H), 4.75 (d, 2H, J =2.6 Hz), 4.31- 4.21 (m, 4H), 3.37-3.52 (m, 4H), 2.53-2.45 (m, 5H), 1.42 (s, 18H), 1.27 (s, 3H). $^{13}$C NMR (100 MHz, *CDCl₃*): $\delta_{ppm}$ 171.8, 171.6, 155.6, 79.2, 76.9, 75.3, 64.9, 53.3, 52.5, 46.2, 35.9, 34.3, 28.2, 17.5. MS Calculated. for $C_{24}H_{38}N_2O_{10}$ 537.2 $[M+Na]^+$. Found (MALDI): 537.2.

**L-G1-NHBOC**. Following the standard protocol, **2** (347 mg, 0.53 mmol), **G1-NHBOC** (183 mg, 0.36 mmol), copper (II) sulfate (36 mg, 0.14 mmol) and sodium ascorbate (86 mg, 0.43 mmol) were dissolved in THF (8 mL) and water (800 µL). Following work-up, the residue was purified by column chromatography (6:4 hexanes:ethyl acetate to 1:1 hexanes:ethyl acetate) to provide 381 mg of material in 91% yield as a white solid in the second fraction (the first fraction contained unreacted excess lipid). Rf = 0.22 (7:3 hexanes:ethyl acetate); $^1$H NMR (400 MHz, *CDCl₃*): $\delta_{ppm}$ 7.65 (s, 1H), 5.34 (qd, *J* = 6.7, 4.8, Hz, 1H), 5.22-5.14 (m, 4H), 4.60 (dd, *J* = 14.4, 4.7 Hz, 1H), 4.55 (dd, *J* = 14.4, 6.7 Hz, 1H), 4.27 (dd, *J* = 12.2, 4.4 Hz, 1H), 4.23-4.10 (m, 4H), 4.02 (dd, *J* = 12.1, 5.3 Hz, 1H), 3.32-3.25 (m, 4H), 2.43 (t, *J* = 6.1, Hz, 4H), 2.28 (t, *J* = 7.5 Hz, 2H), 2.23 (ddd, *J* = 7.4, 7.3, 0.9 Hz, 2H), 1.61-1.46 (m, 4H), 1.43-1.32 (m, 18H), 1.26-1.18 (m, 56H), 0.82 (t, *J* = 6.8 Hz, 6H); $^{13}$C NMR (100 MHz, *CDCl₃*): $\delta_{ppm}$ 172.9, 172.5, 172.3, 170.9, 155.7, 142.3, 124.7, 79.2, 69.2, 64.8, 61.9, 58.1, 50.0, 46.3, 36.0, 34.3, 33.9, 31.8, 29.6, 29.5, 29.5, 29.4, 29.2, 29.15, 29.13, 29.0, 28.9, 28.2, 24.7, 24.6, 22.5, 17.6, 14.0; MS Calculated for $C_{63}H_{113}N_5O_{14}Na$ $[M+Na]^+$: 1186.8. Found (MALDI): 1186.6.

**L-G1-NH₂**. **L-G1-NHBOC** (150 mg, 0.13 mmol) was dissolved in 2 mL of $CH_2Cl_2$ and 2 mL of trifluoroacetic acid. The mixture was stirred for 4 hours, and then evaporated to dryness *in vacuo*

to provide 154 mg of the product as a white solid in quantitative yield. $^1$H NMR (400 MHz, 1:1 *$CD_3OD$:$CDCl_3$*): $\delta_{ppm}$ 7.99 (s, 1H), 5.49-5.41 (m, 1H), 5.23-5.20 (m, 2H), 4.71 (dd, *J* = 14.5, 4.3 Hz, 1H), 4.64 (dd, *J* = 14.5, 7.6 Hz, 1H), 4.40 (dd, *J* = 12.2, 3.5 Hz, 1H), 4.29 (dd, *J* = 11.1, 7.1 Hz, 2H), 4.23 (d, *J* = 11.2 Hz, 2H), 4.07 (dd, *J* = 12.2, 5.9 Hz, 1H), 3.18 (t, *J* = 6.5 Hz, 4H), 2.71 (t, *J* = 6.6 Hz, 4H), 2.33 (dd, *J* = 7.5, 7.5 Hz, 2H), 2.26 (ddd, *J* = 7.4, 7.2, 2.1 Hz, 2H), 1.65-1.47 (m, 4H), 1.33-1.20 (m, 59H), 0.86 (t, *J* = 6.8 Hz, 6H); $^{13}$C NMR (100 MHz, 1:1 *$CD_3OD$:$CDCl_3$*): $\delta_{ppm}$ 173.5, 172.8, 172.3, 170.2, 142.1, 125.7, 69.4, 65.5, 62.2, 57.4, 50.0, 46.2, 34.9, 33.7, 31.7, 30.7, 29.49, 29.45, 29.3, 29.2, 29.12, 29.09, 28.9, 28.8, 26.8, 24.6, 24.6, 22.4, 16.9, 13.4; MS Calculated for $C_{53}H_{98}N_5O_{10}$ $[M+H]^+$: 964.7. Found (MALDI): 964.6.

**L-G1-Gal**. **L-G1-NH$_2$** (80 mg, 0.067 mmol) was dissolved in anhydrous DMSO-$d_6$ (1 mL) to which was added DIPEA (60 μL, 0.3 mmol) and isothiocyanate-activated α-*C*-galactoside **3**[3] (47 mg, 0.19 mmol). The reaction was stirred at ambient temperature or 8 hours, then at 35 ºC for an additional 10 hours. The reaction was then concentrated to dryness *in vacuo* and the mixture was purified by dialysis (1 kg/mol MWCO) against DMF for 12 hours with one change of solvent, then against pure water with two changes of solvent over a period of 10 hours. The dialysate was then lyophilized to provide 63 mg of material as an off-white solid in 65% yield with a 92% functionalization efficiency (see the caption of Figure S26 for details). $T_m$ = 53 ºC; $^1$H NMR (400 MHz, *$(CD_3)_2SO$*): $\delta_{ppm}$ 8.10 (s, 1H), 7.46 (s, 1.3H), 7.32 (s, 1.4H), 5.35 (s, 1H), 5.15 (s, 2H), 4.72 (d, *J* = 3.7 Hz, 1.4H), 4.70-4.58 (m, 2H), 4.57 (d, *J* = 4.0 Hz, 1.5H), 4.48 (s, 1.5H), 4.31 (s, 2.8H), 4.17-4.09 (m, 4H), 4.03-3.97 (m, 1H), 3.79-3.73 (m, 2H), 3.72-3.67 (m, 2H), 3.66-3.61 (m, 2H), 3.59-3.35 (m, 12H), 3.30 (s, 8H), 2.53-2.48 (m, 4H), 2.19 (m, 4H), 1.74-1.65 (m, 4H), 1.48-1.36 (m, 4H), 1.26-1.10 (m, 59H), 0.81 (t, *J* = 6.7 Hz, 6H); $^{13}$C NMR (100 MHz, 1:1, *$CD_3CN$:$CDCl_3$*): $\delta_{ppm}$ 172.8, 172.4, 172.2, 171.4, 163.9, 142.0, 126.0, 73.4, 72.4, 70.8, 69.7, 68.8, 68.36, 65.4, 62.6, 60.6, 58.3, 49.8, 46.4, 33.8, 31.8, 29.6, 29.5, 29.4, 29.24, 29.20, 28.9, 28.8, 25.1, 24.8, 24.7, 22.6, 17.6, 14.3; MS Calculated for $C_{71}H_{128}N_7O_{20}S_2$ $[M+H]^+$: 1462.9. Found (MALDI): 1463.0.

**L-G2-NHBOC.** Following the standard protocol, **2** (60 mg, 0.09 mmol), **G2-NHBOC**[3] (47 mg, 0.04 mmol), copper (II) sulfate (6 mg, 0.02 mmol) and sodium ascorbate (10 mg, 0.05 mmol) were dissolved in THF (1 mL) and water (100 μL). Following work-up, the residue was purified

by column chromatography (6:4 hexanes:ethyl acetate to 1:1 hexanes:ethyl acetate) to provide 58 mg of material in 78% yield as a white solid in the second fraction (the first fraction contained unreacted excess lipid). $^1$H NMR (400 MHz, *CDCl$_3$*): $\delta_{ppm}$ 7.76 (s, 1H), 5.44-5.38 (m, 1H), 5.23-5.19 (m, 4H), 4.66 (dd, *J* = 14.1, 4.4 Hz, 2H), 4.61 (dd, *J* = 14.2, 6.5 Hz, 1H), 4.32 (dd, *J* = 12.1, 4.2 Hz, 1H), 4.27-4.04 (m, 15H), 3.37 (dd, *J* = 11.5, 5.8 Hz, 8H), 2.53 (t, *J* = 6.0 Hz, 8H), 2.33 (t, *J* = 7.6 Hz, 2H), 2.28 (ddd, *J* = 7.3, 7.3, 0.6 Hz, 2H), 1.66-1.51 (m, 4H), 1.42 (s, 36H), 1.32-1.21 (m, 56H), 1.23 (s, 3H), 1.19 (s, 6H), 0.87 (t, *J* = 6.9 Hz, 6H); $^{13}$C NMR (100 MHz, *CDCl$_3$*): $\delta_{ppm}$ 173.1, 172.5, 172.1, 171.9, 171.8, 155.7, 142.1, 125.1, 79.3, 69.2, 65.5, 64.9, 62.1, 58.2, 50.1, 46.6, 46.4, 38.1, 36.1, 34.4, 33.9, 31.8, 29.7, 29.6, 29.5, 29.3, 29.3, 29.2, 29.1, 29.0, 28.4, 24.8, 24.7, 22.7, 17.7, 17.5, 14.1; MS Calculated for $[M+Na]^+$: $C_{89}H_{155}N_7O_{26}Na$: 1761.1; Found (MALDI): 1760.8.

**L-G2-NH$_2$**. **L-G2-NHBOC** (300 mg, 0.17 mmol) was dissolved in 3.5 mL of $CH_2Cl_2$ and 1 mL of trifluoroacetic acid. The mixture was stirred for 4 hours, and then evaporated to dryness *in vacuo* to provide 312 mg of the product as a white solid in quantitative yield. $^1$H NMR (400 MHz, *CD$_3$OD*): $\delta_{ppm}$ 8.11 (s, 1H), 5.53-5.46 (m, 1H), 5.26 (bs, 2H), 4.76 (dd, *J* = 14.4, 4.1 Hz, 1H), 4.69 (dd, *J* = 14.4, 7.6 Hz, 1H), 4.47 (dd, *J* = 12.1, 2.9 Hz, 1H), 4.31-4.19 (m, 12H), 4.09 (dd, *J* = 12.1, 6.3 Hz, 1H), 3.24 (t, *J* = 6.4 Hz, 8H), 2.81 (t, *J* = 6.7 Hz, 8H), 2.33 (dd, *J* = 7.4, 7.4 Hz, 2H), 2.27 (ddd, *J* = 7.1, 6.8, 1.5 Hz, 2H), 1.65-1.50 (m, 4H), 1.36-1.24 (m, 59H), 1.22 (s, 6H), 0.89 (t, *J* = 6.8 Hz, 6H); $^{13}$C NMR (100 MHz, *CD$_3$OD*): $\delta_{ppm}$ 174.7, 174.0, 173.6, 173.4, 171.8, 141.8, 123.7, 71.0, 66.9, 66.7, 63.6, 58.9, 51.3, 47.9, 47.6, 36.3, 35.0, 34.9, 33.1, 32.1, 30.9, 30.8, 30.6, 30.5, 30.3, 30.2, 27.8, 26.04, 25.96, 23.8, 18.0, 17.9, 14.6; MS Calculated for $C_{69}H_{124}N_7O_{18}$ $[M+H]^+$: 1338.9; Found (MALDI): 1338.7.

**L-G2-Gal**. **L-G2-NHBOC** (131 mg, 0.073 mmol) was dissolved in anhydrous DMF (2 mL) to which was added DIPEA (77 μL, 0.44 mmol) and isothiocyanate-activated α-*C*-galactoside **3**[3] (104 mg, 0.41 mmol) in DMF (1 mL). The reaction was stirred at ambient temperature for 8 hours, then at 35 ºC for an additional 10 hours. The reaction was then concentrated to dryness *in vacuo* and the mixture was then purified by dialysis (2 kg/mol MWCO) against DMF with one change of solvent over 12 hours, then against pure water with two changes of solvent over 10 hours. The dialysate was then lyophilized to provide 86 mg of material as an off-white solid in

51% yield with an 81% functionalization efficiency (see the caption of Figure S35 for details). $T_m$ = 36 ºC; $^1$H NMR (400 MHz, 1:1 *(CD$_3$)$_2$SO:CDCl$_3$*): $\delta_{ppm}$ 8.15 (s, 1H), 7.57-7.49 (m, 2H), 7.43-7.36 (m, 2H), 5.38 (bs, 1H), 5.17 (s, 2H), 4.80-4.47 (m, 8H), 4.39-4.30 (m, 3H), 4.23-4.07 (m, 10H), 4.07-3.98 (m, 2H), 3.81-3.75 (m, 3H), 3.74-3.71 (m, 3H), 3.68-3.64 (m, 3H), 3.63-3.22 (m, 31H), 3.07-2.99 (m, 2H), 2.71-2.62 (m, 2H), 2.60-2.52 (m, 4H), 2.31-2.12 (m, 4H), 1.80-1.64 (m, 4H), 1.55-1.36 (m, 4H), 1.31-1.14 (m, 59H), 1.14-1.10 (m, 6H), 1.07-0.99 (m, 3H), 0.83 (t, *J* = 6.53 Hz, 6H); $^{13}$C NMR (100 MHz, 1:1 *(CD$_3$)$_2$SO:CDCl$_3$*) 0.5Hz line broadening applied: $\delta_{ppm}$ 182.9, 172.8, 172.2, 172.1, 171.5, 170.3, 141.8, 126.2, 73.4, 72.4, 70.8, 69.7, 68.8, 68.5, 65.8, 65.4, 64.1, 62.7, 60.6, 58.3, 49.8, 48.5, 46.5, 46.44, 46.37, 35.7, 35.0, 33.79, 33.77, 31.8, 29.6, 29.5, 29.4, 29.2, 28.9, 28.8, 25.1, 24.81, 24.75, 22.5, 17.5, 17.3, 14.3. MS Calculated for $C_{105}H_{181}DN_{11}O_{38}NaS_4$ $[M+Na]^+$: 2358.2. Found (ESI): 2358.1.

**L-G3-NHBOC**. Following the standard protocol, **2** (391 mg, 0.60 mmol), **G3-NHBOC** (550 mg, 0.246 mmol),[3] copper (II) sulfate (37 mg, 0.142 mmol) and sodium ascorbate (62 mg, 0.31 mmol) were dissolved in THF (1800 µL) and water (200 µL). Following work-up, the residue was purified by column chromatography (1:2 hexanes:ethyl acetate to 1:4 hexanes:ethyl acetate) to provide 450 mg of material in 64 % yield as a white solid in the second fraction (the first fraction contained unreacted excess lipid). $^1$H NMR (400 MHz, *CDCl$_3$*): $\delta_{ppm}$ 7.75 (s, 1H), 5.41-5.33 (m, 1H), 5.31-5.11 (m, 8H), 4.61 (dd, *J* = 14.4, 4.7 Hz, 1H), 4.56 (dd, *J* = 14.5, 6.8 Hz, 1H), 4.30 (dd, *J* = 12.1, 3.8 Hz, 1H), 4.23-3.98 (m, 31H), 3.31 (dd, *J* = 11.6, 5.8 Hz, 16H), 2.48 (t, *J* = 6.0 Hz, 16H), 2.27 (t, *J* = 7.6 Hz, 2H), 2.22 (ddd, *J* = 9.2, 7.4, 1.4 Hz, 2H), 1.59-1.46 (m, 4H), 1.36 (s, 72H), 1.26-1.16 (m, 71H), 1.15 (s, 6H), 0.81 (t, *J* = 6.8 Hz, 6H); $^{13}$C NMR (100 MHz, *CDCl$_3$)*: $\delta_{ppm}$ 173.1, 172.6, 172.0, 171.8, 171.45, 171.41, 155.8, 142.0, 125.1, 79.3, 69.31, 69.29, 65.3, 64.8, 62.2, 59.5, 58.3, 50.1, 46.6, 46.4, 38.1, 36.1, 34.4, 34.0, 33.9, 31.9, 31.2, 29.7, 29.6, 29.3, 29.1, 29.0, 28.4, 24.8, 24.7, 22.7, 17.8, 17.4, 14.1. MS Calculated for $C_{144}H_{239}N_{11}O_{50}$ $[M+Na]^+$: 2909.6; Found (MALDI): 2909.5.

**L-G3-NH$_2$**. **L-G3-NHBOC** (34 mg, 0.012mmol) was dissolved in 1 mL of $CH_2Cl_2$ and 1 mL of trifluoroacetic acid. The mixture was stirred for 2 hours, and then evaporated to dryness *in vacuo* to provide 32 mg of the product as a white solid, after triteration with diethyl ether and hexanes, in quantitative yield. $^1$H NMR (400 MHz, 1:1 *(CD$_3$)$_2$CO:CDCl$_3$*): $\delta_{ppm}$ 8.12 (s, 1H), 5.53-5.45

(m, 1H), 5.32-5.24 (m, 24H-exchangeable), 4.75 (dd, *J* = 14.5, 4.2 Hz, 1H), 4.68 (dd, *J* = 14.5, 7.6 Hz, 1H), 4.46 (dd, *J* = 12.1, 2.9 Hz, 1H), 4.35-4.21 (m, 30H), 4.09 (dd, *J* = 12.0, 6.3 Hz, 1H), 3.23 (t, *J* = 6.6 Hz, 16H), 2.80 (t, *J* = 6.7 Hz, 16H), 2.33 (t, *J* = 7.4 Hz, 2H), 2.27 (ddd, *J* = 7.3, 7.1, 2.3 Hz, 2H), 1.65-1.49 (m, 4H), 1.34-1.24 (m, 71H), 1.23 (s, 6H), 0.88 (t, *J* = 6.8 Hz, 6H); $^{13}$C NMR (150 MHz, *$CD_3OD$*): $\delta_{ppm}$ 174.7, 174.1, 173.6, 173.5, 173.2, 171.8, 143.6, 127.4, 71.0, 67.4, 66.9, 66.6, 63.7, 59.0, 51.3, 48.0, 47.9, 47.6, 36.3, 36.0, 34.93, 34.88, 33.1, 32.2, 30.8, 30.7, 30.5, 30.3, 30.2, 26.01, 25.9, 23.8, 18.1, 18.0, 14.5. MS Calculated for $C_{101}H_{175}N_{11}O_{34}$ $[M+H]^+$: 2087.2; Found (MALDI): 2087.0.

**L-G3-Gal**. **L-G3-$NH_2$** (96 mg, 0.032 mmol) was dissolved in anhydrous DMF (2 mL) to which were added DIPEA (557 μL, 3.2 mmol) and isothiocyanate-activated α-*C*-galactoside **3**[3] (130 mg, 0.51 mmol) in DMF (1 mL). The reaction was stirred at ambient temperature for 8 hours, then at 35 ºC for an additional 10 hours, then at 45 ºC for an additional 24 hours. The reaction was then concentrated to dryness *in vacuo* and the mixture was then purified by dialysis (2 kg/mol MWCO) against DMF with one change of solvent over 12 h, then against pure water with two changes of solvent over 10 h. The dialysate was then lyophilized to provide 90 mg of material as a light-yellow solid in 69% yield with a 95% functionalization efficiency (see the caption of Figure S44 for details).. $T_m$ = 18 ºC; $T_g$ = -8 ºC; $^1$H NMR (600 MHz, *$(CD_3)_2SO$*): $\delta_{ppm}$ 8.11 (s, 1H), 7.46 (s, 4.2H), 7.32 (s, 5.3H), 5.35 (s, 1H), 5.18-5.13 (m, 2H), 4.75-4.71 (m, 4.7H-exch), 4.70-4.65 (m, 2H), 4.63-4.55 (m, 6.3H-exch), 4.51-4.47 (m, 5.2H-exch), 4.37-4.28 (m, 6.7H-exch), 4.20-4.01 (m, 30H), 3.79-3.74 (m, 8H), 3.71-3.68 (m, 8H), 3.67-3.61 (m, 8H), 3.59-3.25 (m, 63H), 2.61-2.48 (m, 16H), 2.24 (t, *J* = 6.8 Hz, 2H), 2.17 (t, *J* = 6.4 Hz, 2H), 1.77-1.62 (m, 16H), 1.50-1.43 (m, 2H), 1.43-1.37 (m, 2H), 1.26-1.08 (m, 83H), 1.04 (s, 3H), 0.82 (t, *J* = 6.7 Hz, 6H); $^{13}$C NMR (100 MHz, *$CD_3OD$*): $\delta_{ppm}$ 182.3, 172.8, 172.4, 171.8, 171.6, 171.2, 171.0, 141.4, 125.7, 72.9, 71.9, 70.3, 69.2, 68.3, 68.0, 68.0, 64.8, 62.1, 60.1, 57.9, 49.3, 48.0, 46.1, 45.9, 41.1, 33.3, 31.2, 29.01, 28.97, 28.90, 28.7, 28.4, 28.3, 24.6, 24.3, 22.0, 17.1, 16.8, 13.9.

**L-G4-NHBOC**. Following the standard protocol, **2** (80 mg, 0.12 mmol), **G4-NHBOC** (267 mg, 0.059 mmol),[3] copper (II) sulfate (7.4 mg, 0.03 mmol) and sodium ascorbate (12 mg, 0.059 mmol) were dissolved in THF (900 μL) and water (100 μL). Following work-up, the residue was purified by column chromatography (1:4 hexanes:ethyl acetate) to provide 251 mg of material in 82 % yield as a thick clear gel in the third fraction (the first fraction contained unreacted excess

lipid and the second unreacted dendron).$^{1}$H NMR (400 MHz, *CDCl$_3$*): $\delta_{ppm}$ 7.78 (s, 1H), 5.43-5.36 (m, 1H), 5.34-5.03 (m, 16H), 4.63 (dd, *J* = 15.1, 4.9 Hz, 1H), 4.58 (dd, *J* = 14.5, 7.0 Hz, 1H), 4.37-4.32 (m, 1H), 4.33-3.96 (m, 63H), 3.33 (dd, *J* = 11.3, 5.9 Hz, 32H), 2.50 (t, *J* = 5.8, 5.8 Hz, 32H), 2.29 (t, *J* = 7.7 Hz, 2H), 2.24 (ddd, *J* = 7.6, 7.3, 1.5 Hz, 2H), 1.62-1.48 (m, 4H), 1.47-1.33 (m, 144H), 1.31-1.11 (m, 97H), 1.07 (s, 3H), 0.84 (t, *J* = 6.8 Hz, 6H); $^{13}$C NMR (100 MHz, *CDCl$_3$*): $\delta_{ppm}$ 173.1, 172.6, 172.1, 172.0, 171.8, 171.5, 171.3, 155.8, 142.1, 125.1, 79.3, 69.3, 65.9, 65.7, 65.1, 64.8, 62.2, 58.2, 50.0, 46.6, 46.4, 37.4, 36.1, 34.4, 34.0, 33.9, 31.9, 29.7, 29.6, 29.5, 29.31, 29.27, 29.1, 29.0, 28.4, 24.8, 24.7, 22.6, 17.8, 17.6, 17.5, 17.4, 14.1; MS Calculated for $C_{245}H_{407}CsN_{19}O_{98}$ $[M+Cs]^+$: 5316.7; Found (ESI): 5316.7.

**L-G4-NH$_2$**. **L-G4-NHBOC** (150 mg, 0.029 mmol) was dissolved in 2 mL of $CH_2Cl_2$ and 2 mL of trifluoroacetic acid. The mixture was stirred for 2 hours, and then evaporated to dryness *in vacuo* to provide 150 mg of the product as a white solid, after triteration with diethyl ether and hexanes, in quantitative yield. $^{1}$H NMR (400 MHz, *CD$_3$OD*): $\delta_{ppm}$ 8.14 (s, 1H), 5.55-5.47 (m, 1H), 5.17-4.93 (m, 48H), 4.82-4.65 (m, 2H), 4.52-4.42 (m, 1H), 4.39-4.18 (m, 60H), 4.15-4.06 (m, 2H), 3.29-3.20 (m, 32H), 2.87-2.75 (m, 32H), 2.34 (t, *J* = 7.5 Hz, 2H), 2.28 (ddd, *J* = 7.2, 7.0, 2.7 Hz, 2H), 1.67-1.48 (m, 4H), 1.41-1.09 (m, 101H), 0.89 (t, *J* = 6.8 Hz, 6H); $^{13}$C NMR (100 MHz, *CD$_3$OD*): $\delta_{ppm}$ 173.5, 171.87, 171.84, 171.79, 171.71, 171.66, 144.3, 127.3, 71.4, 67.5, 67.0, 66.9, 66.86, 66.7, 48.0, 47.7, 36.3, 34.93, 34.92, 33.1, 32.2, 30.8, 30.5, 27.8, 26.0, 23.8, 18.2, 18.11, 18.07, 14.5; MS Calculated for $C_{165}H_{280}N_{19}O_{66}$ $[M+H]^+$: 3583.9; Found (MALDI): 3584.5.

**L-G4-Gal**. **L-G4-NH$_2$** (70 mg, 0.0129 mmol) was dissolved in anhydrous DMF (2 mL) to which were added DIPEA (431 µL, 2.6 mmol) and isothiocyanate-activated α-*C*-galactoside **3**[3] (103 mg, 0.414 mmol) in DMF (1 mL). The reaction was stirred at ambient temperature for 8 hours, then at 35 ºC for an additional 10 hours, then at 45 ºC for an additional 24 hours. The reaction was then concentrated to dryness *in vacuo* and the mixture was purified by dialysis (2 kg/mol MWCO) against DMF with one change of solvent over 12 hours, then against pure water with two changes of solvent over 10 hours. The dialysate was then lyophilized to provide 91 mg of material as an off-white amorphous solid in 93% yield with a 92% functionalization efficiency (see the caption of Figure S52 for details). $^{1}$H NMR (400 MHz, (*CD$_3$)$_2$SO*): $\delta_{ppm}$ 8.10 (s, 1H), 7.71-7.19 (m, 17.3H), 5.36 (bs, 1H), 5.17-5.11 (m, 2H), 4.77-4.70 (m, 10.9H), 4.59 (s, 12.1H),

4.50 (s, 9.8H), 4.33 (s, 12.4H), 4.26-3.96 (m, 48H), 3.83-3.73 (m, 16H), 3.73-3.68 (m, 16H), 3.67-3.60 (m, 16H), 3.60-3.09 (m, 124H), 2.62-2.41 (m, 32H), 2.27-2.13 (m, 4H), 1.80-1.56 (m, 32H), 1.51-1.35 (m, 4H), 1.31-0.89 (m, 101H), 0.86-0.77 (m, 6H); $^{13}$C NMR (100 MHz, *$CD_3OD$*): $\delta_{ppm}$ 182.3, 172.8, 172.3, 171.8, 171.6, 171.2, 171.0, 141.3, 125.5, 72.9, 71.9, 70.3, 68.3, 68.0, 64.8, 63.6, 60.1, 49.3, 47.9, 46.1, 45.9, 41.1, 33.3, 31.2, 28.98, 28.87, 28.62, 28.39, 28.24, 24.6, 24.3, 24.2, 22.0 ,17.1, 17.09, 16.8, 16.6, 13.8.

**L-G3-Acet**. Following the standard protocol, **2** (240 mg, 0.73 mmol), **G3-Acet** (250 mg, 0.49 mmol)[3], copper (II) sulfate (25 mg, 0.19 mmol) and sodium ascorbate (40 mg, 0.39 mmol) were dissolved in THF (1.8 mL) and water (200 μL). Following work-up, the residue (500 mg of brown oil) was purified by column chromatography (7:3 hexanes:ethyl acetate to 3:7 hexanes:ethyl acetate) to provide 370 mg of pure material in 45 % yield as a white solid in the second fraction (the first fraction contained unreacted excess lipid). $^1$H NMR (400 MHz, *$CDCl_3$*): $\delta_{ppm}$ 7.78 (s, 1H), 5.43-5.34 (m, 1H), 4.62 (d, *J* = 4.6 Hz, 1H), 4.61 (d, *J* = 6.8 Hz, 1H), 4.33-4.16 (m, 13H), 4.14-4.04 (m, 10H), 3.59 (d, *J* = 12.1 Hz, 9H), 2.30 (t, *J* = 7.6 Hz, 2H), 2.24 (dt, *J* = 7.6, 0.9 Hz, 2H), 1.64-1.46 (m, 4H), 1.38 (s, 14H), 1.33-1.29 (m, 14H), 1.27-1.19 (m, 62H), 1.11-1.09 (m, 12H), 0.84 (t, *J* = 6.8 Hz, 6H); $^{13}$C NMR (150 MHz, *$CDCl_3$*) $\delta_{ppm}$ 173.4, 173.0, 172.4, 172.0, 171.6, 142.1, 125.2, 98.0, 69.2, 65.8, 64.8, 62.0, 58.2, 50.0, 46.7, 46.5, 42.0, 33.89, 33.87, 31.8, 29.59, 29.56, 29.55, 29.53, 29.39, 29.25, 29.19, 29.17, 29.0, 28.9, 25.3, 24.7, 24.6, 22.6, 18.4, 17.5, 17.4, 14.0; MS Calculated for $C_{89}H_{152}N_3O_{26}$ $[M+H]^+$: 1679.0586. Found (ESI): 1679.0620.

**L-G3-OH**. **L-G3-Acet** (73 mg, 0.044 mmol) was dissolved in methanol (1 mL) and chloroform (2 mL). Dowex-50WX-8 (25 mg), was added and the reaction was stirred at 45 ºC for 14 hours. When TLC analysis showed completion, the material was filtered through a glass frit, and the filtrate was concentrated to dryness and purified by preparative TLC (100 % ethyl acetate) to provide 55 mg of the product as white solid in 83 % yield. $^1$H NMR (400 MHz, *$CDCl_3$*): $\delta_{ppm}$ 8.11 (s, 1H), 5.53-5.46 (m, 1H), 4.80 (dd, *J* = 14.5, 4.3 Hz, 1H), 4.74 (dd, *J* = 14.6, 7.3 Hz, 1H), 4.41 (dd, *J* = 12.1, 3.7 Hz, 1H), 4.37-4.16 (m, 12H), 4.15-4.09 (m, 5H), 3.72-3.61 (m, 14H), 2.35 (t, *J* = 7.5 Hz, 2H), 2.29 (t, *J* = 7.4 Hz, 2H), 1.66-1.48 (m, 4H), 1.35-1.22 (m, 65H), 1.15-1.12 (m, 12H), 0.88 (t, *J* = 6.8 Hz, 6H); $^{13}$C NMR (100 MHz, *$(CD_3)_2CO$*): $\delta_{ppm}$ 176.2, 175.2, 174.4, 173.9, 173.8, 144.0, 127.4, 71.4, 67.8, 67.4, 66.8, 66.4, 64.1, 60.1, 52.3, 51.8, 48.6, 48.4, 43.7,

35.5, 35.4, 33.6, 31.3, 31.1, 26.6, 26.5, 24.3, 19.8, 19.0, 18.9, 18.41, 18.37, 15.4. MS Calculated for $C_{77}H_{133}N_3O_{25}Cs$ $[M\text{-}H_2O+Cs]^+$: 1632.9. Found (MALDI): 1633.2.

**Self-assembly of dendron-lipid amphiphiles**

The amphiphile was dissolved in either THF (**L-G0-Gal**, **L-G1-Gal**) or DMSO (**L-G2-Gal**, **L-G3-Gal**, **L-G4-Gal**, **L-G3-OH**) at a concentration of 10 mg/mL. 100 μL of this solution was added to a vial equipped with a stir bar stirring at 3500 rpm. Millipore purified water (900 μL) was then added to the stirring solution over a period of 1 minute. The mixture was then continually stirred for 30 minutes and then removed from the stir plate. The samples were then dialyzed against 10 mM phosphate buffer (2 kg/mol MWCO) over a period of 24 hours with three changes of the dialysate.

**Determination of CACs based on fluorescence emission of pyrene**

Assemblies were prepared as previously described above, and then dialyzed against 0.1 M phosphate buffer (pH = 7.4). The resulting solution (1000 μg/mL) was diluted to prepare amphiphile concentrations from 1000 ug/mL to 0.001 ug/mL (30 different concentrations, 1 mL of each). Each of these solutions was added to a vial containing 0.005 mg of pyrene, which had been prepared in the following manner. Pyrene (1.00 mg), was dissolved in 10.0 mL of freshly distilled $CH_2Cl_2$. 50 μL of this solution was then injected into each glass vial, and the $CH_2Cl_2$ was evaporated over 6 hours to provide the pyrene-charged vials. Following the addition of the amphiphile solutions, all the vials were sealed, placed in a mechanical shaker, and mixed for 16 hours at ambient temperature to allow for encapsulation of the pyrene into the hydrophobic domains of the assemblies. The fluorescence emission spectrum (365-450 nm) of each solution was then obtained using an excitation wavelength of 334 nm in quartz cuvettes. The emission intensities of the first ($I_1$) and third ($I_3$) vibronic bands of pyrene at 371 and 382 nm respectively were obtained and to determine the CAC, the $I_1/I_3$ ratio was plotted against the log[concentration (mg/L)] to give a sigmoidal curve. The CAC was determined to be the point of intersection between the horizontal linear segment at low concentration and the linear region of negative slope.

*A note on the choice of intercept:*

Figures S61-S66 shows the $I_1/I_3$ (emission at 371/emission at 382 nm) ratio plotted against concentration for the amphiphiles. There is debate in the literature regarding how to interpret this data as there are three potential points of measurement. A) The intersection of the high concentration horizontal linear region with the decreasing linear region;[5,6] B) the intersection of the low concentration horizontal linear region with the decreasing linear region;[7] or C) the point of inflection of the sigmoidal curve.[8,9] In simple cases these three points may be nearly identical, however in more complex cases, such as amphiphilic block copolymers the three points might vary over orders of magnitude. This is what is observed in this case. There are only a limited number of investigations into the CAC of dendron-based amphiphiles using the pyrene method.[10,11] In both cases the CAC was determined by at least two methods, including the surface tension measurement, and in both cases the secondary methods supported a CAC at point B. In the case of the current study, a dynamic light scattering measurement taken at different dilutions of the dendron also supported a CAC at point B. Conceptually this point can be thought of as the lowest concentration in which any pyrene is localized within a hydrophobic environment. At lower concentrations all amphiphiles are molecularly dissolved, whereas at higher concentrations a higher volume of hydrophobic environments are available indicating an increased assembly concentration, leading to a growing percentage of the pyrene molecules being segregated from the water. At the second high horizontal linear region, essentially all pyrene present is incorporated into the hydrophobic domains. Consequently, point B would, in the absence of the ability of unimolecular particles being able to adsorb the pyrene, be the lowest concentration where nanostructures are present, or the CAC. This choice was validated by a dynamic light scattering experiment (see below).

**Determination of CAC by dynamic light scattering (DLS)**

The assemblies were prepared as described above. Serial dilutions were then prepared to encompass concentrations of each sample that were within the high concentration horizontal linear region, the rapidly varying region and in the low concentration horizontal linear region as determined by the pyrene analysis. Each sample was then analyzed using a Malvern nano-ZS instrument equipped with a 4 mW helium-neon laser emitting at 633 nm. All data were collected and analyzed using Malvern zetasizer software V 6.20. For the DLS study, 1 mL solutions of the serial dilutions were analyzed in quartz cuvettes using a constant attenuator setting of 10, and a

laser power of 1.2 mW. The count rates were measured over a minimum of 15 scans and were averaged for each sample, as were the count rates of 5 blank samples. The background count rate was determined to be about 25 counts per second. Any count rate above 100 was considered to be indicative of the presence of assemblies. The lowest concentration at which such a number was observed was determined to be the maximum possible value for the CAC.

**Lectin-binding studies**

*Sample preparation.* GSL 1-coated agarose beads (17 μL) (Vector Laboratories, Burlingame California, 20 mg/mL protein concentration, 1:1 buffer:agarose bead v/v) were washed extensively (10 times) with 0.1 M phosphate buffered saline (PBS). The beads were then suspended in 150 μL phosphate buffered saline (137 mM NaCl, 2.7 mM KCl, 0.012 M phosphate buffer, pH 7.4; 1x PBS), and stored for 16 hours at 4 ºC.

Meanwhile, nile red was dissolved in organic solvent (THF or DMSO) at a known concentration. The solution was diluted to 0.01 mg/mL, and then filtered through a 0.2 μm syringe filter. Each dendron-lipid amphiphile was then dissolved in the same solution at 10 mg/mL (**L-G0-Gal**, **L-G1-Gal**, and **L-G3-OH** in THF; **L-G2-Gal**, **L-G3-Gal**, and **L-G4-Gal** in DMSO). 100 μL was added to a vial equipped with a stir bar and the suspension was stirred at 3500 rpm. Purified water (900 μL) was then added to the stirring solution over a period of 1 minute. The resulting suspension was stirred for 30 minutes and then dialyzed against 0.1x PBS (diluted PBS, see above) using a 2 kg/mol MWCO membrane with three changes of dialysate over a period of 24 hours. The material was then recovered and stored at 4 ºC until needed for up to 3 days. The fluorescence of each assembly sample (at 1 mg/mL dendron-lipid) was measured using an excitation wavelength of 550 nm and the emission spectra were measured from 565 to 700 nm. The relative magnitudes of the fluorescence are given in Table S1.

50 μL of the dendron-lipid assembly suspension was then added to a batch of the lectin beads (150 μL, prepared as described above) in a 2 mL Eppendorf tube. Each sample was prepared in triplicate. For the galactose-competition studies, 100 μL of the PBS solution was removed from the beads prior to the addition of the assemblies, and replaced with 100 μL of PBS containing the appropriate amount of galactose (1.77 mg, 0.0098 mmol for the 100-fold excess sample, 0.177 mg, 0.00098 mmol for the 10-fold excess sample). For the blank, 50 μL of 0.1x PBS was added instead of the assembly suspension. All tubes were then gently shaken in a

mechanical shaker for 3 hours. Tubes were then centrifuged at 3500 rpm for three minutes, and then allowed to stand for five minutes. 150 μL of supernatant was then removed and discarded and replaced with 150 μL of fresh 0.1x PBS. The beads were resuspended by vortexing and then the centrifugation/solvent exchange process was repeated. The tube was then vortexed and 50 μL of bead suspension was then removed from each tube, transferred to a new Eppendorf tube and then diluted with 75 μL of 0.1x PBS. This aliquot corresponded to "Wash 1". The original tubes were then reshaken for an additional three hours, and the entire process above was repeated to obtain the sample referred to as "Wash 2". All tubes were stored at 4 ºC until needed for microscopy which was at most 72 hours. For this analysis, each sample was briefly vortexed, and 25 μL of bead suspension was deposited on a microscopy slide and a cover slip was placed on top. Slides were created no more than 18 at a time to avoid samples drying out.

*Image acquisition.* The samples were imaged using a Zeiss Compound Fluorescence Imager Z1 microscope equipped with a rhodamine filter (excitation 575-625 nm; emission 660-710 nm) and a 40X (PH2 DIC EC Plan Neofluar) objective lens. Images were captured using a 1.4 megapixel monochrome Zeiss MRm camera. The images were acquired and initially processed using Zen software (Zeiss) and analyzed using Image Pro Plus (MediaCybernetics) on PCs using a Windows-based interface. The difference in fluorescence intensity was managed by changing the exposure time of the image from 0.30 s to 7.20 s. A calibration curve was then created by imaging one field with different exposure times to confirm the linear dependence of fluorescence intensity and exposure time (Figure S68).

*Image processing*. All images were exported from the Zen software as .tif files without any compression or change in the dynamic range of the pixel brightness (12 bit). The pictures were corrected for dark pixel effect, and the background was zeroed.[12] The mean fluorescence intensity of all the pixels in a bead for a minimum of at least 4 images and at least 15 beads per sample (number of beads analyzed per sample varied from 15 to 73, and the number of images from 4 to 10) was determined. The mean fluorescence for each bead was then averaged to provide a mean fluorescence intensity for the sample. The autofluorescence of the beads alone was then subtracted from this value (a control sample of beads without any added compound in the PBS vehicle, was treated with the same wash sequence as all the other samples to obtain a background control). This fluorescence was then normalized to take into account the differences in nile red fluorescence intensity between the different assemblies. Finally, this normalized data

was averaged over the three replicates of the study to provide the means ± standard error presented in Figure 4.

**Evaluation of the stability of assemblies formed from L-G0-Gal**

The assemblies were prepared as described above for the lectin binding studies in 10 mM pH 7.4 phosphate buffer at a concentration of 0.5 mg/mL, but without nile red. The count rate was measured using a Malvern nano-ZS instrument equipped with a 4 mW helium-neon laser emitting at 633 nm. The attenuator setting was fixed at 10. The initial count rate was greater than 3000 kilocounts per second (kcps). The sample was then diluted to 0.075 mg/mL, well below the CAC. The count rate immediately dropped to ~2200 kcps, but was well above that of buffer alone, which was ~12 kcps. The count rate was measured over a period of 20 h following the dilution. 3 measurements were taken at each time point.

***In vitro i*NKT cell activation bioassay**

The mouse *i*NKT hybridoma cell line DN32.D3[13] was provided by Dr. Albert Bendelac (The University of Chicago) and maintained in RPMI-1640 medium supplemented with 10% heat-inactivated fetal bovine serum, nonessential amino acids, 2 mM L-glutamine, 1 mM sodium pyruvate, and 50 μM 2-mercaptoethanol. Cells were seeded at $10^5$ cells per well of a flat bottom microplate and stimulated with indicated doses of the test compounds in parallel with 100 ng/mL of KRN7000 (Funakoshi Co Ltd., Tokyo, Japan), which was used as a positive control. 24 hours later, culture supernatants were harvested and their IL-2 content was quantified using an ELISA kit from eBioscience (San Diego, USA). The experiment included triplicate measurements for each condition.

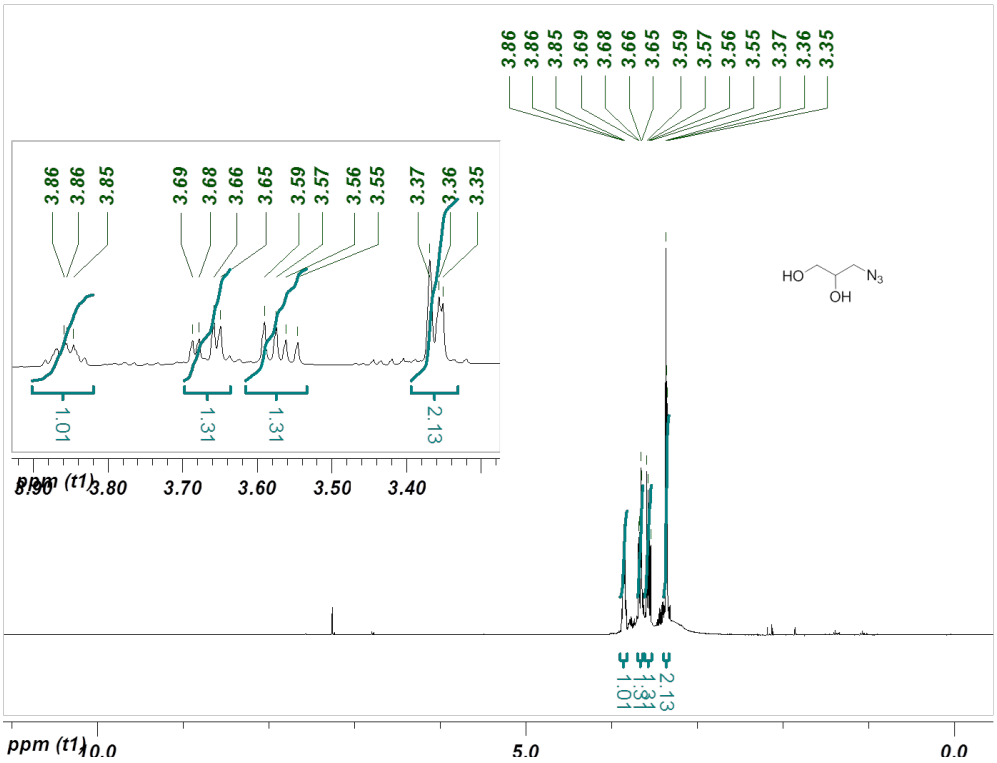


**Figure S1.** $^{1}$H NMR spectrum of *rac*-3-azido-1,2-propandiol (400 MHz, $CDCl_3$).

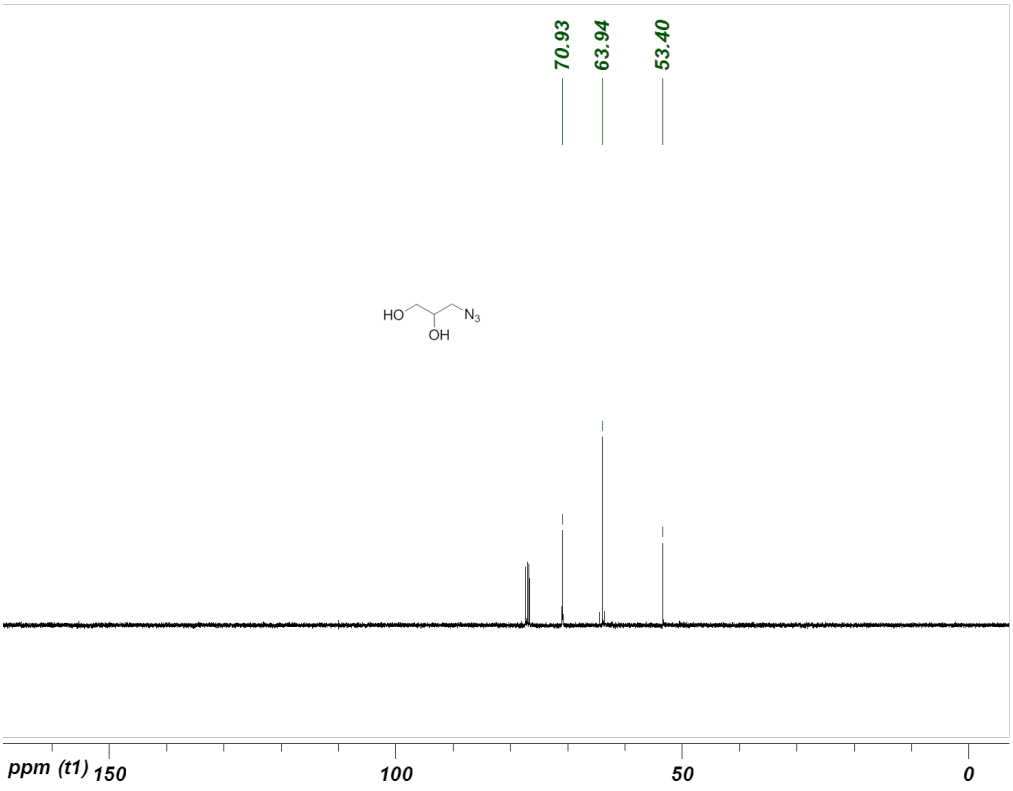


**Figure S2.** $^{13}$C NMR spectrum of *rac*-3-azido-1,2-propandiol (100 MHz, $CDCl_3$).

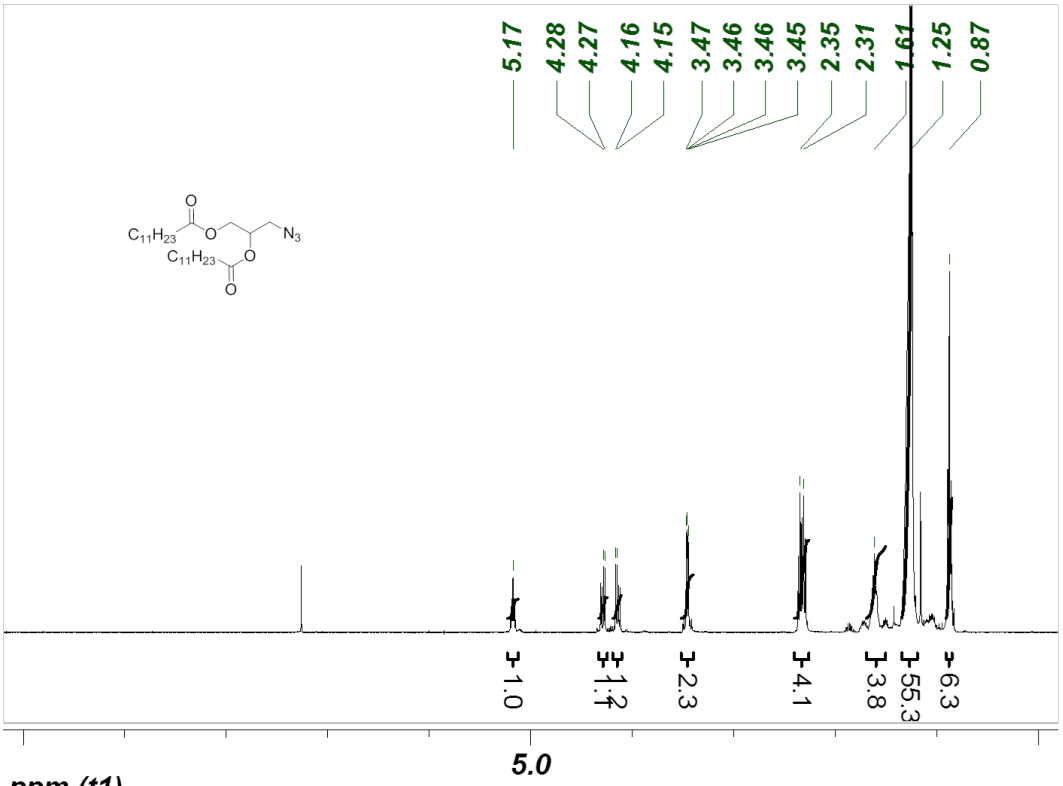


**Figure S3.** $^{1}$H NMR spectrum of azido diglyceride **2** (400 MHz, $CDCl_3$).

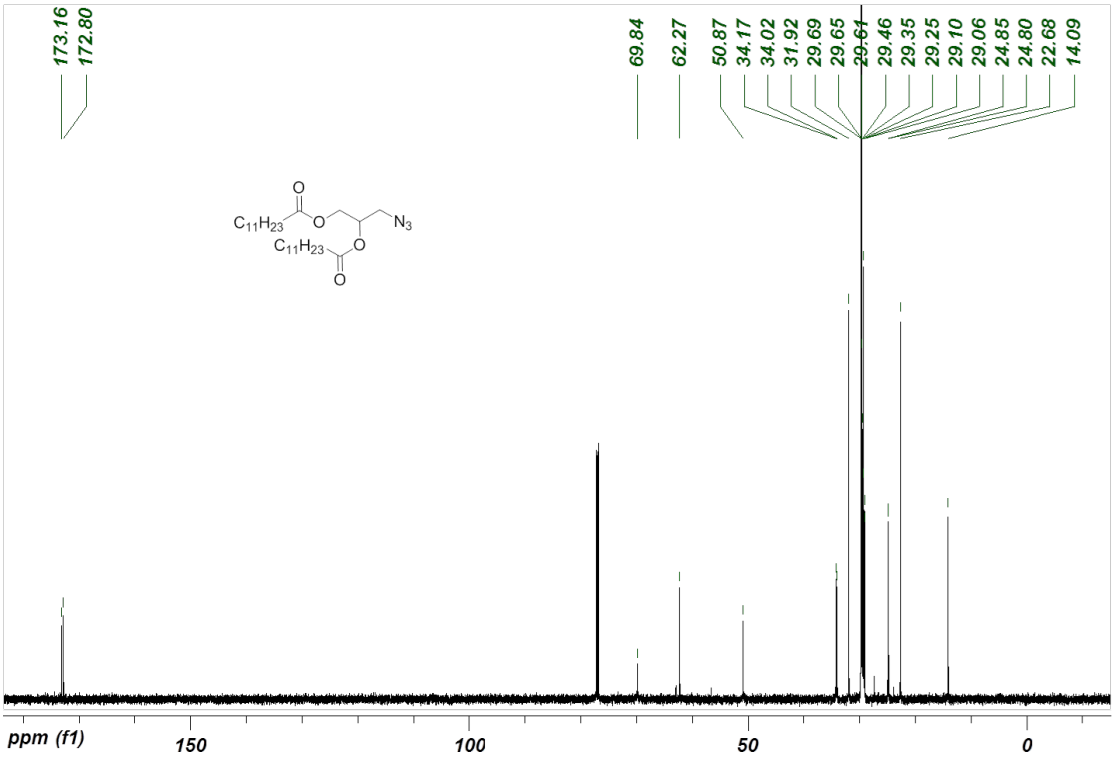


**Figure S4.** $^{13}$C NMR spectrum of azido diglyceride **2** (150 MHz, $CDCl_3$).

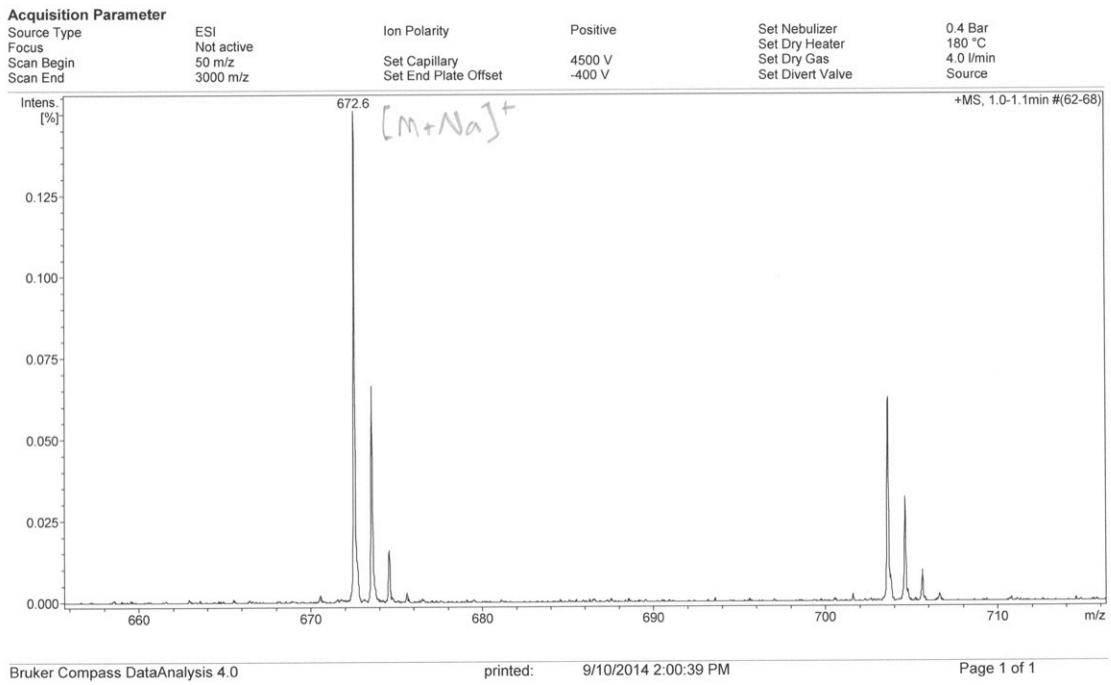


**Figure S5**. Mass spectrum of azido diglyceride **2** (ESI, $CH_2Cl_2$).

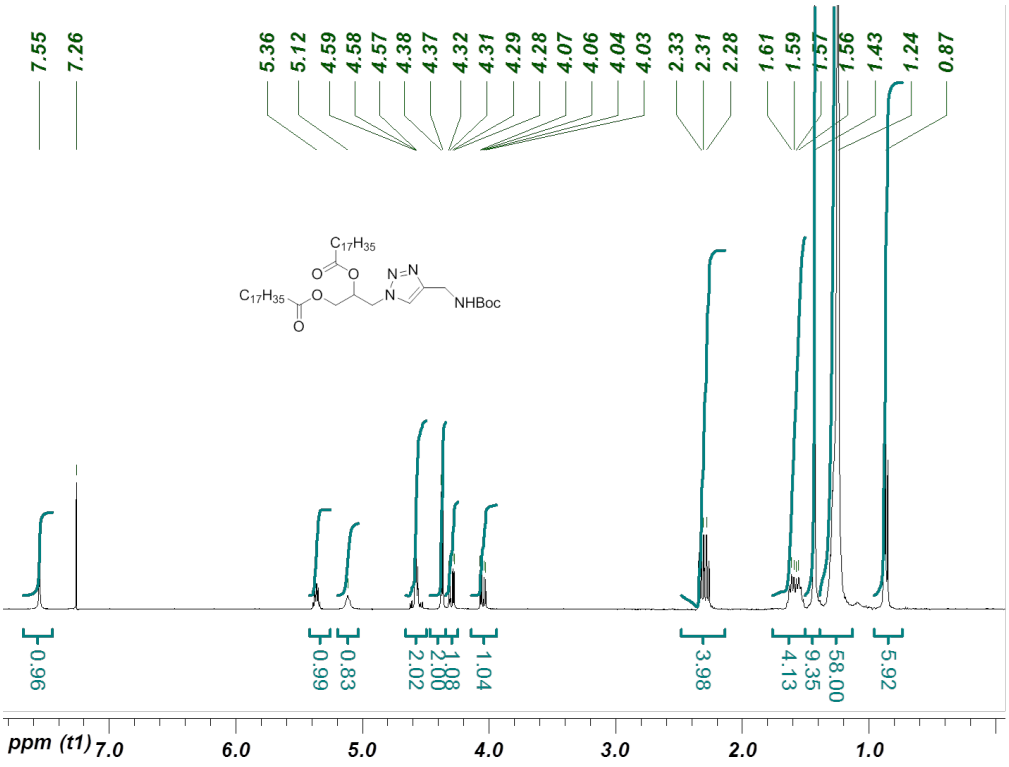


**Figure S6.** $^1$H NMR spectrum of **L-G0-NHBOC** (400 MHz, $CDCl_3$).

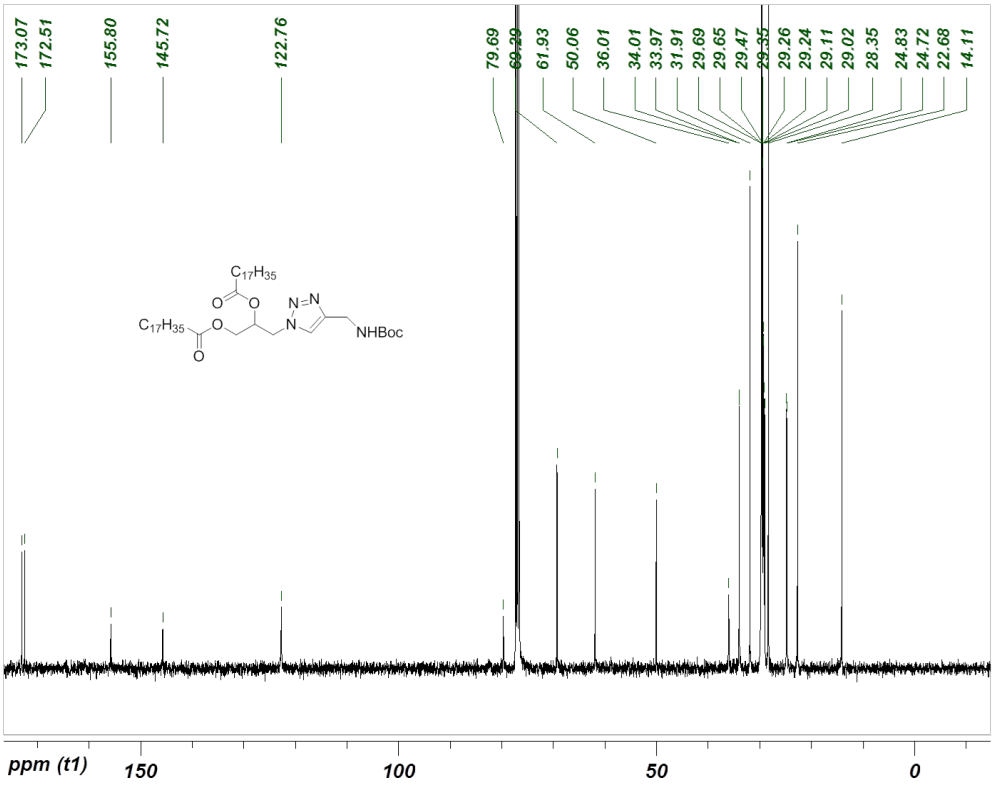


**Figure S7.** $^{13}C$ NMR spectrum of **L-G0-NHBOC** (150 MHz, $CDCl_3$).

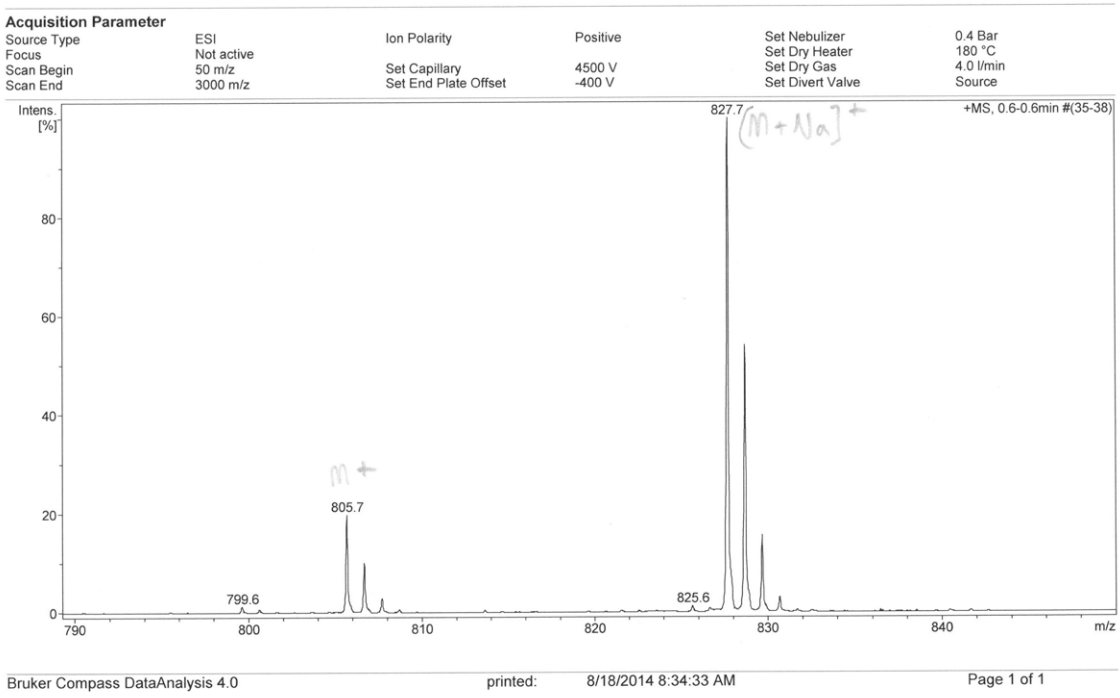


**Figure S8**. Mass spectrum of **L-G0-NHBOC** (ESI, $CH_2Cl_2$).

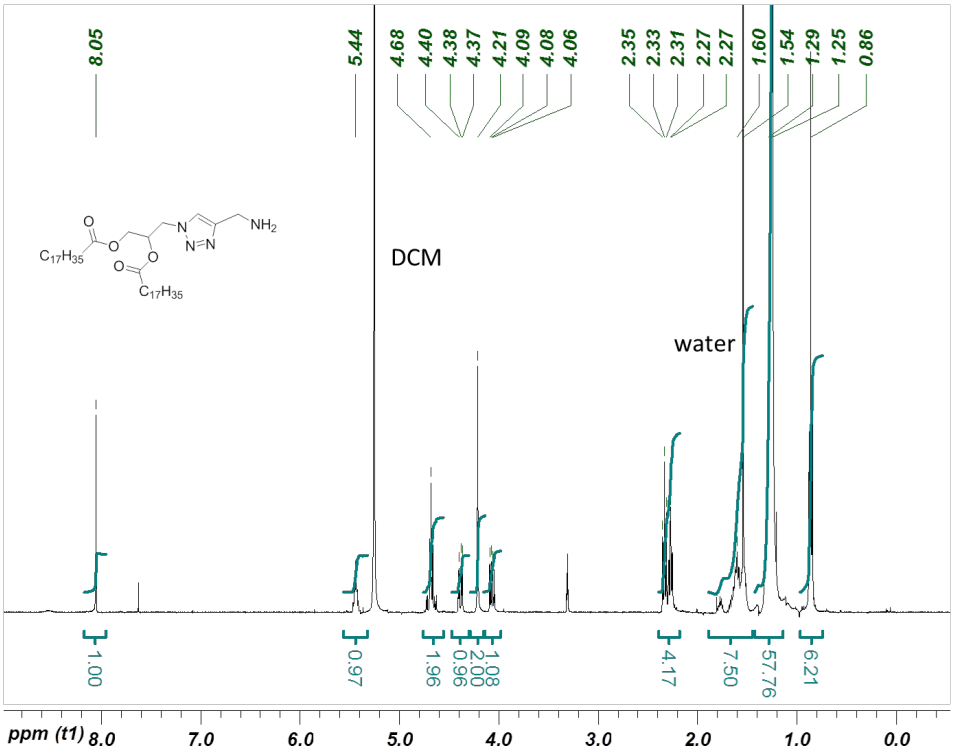


**Figure S9.** $^{1}$H NMR spectrum of **L-G0-NH$_2$** (400 MHz, 1:1 $CD_3OD$:$CDCl_3$).

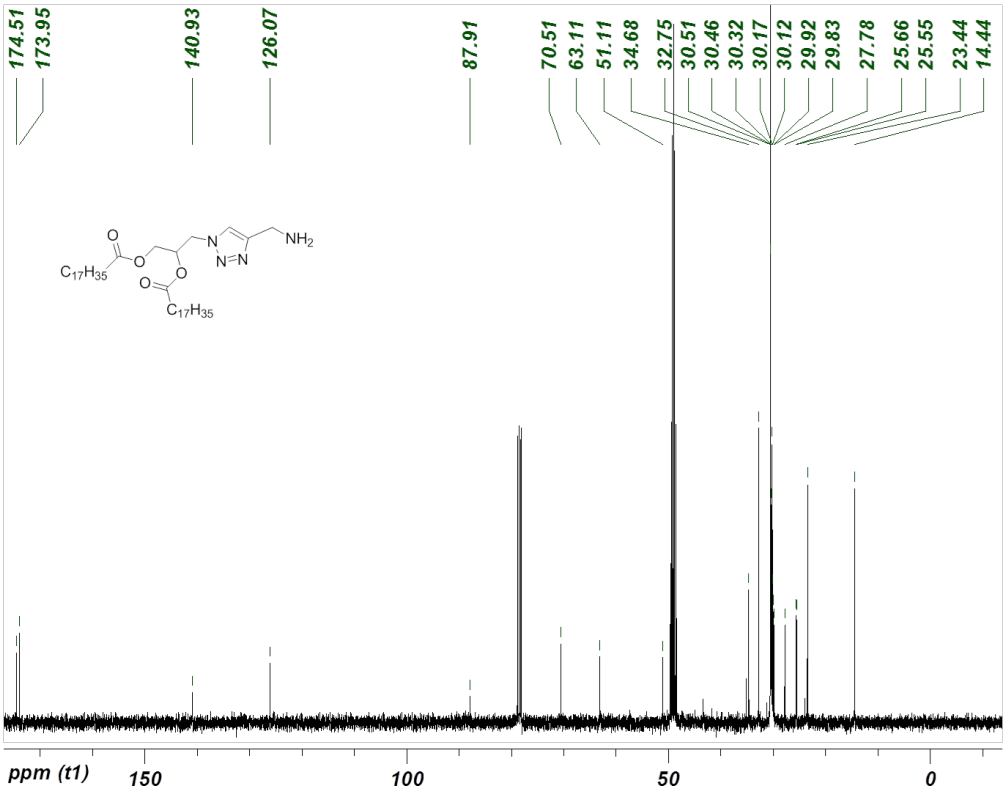


**Figure S10.** $^{13}$C NMR spectrum of **L-G0-NH$_2$** (100 MHz, 1:1 $CD_3OD$:$CDCl_3$).

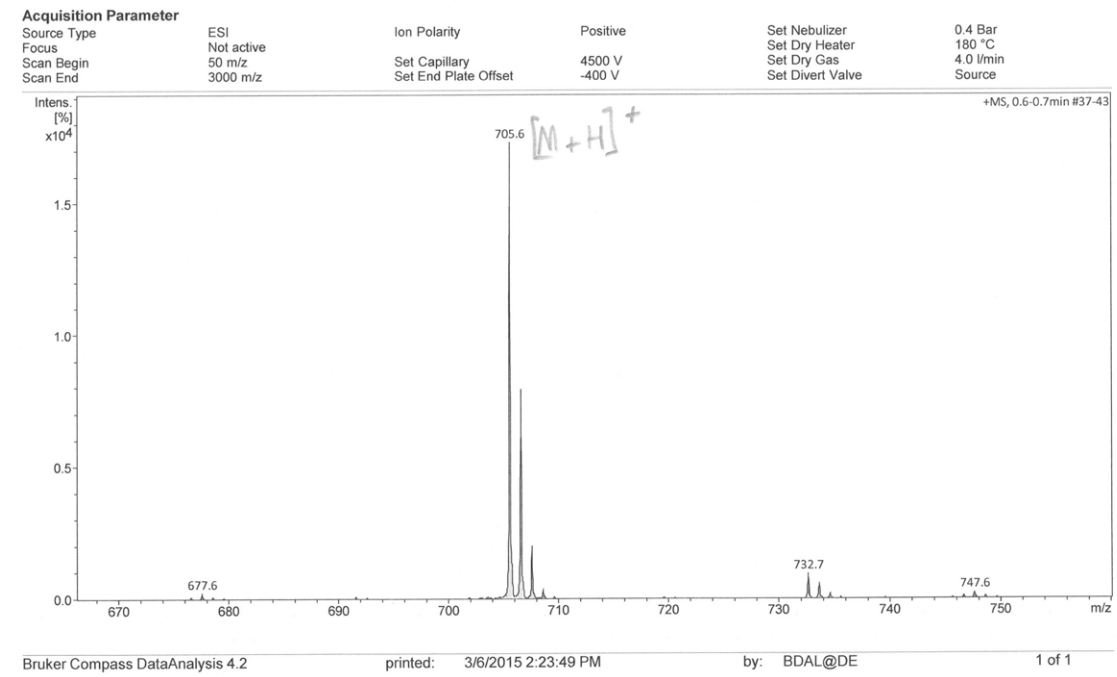


**Figure S11**. Mass spectrum of **L-G0-NH$_2$** (ESI, THF).

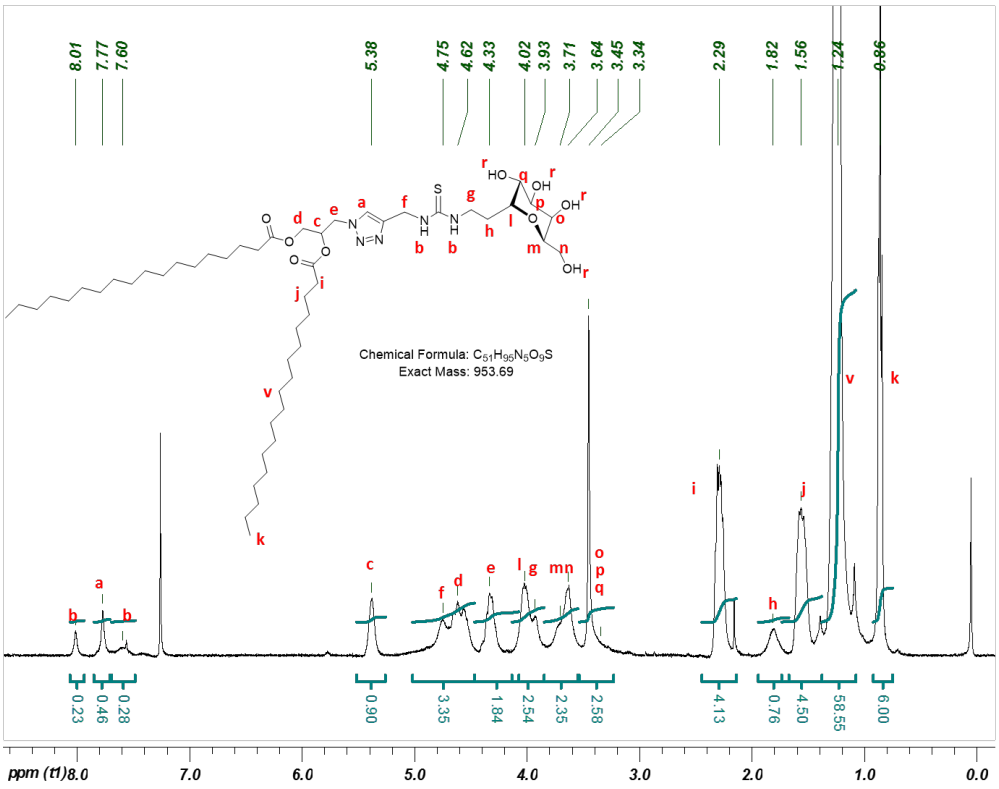


**Figure S12.** $^1$H NMR spectrum of **L-G0-Gal** (400 MHz, $CDCl_3$). Peaks corresponding to the sugar integrate low in this solvent due to selective solubilization of the lipid. The spectrum was also obtained in 1:1 $(CD_3)_2SO$:$CDCl_3$ (Figure S13).

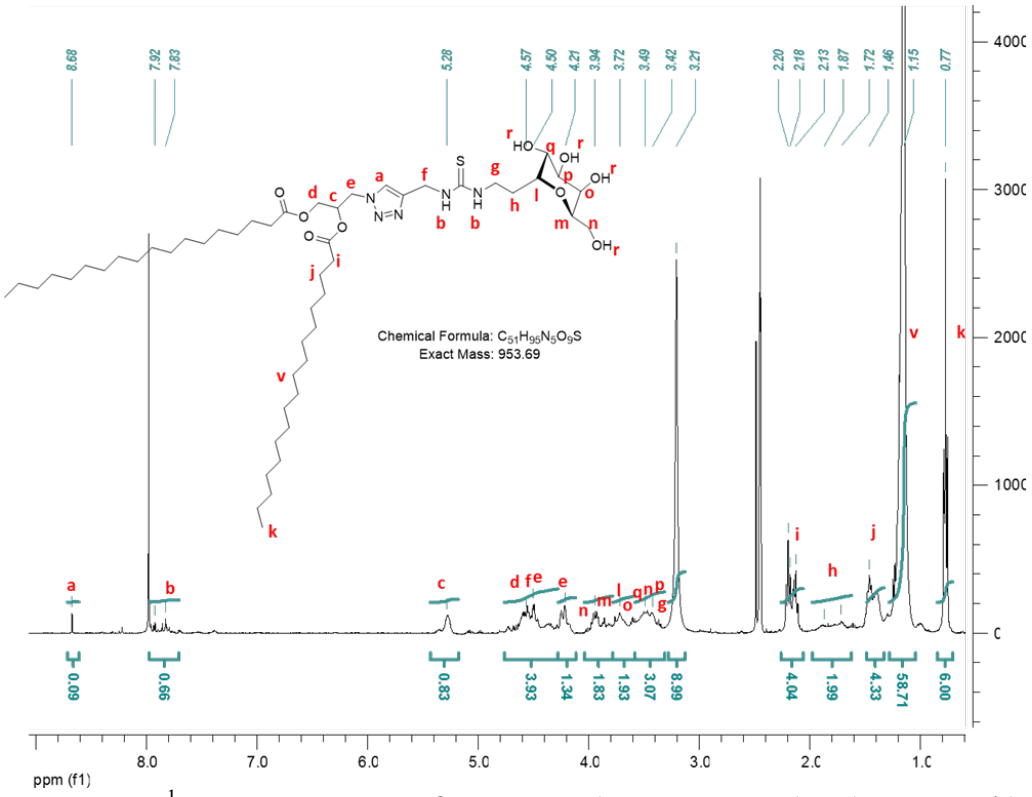


**Figure S13.** $^{1}$H NMR spectrum of **L-G0-Gal** (400 MHz, 1:1 $(CD_3)_2SO$:$CDCl_3$). Proper relative integration of peaks k (6H) vs h (2H) shows full functionalization with the sugar.

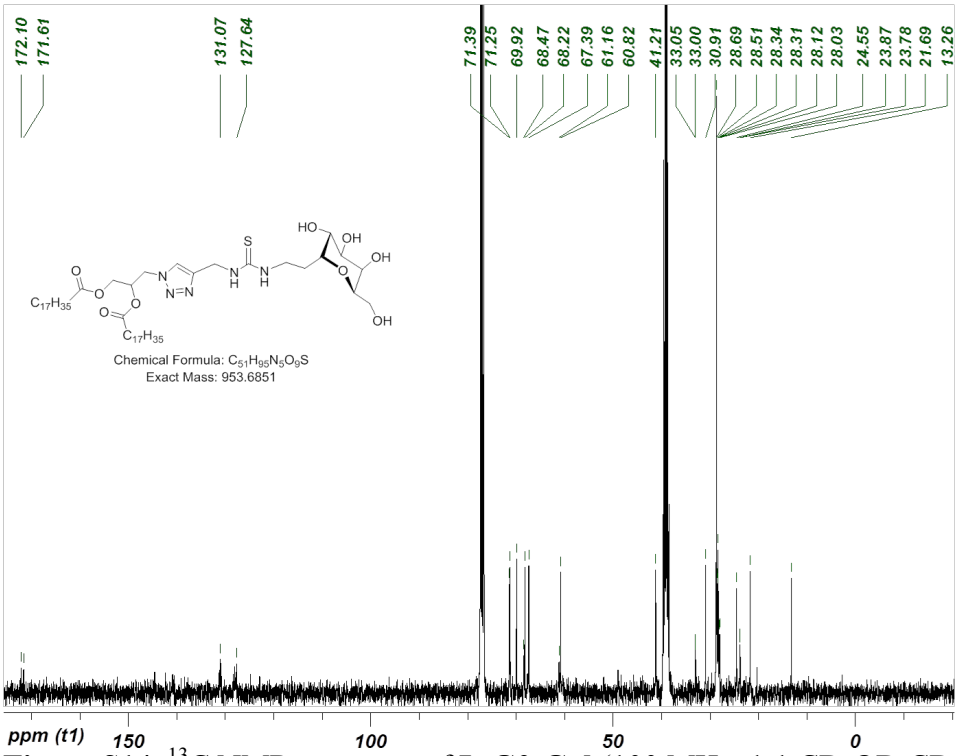


**Figure S14.** $^{13}$C NMR spectrum of **L-G0-Gal** (100 MHz, 1:1 $CD_3OD$:$CDCl_3$).

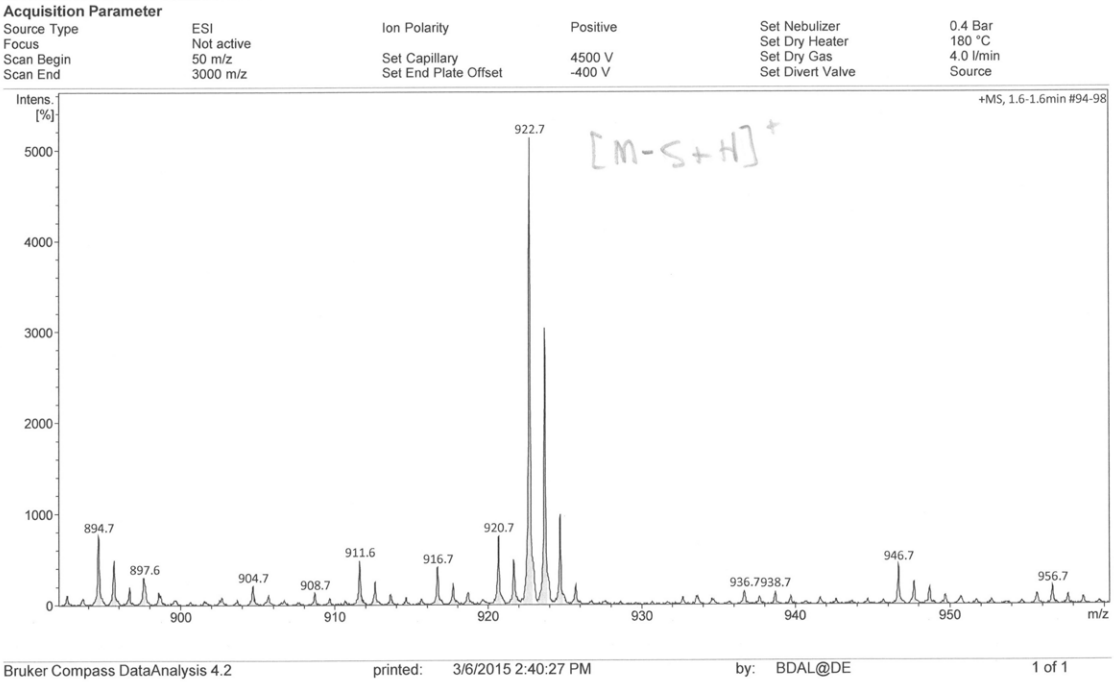


**Figure S15**. Mass spectrum of **L-G0-Gal** (ESI, THF). Fragmentation *via* loss of sulfur was confirmed by high resolution MS (Figure S16).

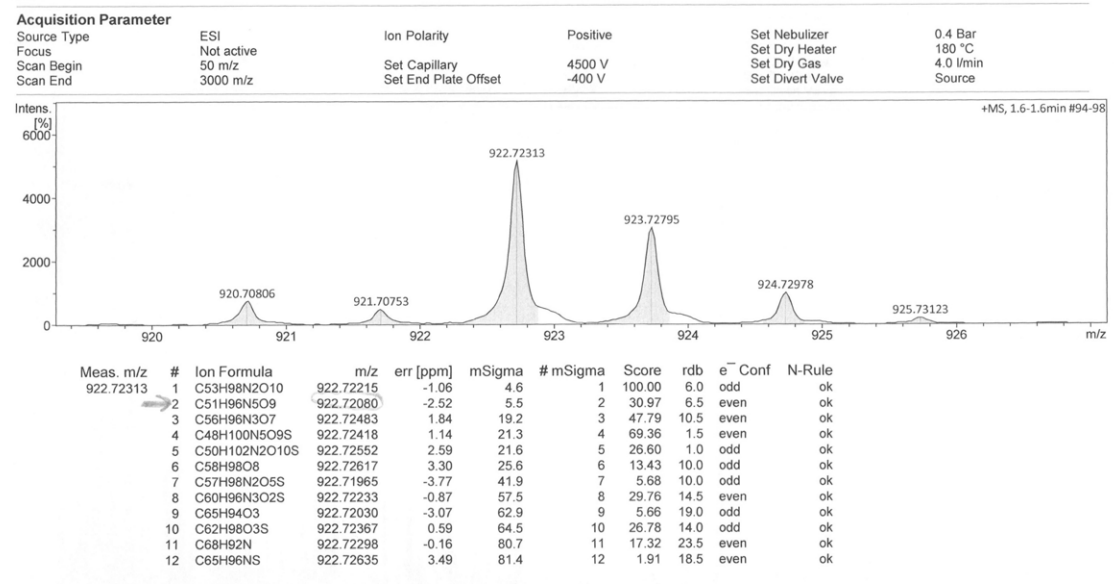


| Meas. m/z | # | Ion Formula | m/z | err [ppm] | mSigma | # mSigma | Score | rdb | e⁻ Conf | N-Rule |
|---|---|---|---|---|---|---|---|---|---|---|
| 922.72313 | 1 | C53H98N2O10 | 922.72215 | -1.06 | 4.6 | 1 | 100.00 | 6.0 | odd | ok |
| | 2 | C51H96N5O9 | 922.72080 | -2.52 | 5.5 | 2 | 30.97 | 6.5 | even | ok |
| | 3 | C56H96N3O7 | 922.72483 | 1.84 | 19.2 | 3 | 47.79 | 10.5 | even | ok |
| | 4 | C48H100N5O9S | 922.72418 | 1.14 | 21.3 | 4 | 69.36 | 1.5 | even | ok |
| | 5 | C50H102N2O10S | 922.72552 | 2.59 | 21.6 | 5 | 26.60 | 1.0 | odd | ok |
| | 6 | C58H98O8 | 922.72617 | 3.30 | 25.6 | 6 | 13.43 | 10.0 | odd | ok |
| | 7 | C57H98N2O5S | 922.71965 | -3.77 | 41.9 | 7 | 5.68 | 10.0 | odd | ok |
| | 8 | C60H96N3O2S | 922.72233 | -0.87 | 57.5 | 8 | 29.76 | 14.5 | even | ok |
| | 9 | C65H94O3 | 922.72030 | -3.07 | 62.9 | 9 | 5.66 | 19.0 | odd | ok |
| | 10 | C62H98O3S | 922.72367 | 0.59 | 64.5 | 10 | 26.78 | 14.0 | odd | ok |
| | 11 | C68H92N | 922.72298 | -0.16 | 80.7 | 11 | 17.32 | 23.5 | even | ok |
| | 12 | C65H96NS | 922.72635 | 3.49 | 81.4 | 12 | 1.91 | 18.5 | even | ok |

**Figure S16**. High resolution mass spectrum of **L-G0-Gal** (ESI, THF), confirming fragmentation via loss of sulfur.

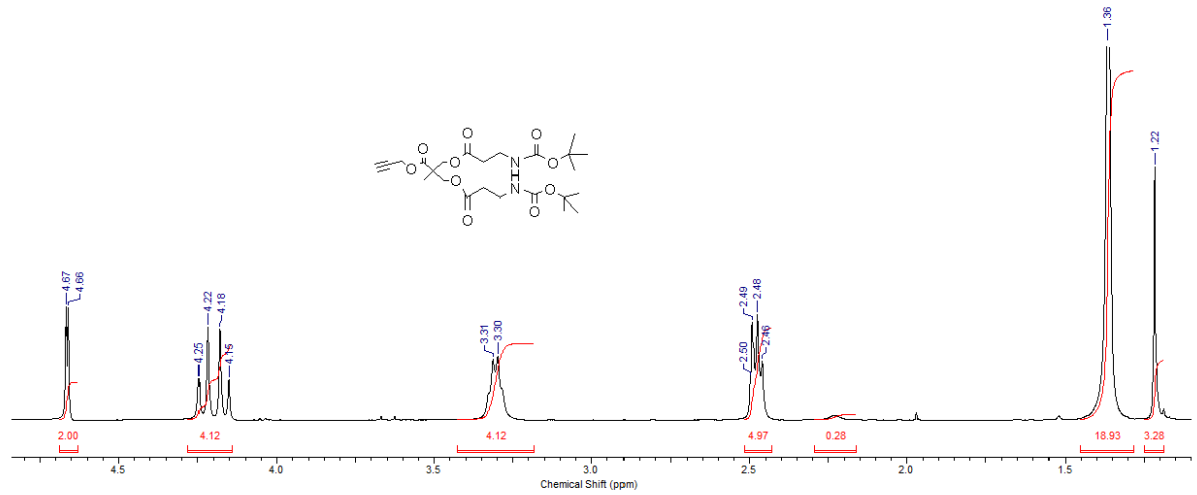


**Figure S17**. $^{1}$H NMR spectrum of **G1-NHBOC** (400 MHz, $CDCl_3$).

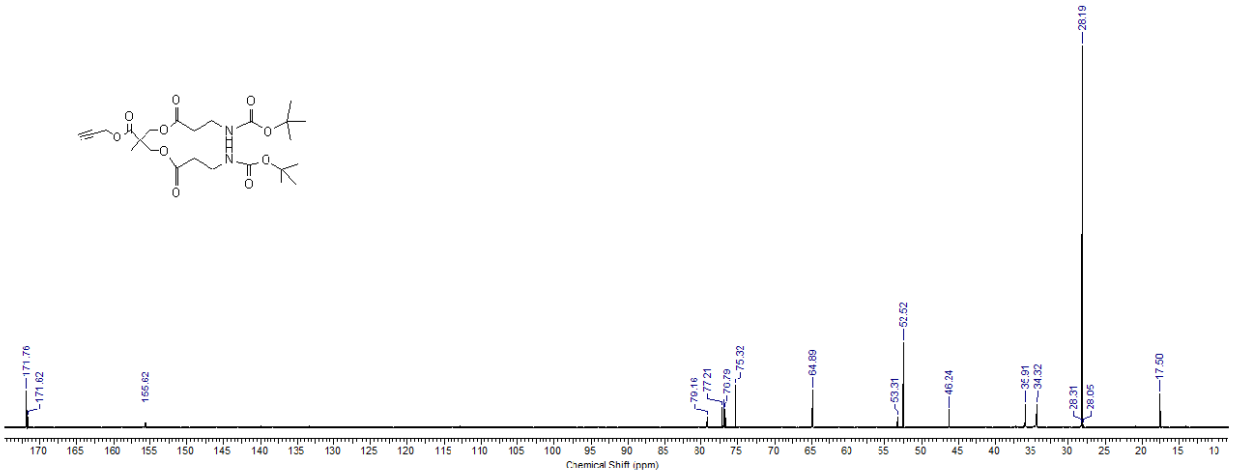


**Figure S18**. $^{13}$C NMR spectrum of **G1-NHBOC** (100 MHz, $CDCl_3$).

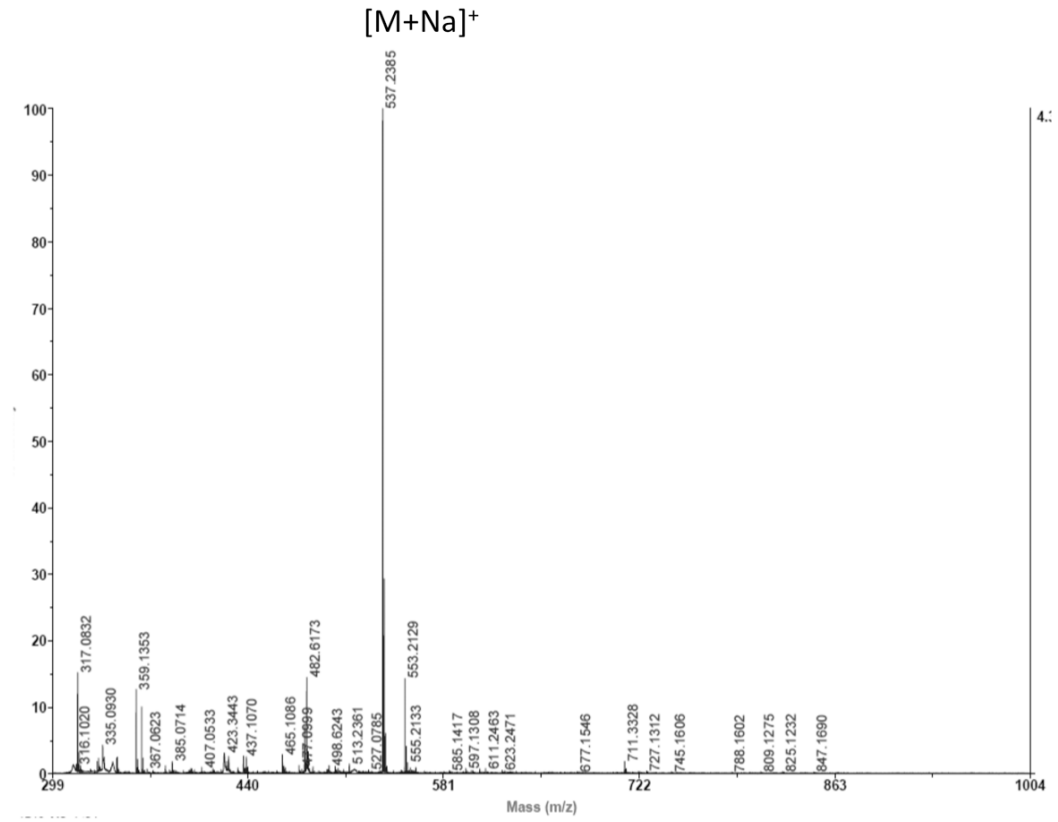


**Figure S19**. Mass spectrum of **G1-NHBOC** (MALDI, 7:3 $CH_3CN$:$H_2O$).

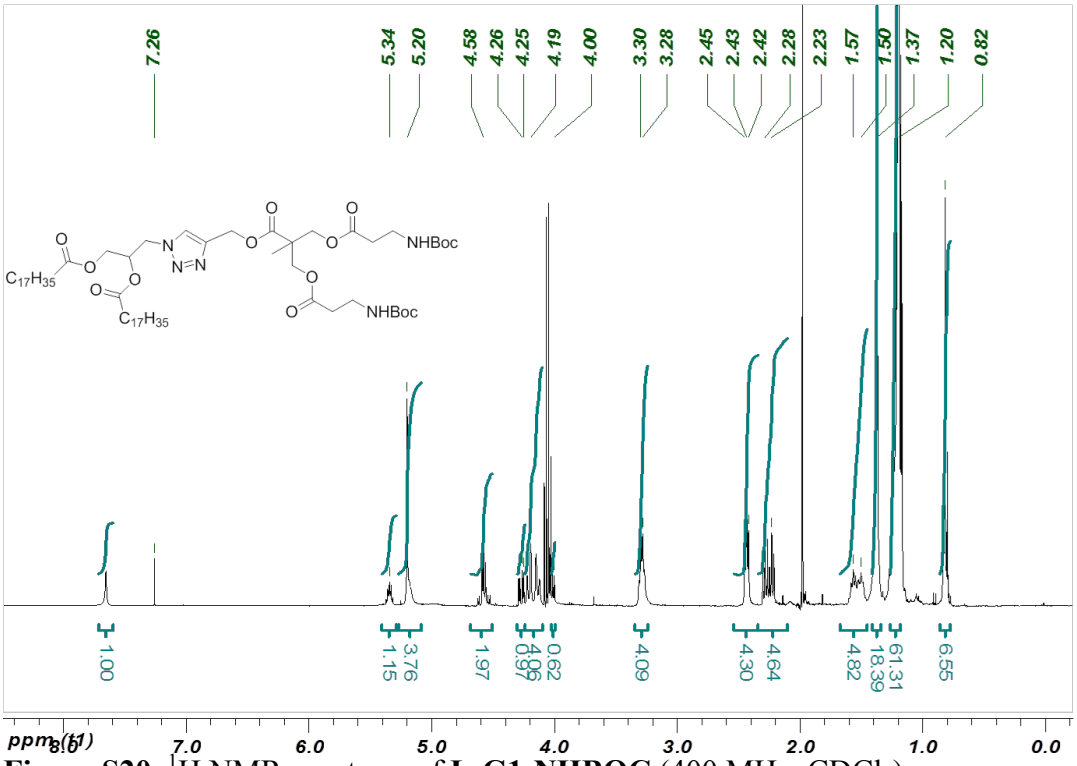


**Figure S20.** $^1$H NMR spectrum of **L-G1-NHBOC** (400 MHz, $CDCl_3$).

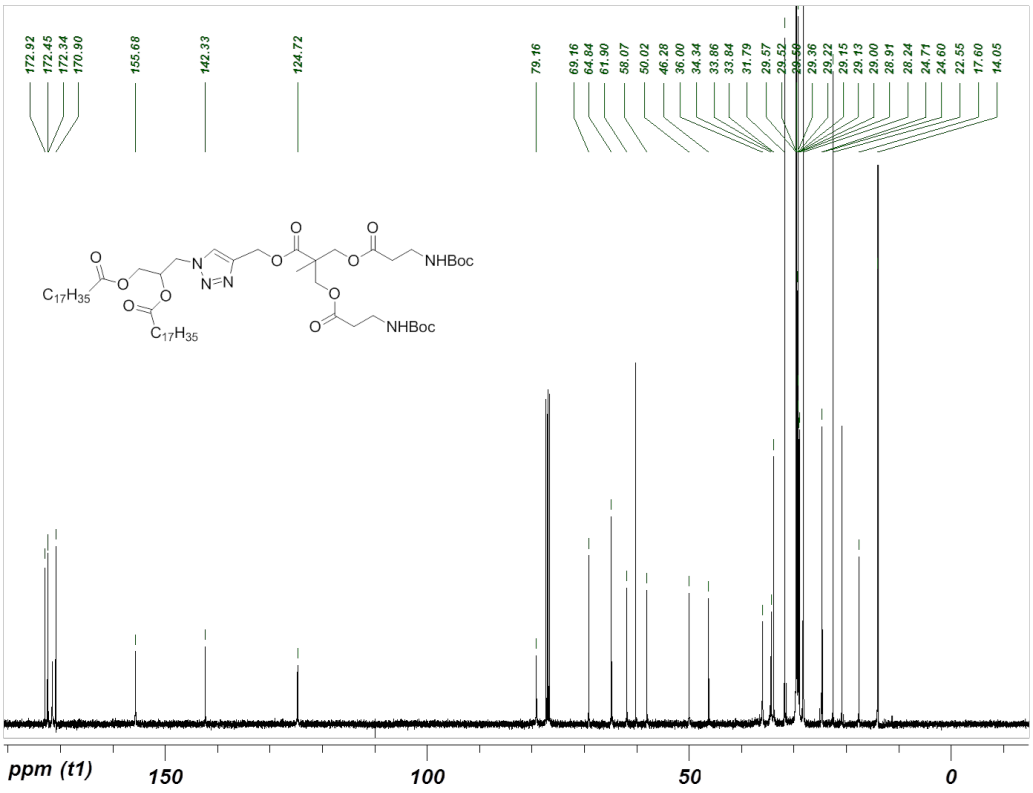


**Figure S21.** $^{13}C$ NMR spectrum of **L-G1-NHBOC** (100 MHz, $CDCl_3$).

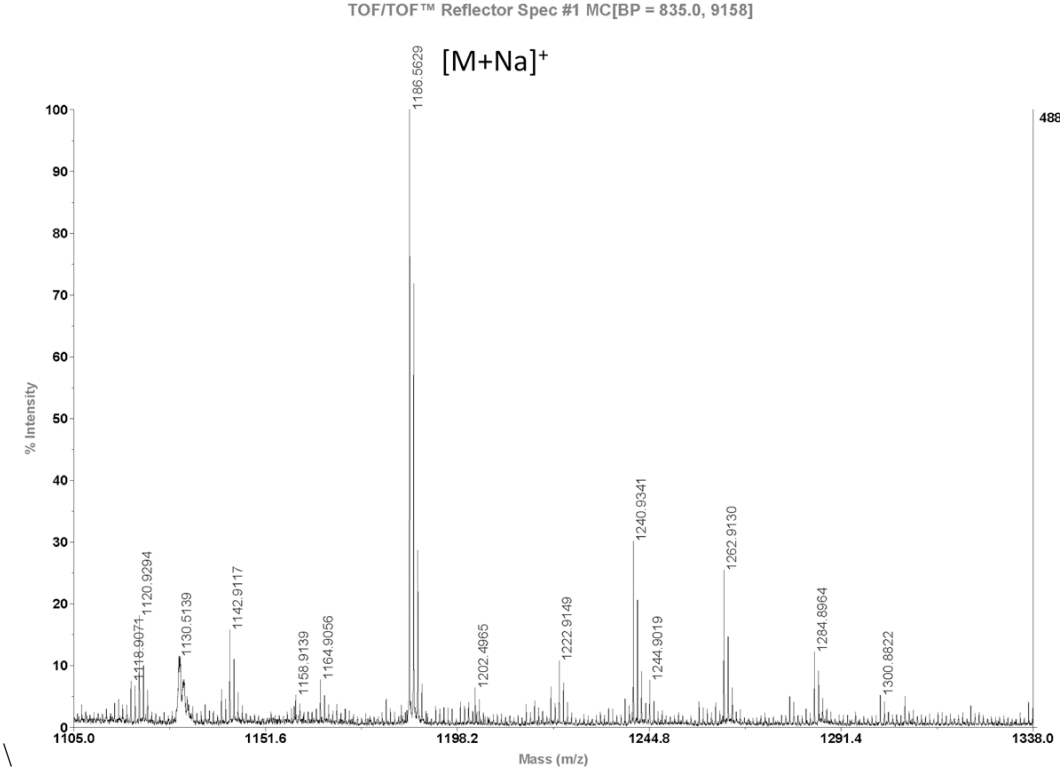


**Figure S22**. Mass spectrum of **L-G1-NHBOC** (MALDI, 1:1 $CH_3CN$:$H_2O$).

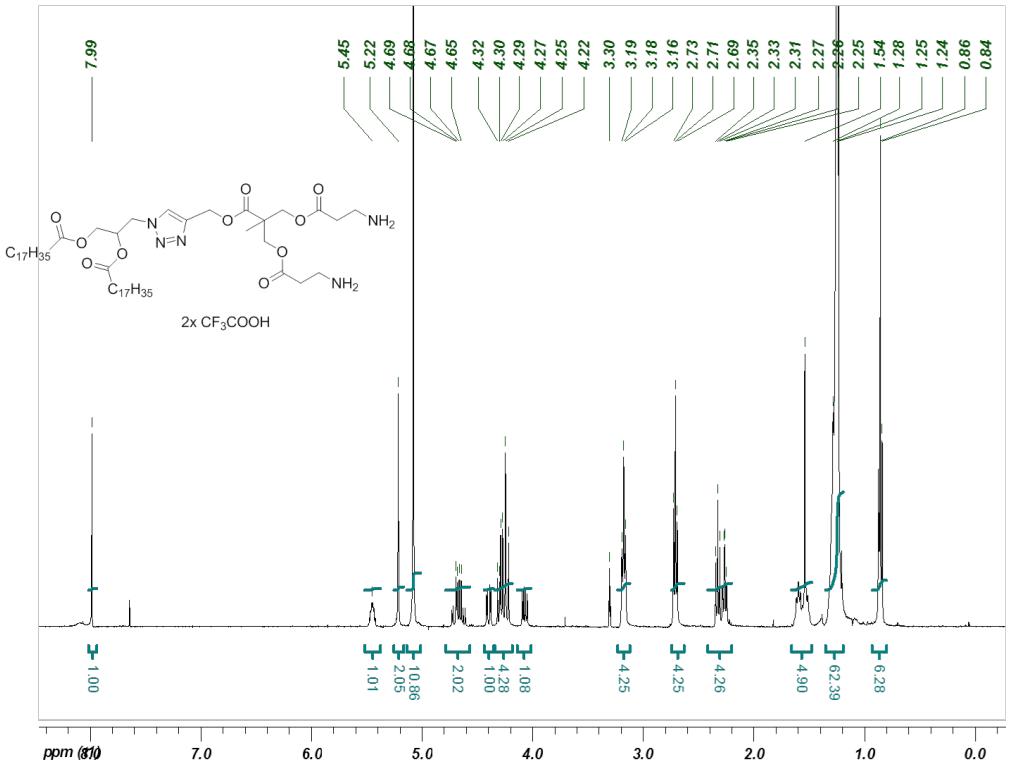


**Figure S23.** $^{1}$H NMR spectrum of **L-G1-NH$_2$** (400 MHz, 1:1 $CD_3OD$:$CDCl_3$).

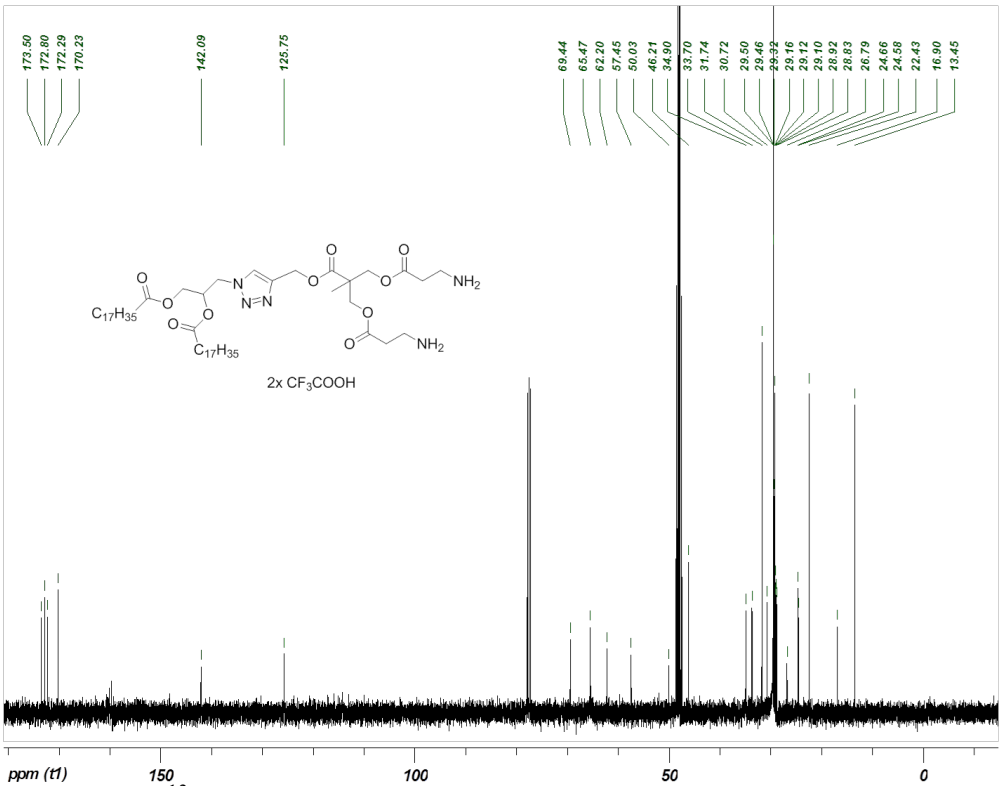


**Figure S24.** $^{13}$C NMR spectrum of **L-G1-NH$_2$** (100 MHz, 1:1 $CD_3OD$:$CDCl_3$).

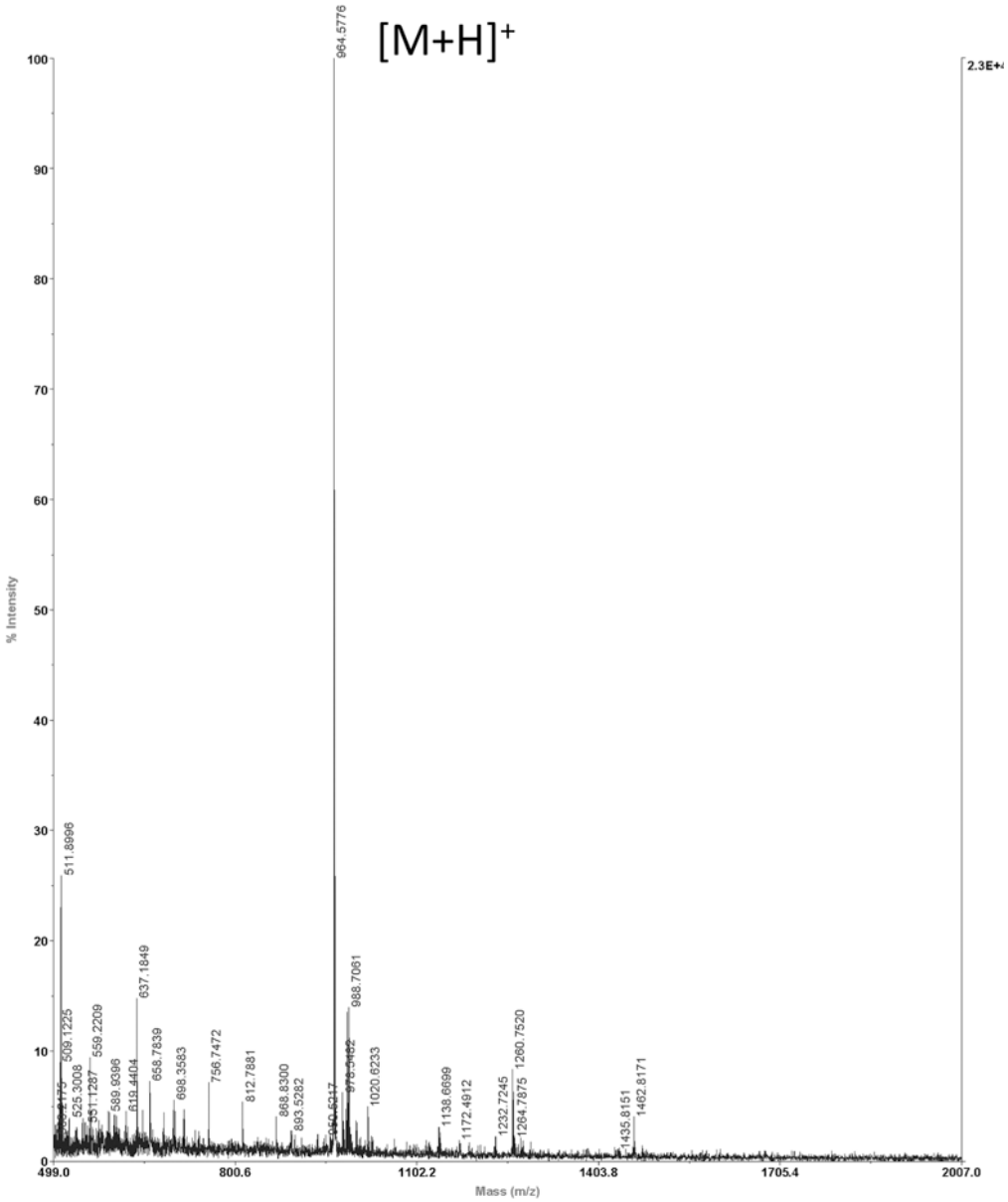


**Figure S25**. Mass spectrum of **L-G1-NH$_2$** (MALDI, 7:3 $CH_3CN$:$H_2O$).

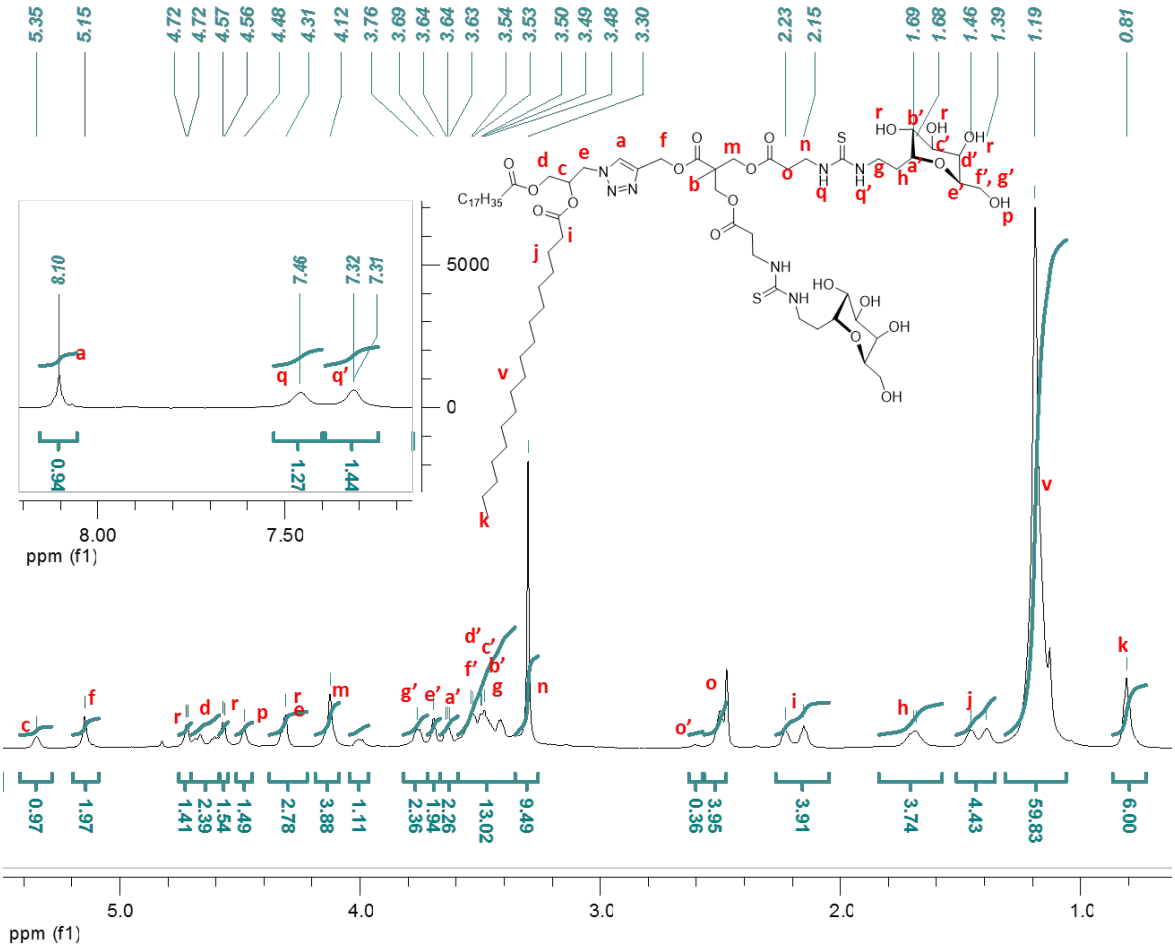


**Figure S26.** $^{1}$H NMR spectrum of **L-G1-Gal** (400 MHz, $(CD_3)_2SO$). The extent of functionalization of the amines with α-Gal was calculated to be 92% based on the ratio of the integrations of the peaks labelled o and o', where o' corresponds to protons on an unfunctionalized β-alanine moiety (with the amine in its protonated form).

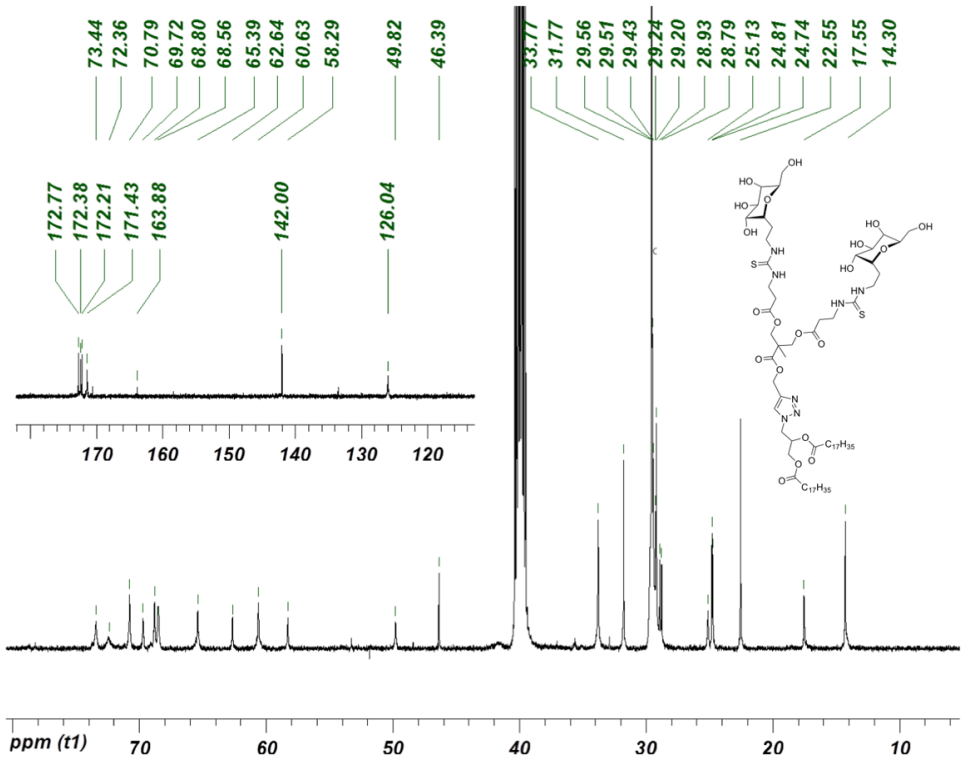


**Figure S27.** $^{13}$C NMR spectrum of **L-G1-Gal** (100 MHz, 1:1 $CD_3CN$:$CDCl_3$).

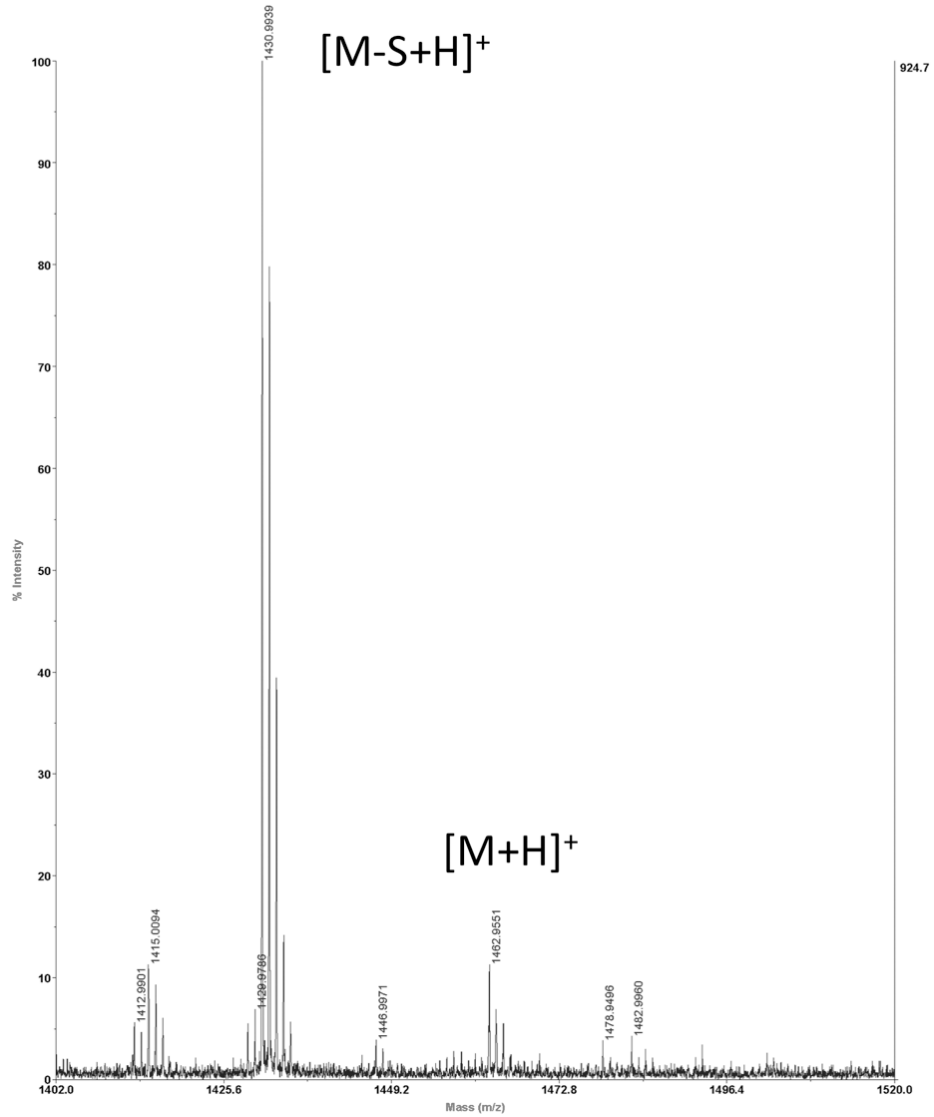


**Figure S28**. Mass spectrum of **L-G1-Gal** (MALDI, 1:1 EtOH:$H_2O$).

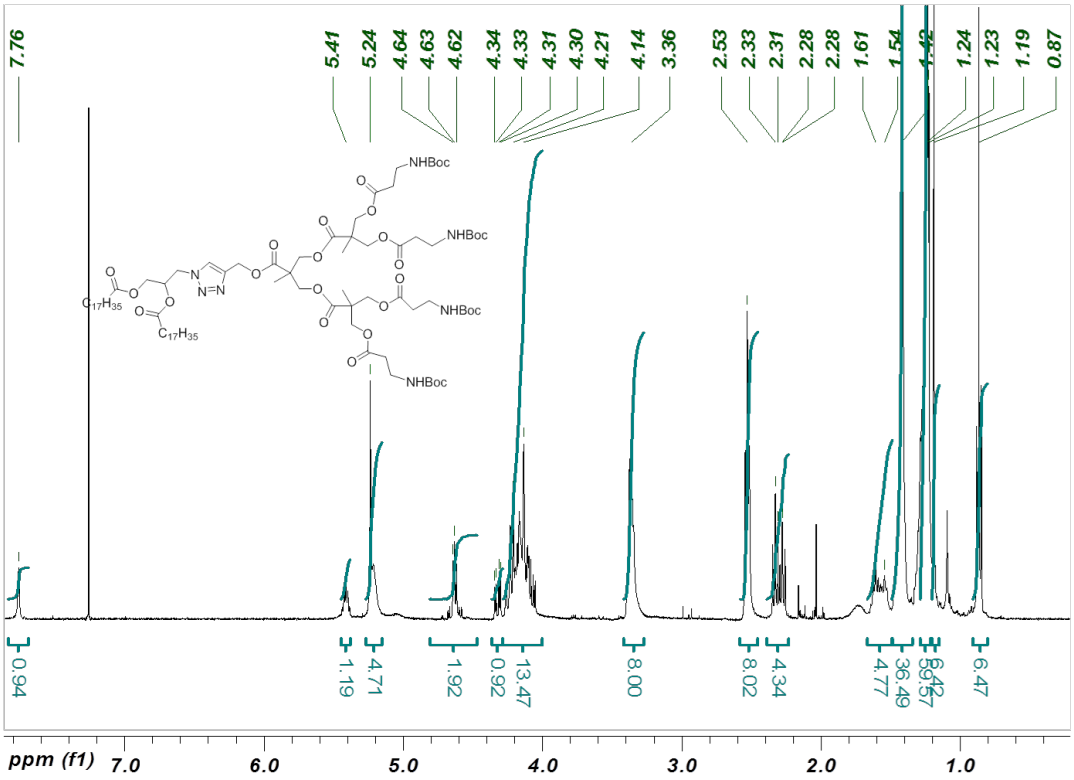


**Figure S29.** $^{1}$H NMR spectrum of **L-G2-NHBOC** (400 MHz, $CDCl_3$).

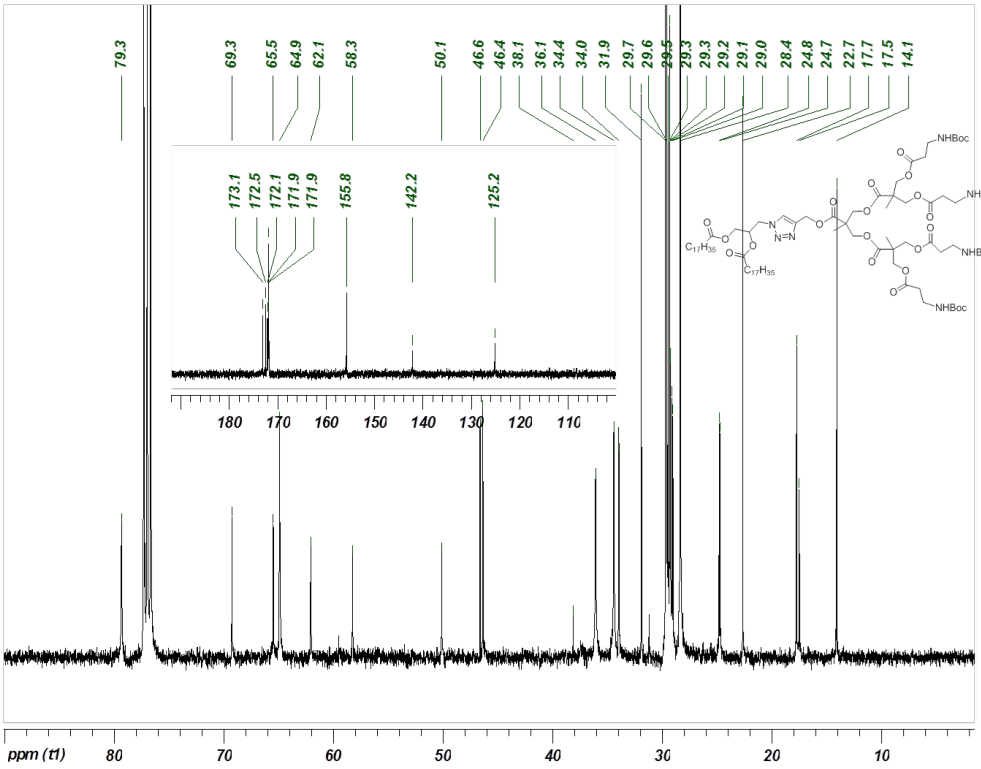


**Figure S30.** $^{13}$C NMR spectrum of **L-G2-NHBOC** (100 MHz, $CDCl_3$).

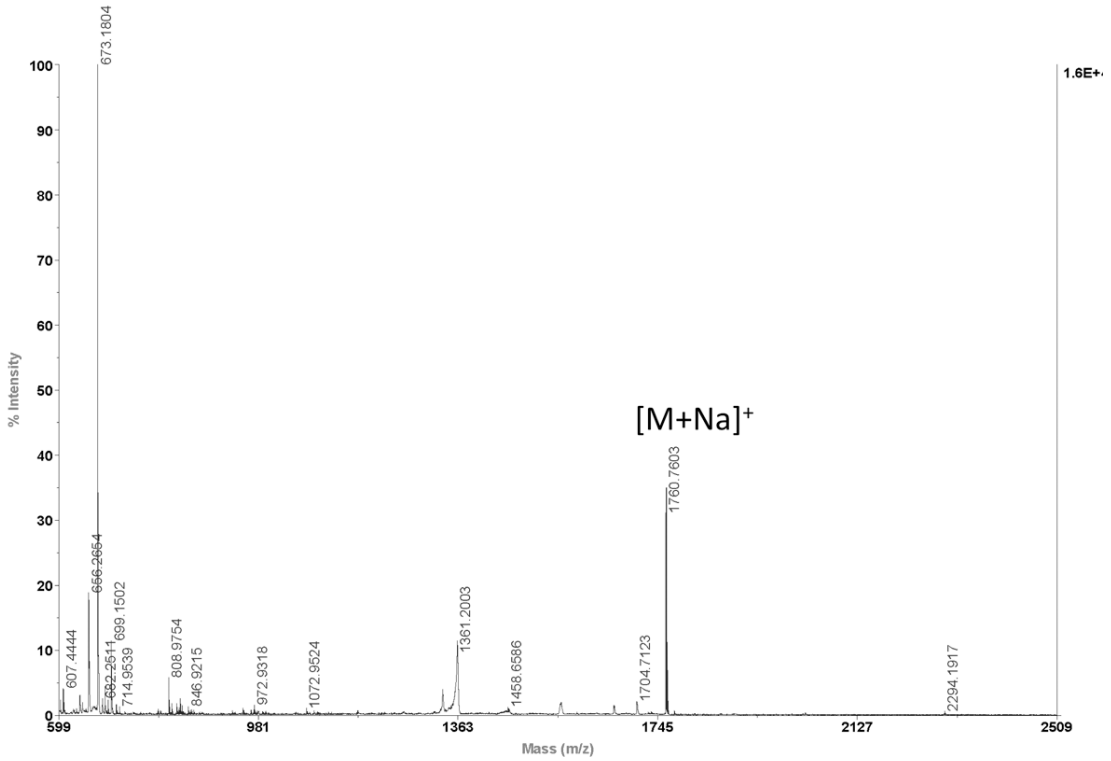


**Figure S31**. Mass spectrum of **L-G2-NHBOC** (MALDI, 1:1 $CH_3CN$:$H_2O$).

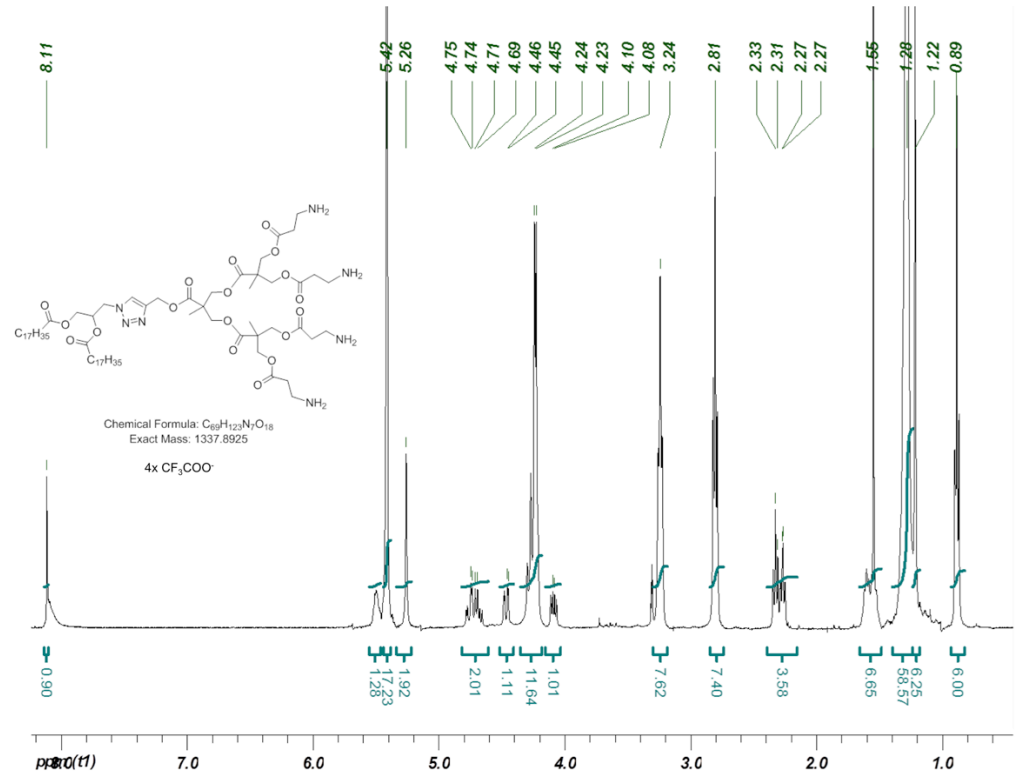


**Figure S32.** $^1$H NMR spectrum of **L-G2-NH$_2$** (400 MHz, $CD_3OD$).

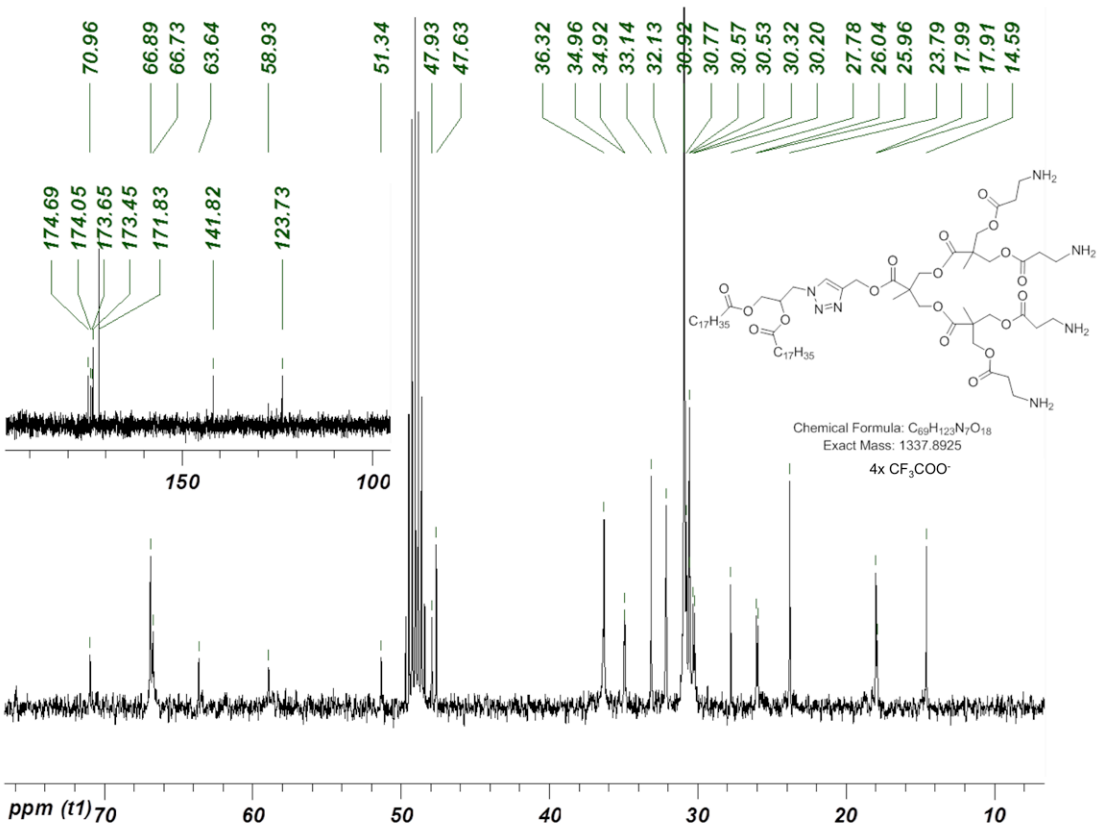


**Figure S33.** $^{13}$C NMR spectrum of **L-G2-NH$_2$** (100 MHz, $CD_3OD$).

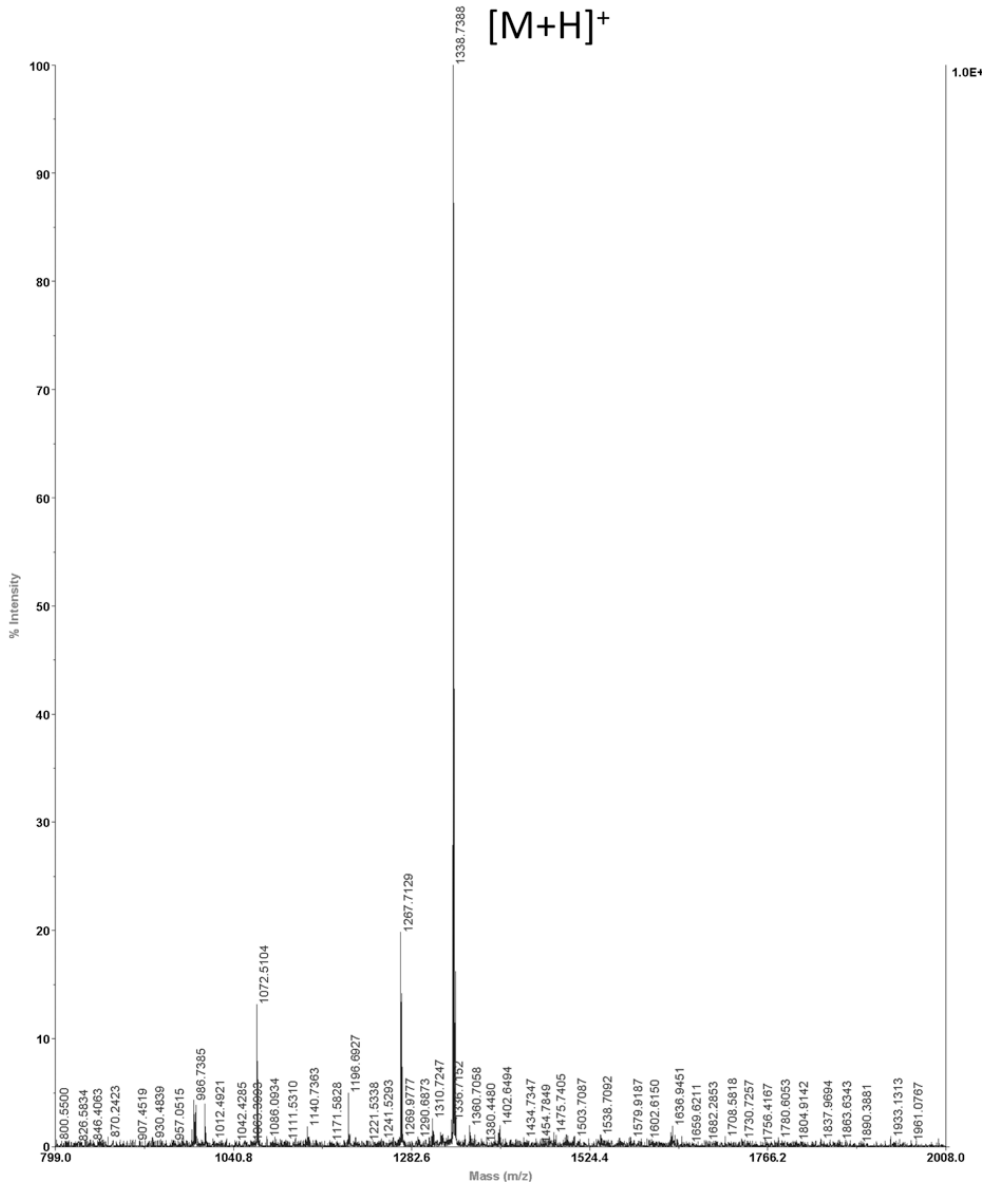


**Figure S34**. Mass spectrum of **L-G2-NH$_2$** (MALDI, 7:3 $CH_3CN$:$H_2O$).

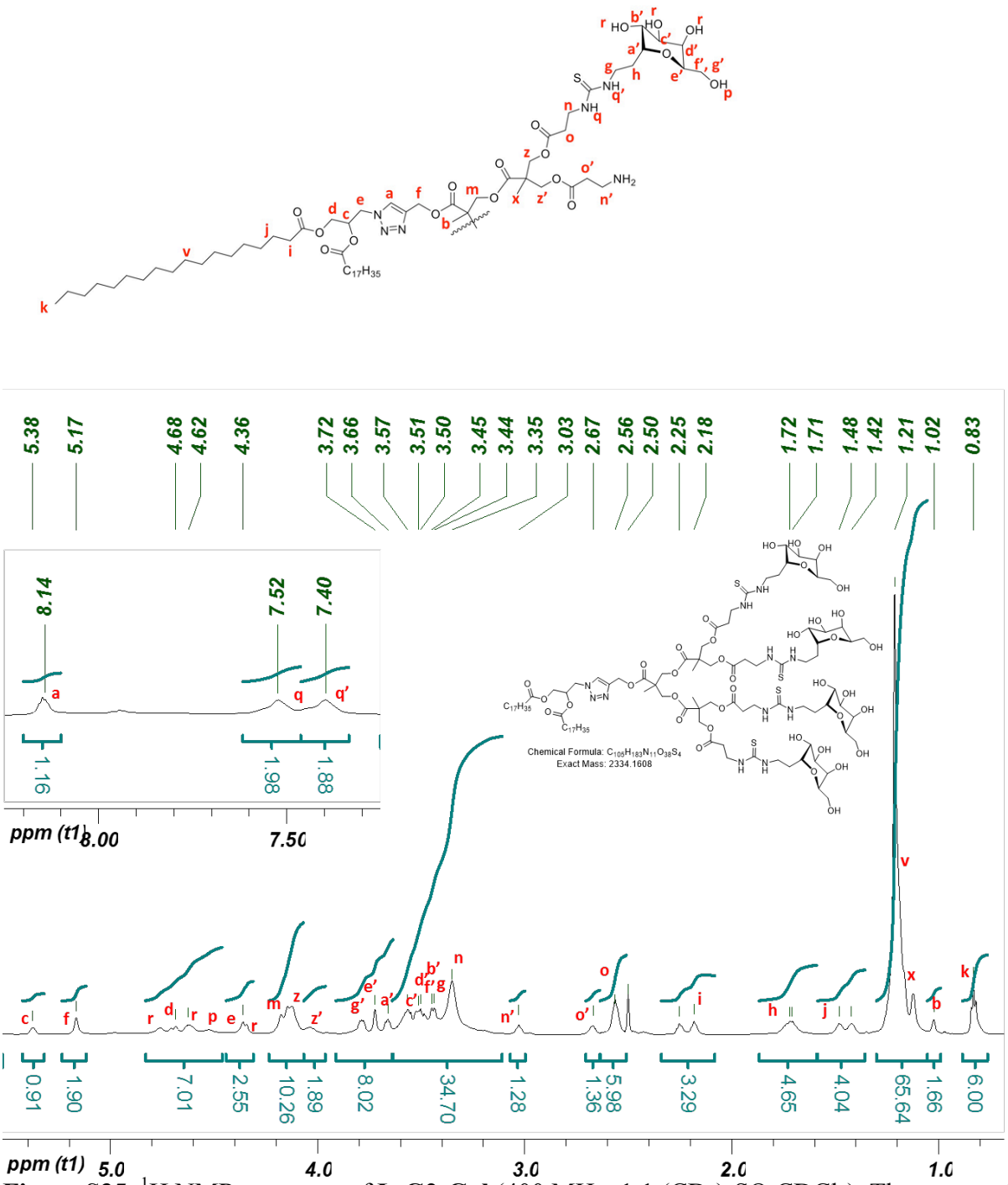


**Figure S35.** $^{1}$H NMR spectrum of **L-G2-Gal** (400 MHz, 1:1 $(CD_3)_2SO$:$CDCl_3$). The extent of functionalization of the amines with α-Gal was calculated to be 81% based on the ratio of the integrations of the peaks labelled o and o', where o' corresponds to protons on an unfunctionalized β-alanine moiety (with the amine in its protonated form).

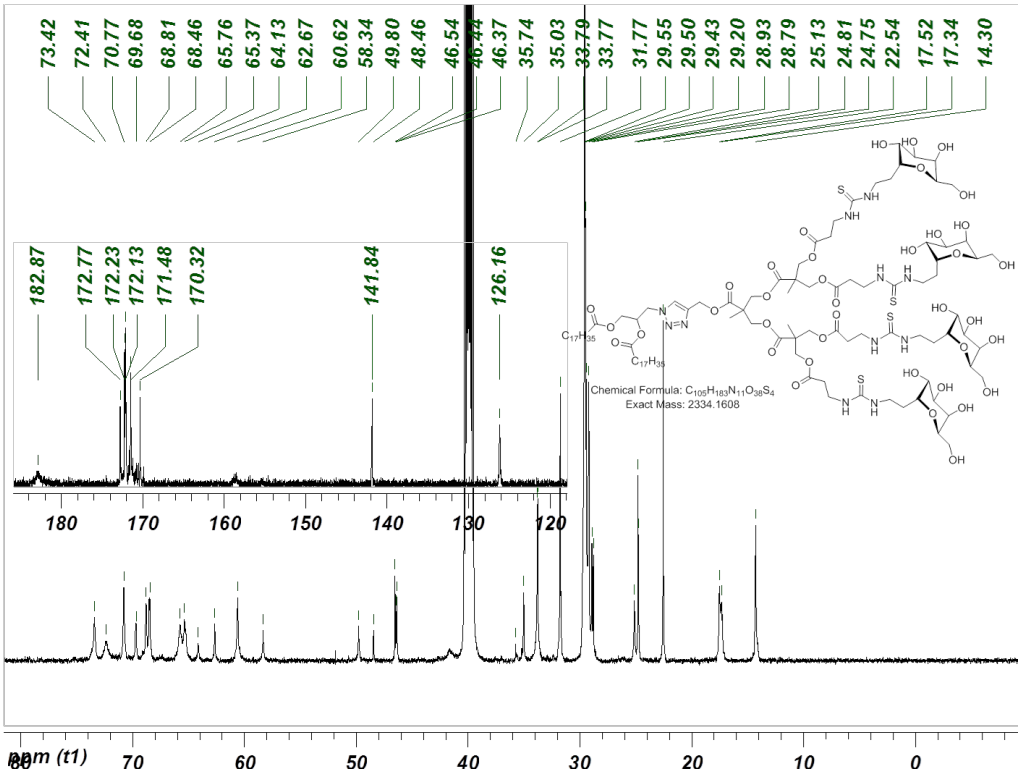


**Figure S36.** $^{13}C$ NMR spectrum of **L-G2-Gal** (100 MHz, 1:1 $(CD_3)_2SO$:$CDCl_3$).

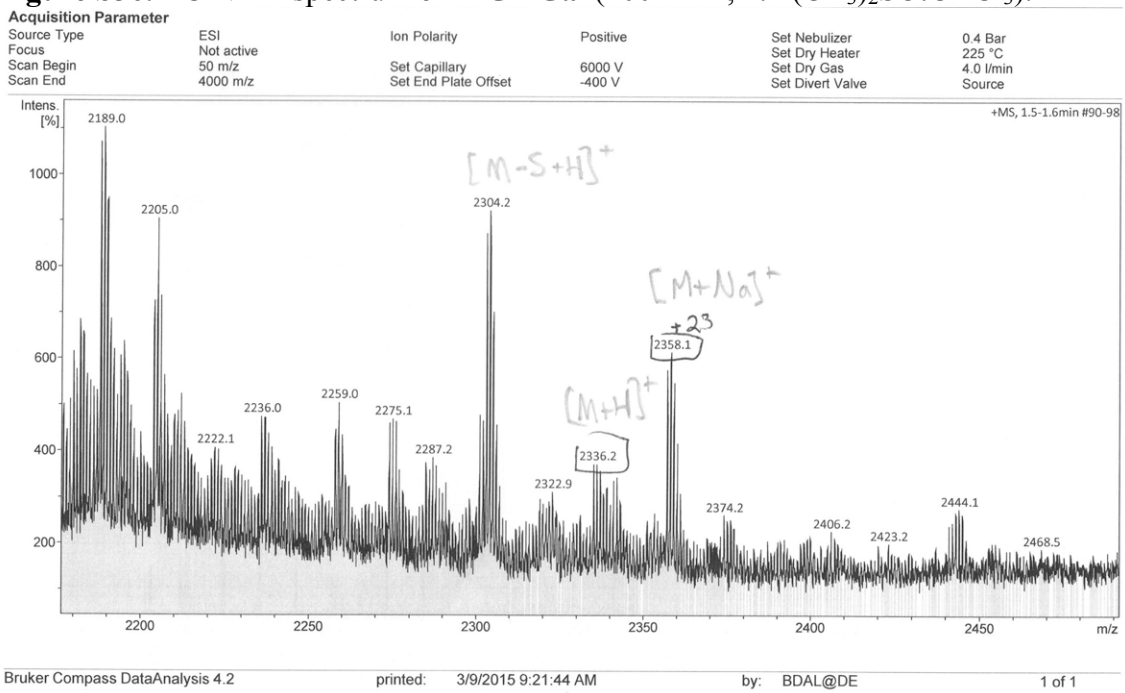


**Figure S37**. Mass spectrum of **L-G2-Gal** (ESI, MeOH).

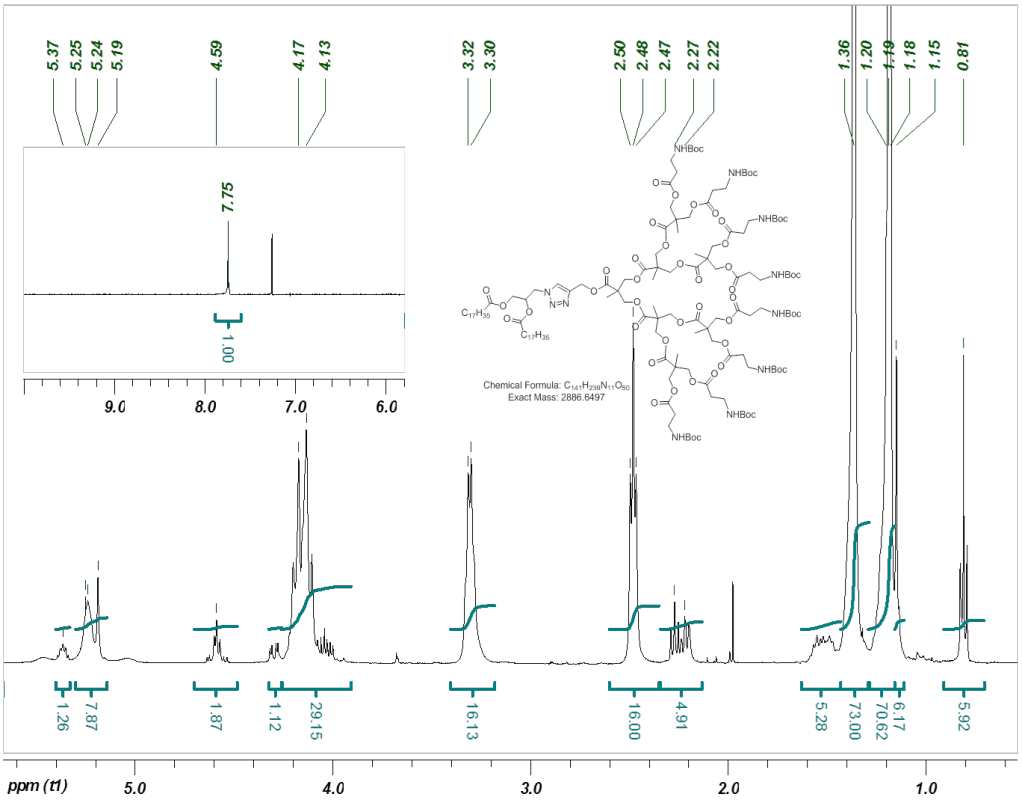


**Figure S38.** $^{1}$H NMR spectrum of **L-G3-NHBOC** (400 MHz, $CDCl_3$).

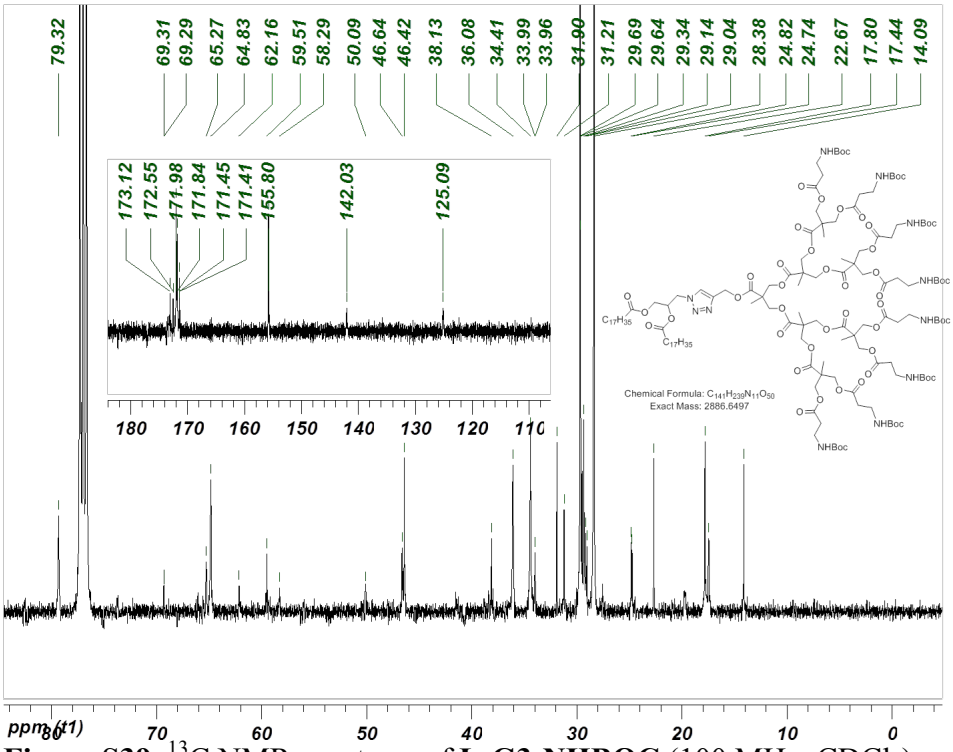


**Figure S39.** $^{13}$C NMR spectrum of **L-G3-NHBOC** (100 MHz, $CDCl_3$).

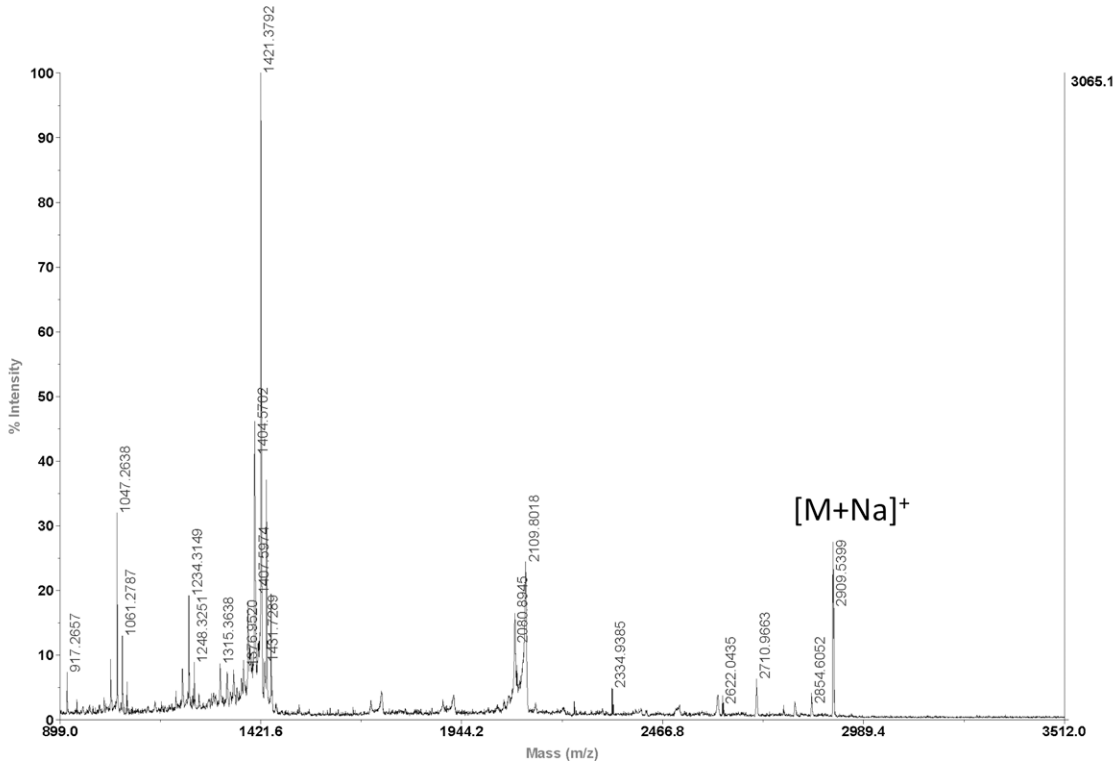


**Figure 40**. Mass spectrum of **L-G3-NHBOC** (MALDI, 7:3 $CH_3CN$:$H_2O$).

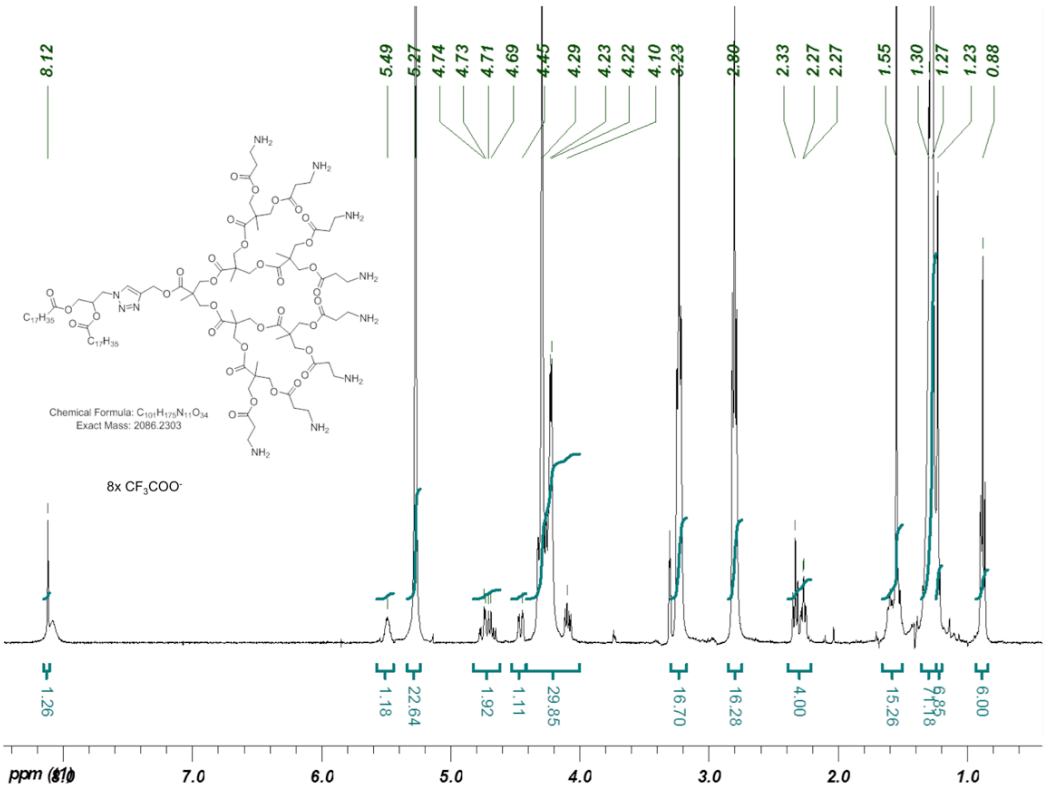


**Figure S41.** $^1$H NMR spectrum of **L-G3-$NH_2$** (400 MHz, 1:1 $(CD_3)_2CO$:$CDCl_3$).

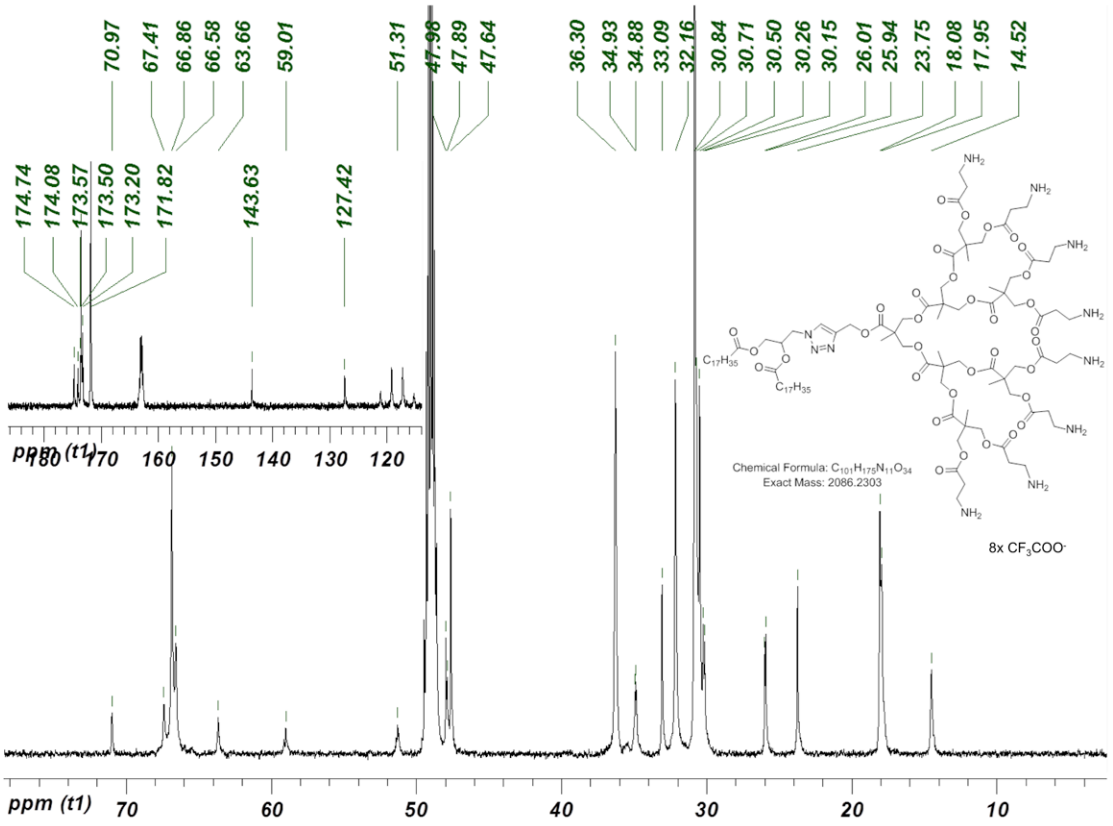


**Figure S42.** $^{13}$C NMR spectrum of **L-G3-NH$_2$** (150 MHz, $CD_3OD$).

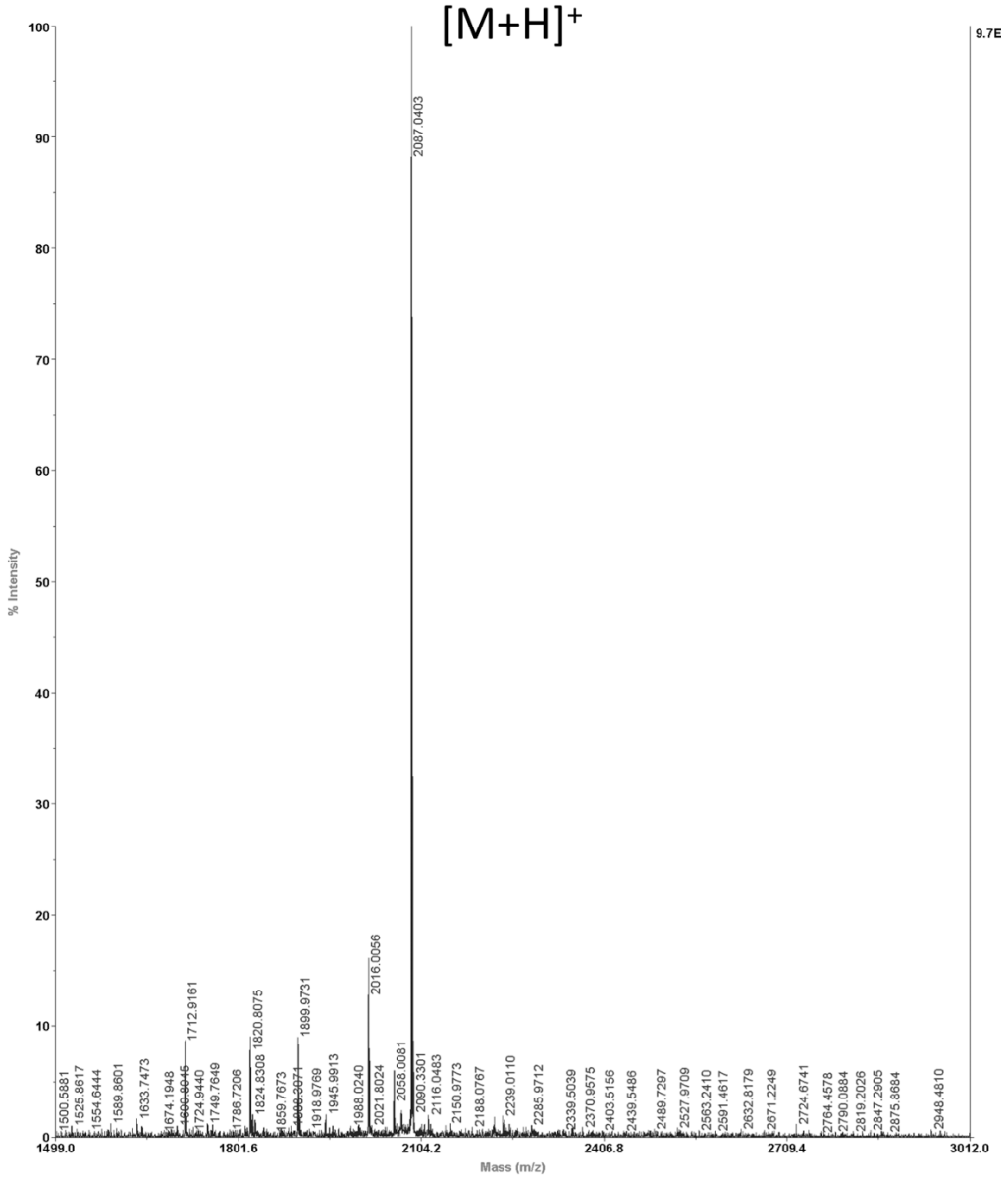


**Figure S43**. Mass spectrum of **L-G3-$NH_2$** (MALDI, 1:1 $CH_3CN$:$H_2O$).

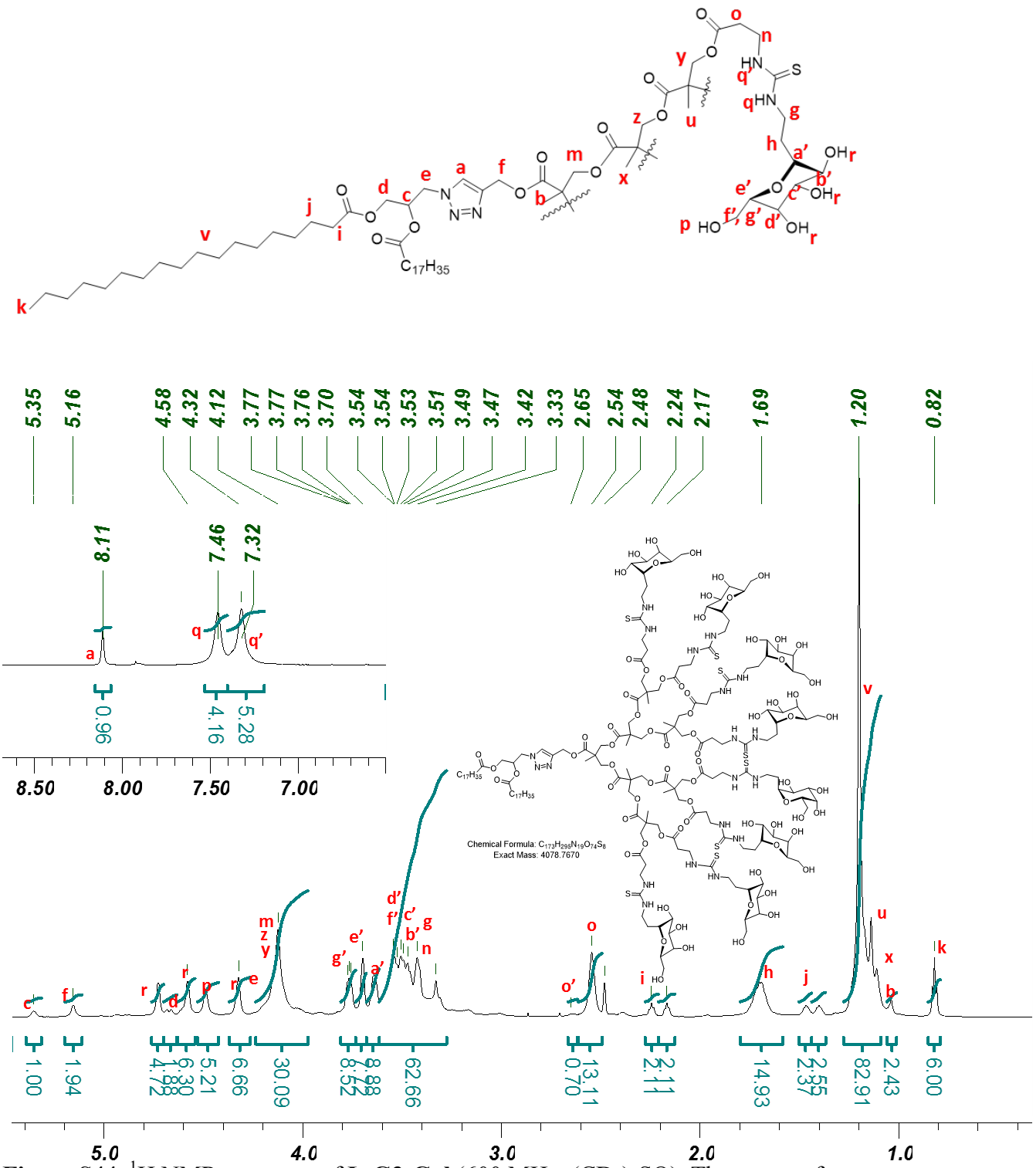


**Figure S44.** $^{1}$H NMR spectrum of **L-G3-Gal** (600 MHz, $(CD_3)_2SO$). The extent of functionalization of the amines with α-Gal was calculated to be 95% based on the ratio of the integrations of the peaks labelled o and o', where o' corresponds to protons on an unfunctionalized β-alanine moiety (with the amine in its protonated form).

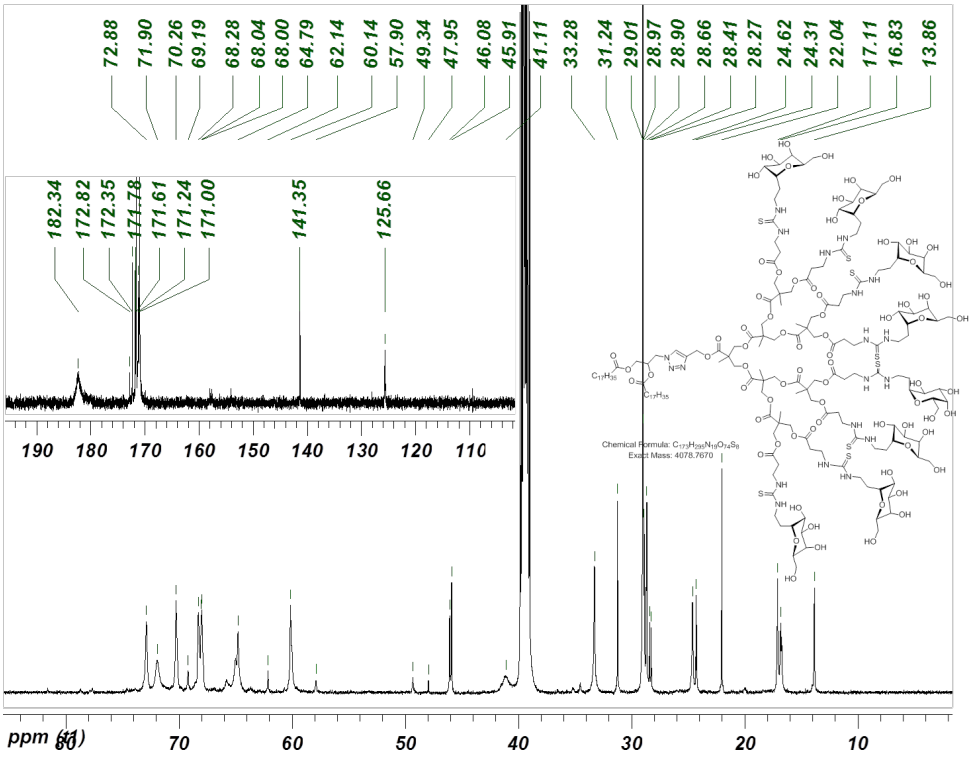

**Figure S45.** $^{13}$C NMR spectrum of **L-G3-Gal** (100 MHz, $(CD_3)_2SO$).

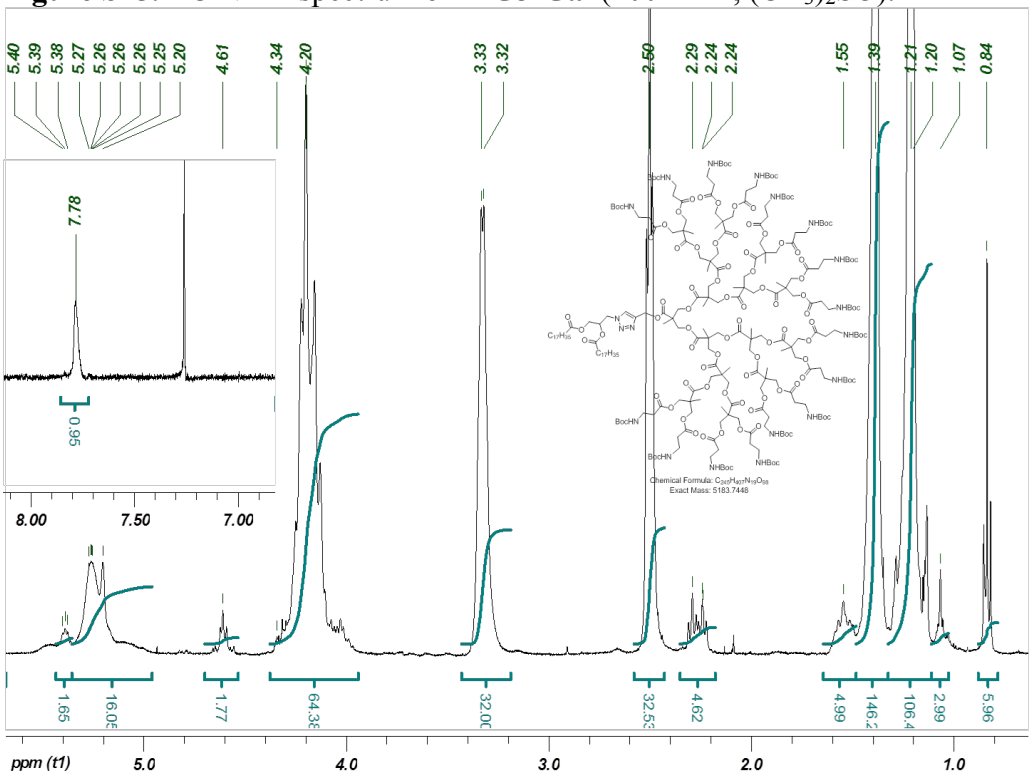

**Figure S46.** $^{1}$H NMR spectrum of **L-G4-NHBOC** (400 MHz, $CDCl_3$).

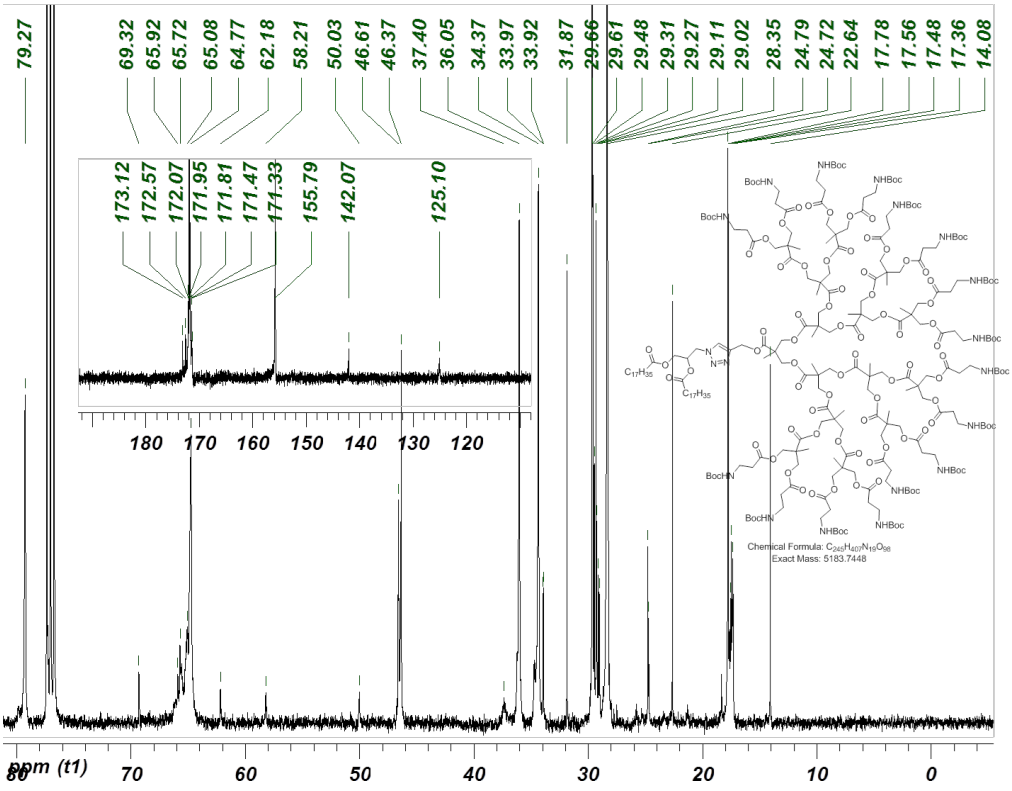


**Figure S47.** $^{13}C$ NMR spectrum of **L-G4-NHBOC** (100 MHz, $CDCl_3$).

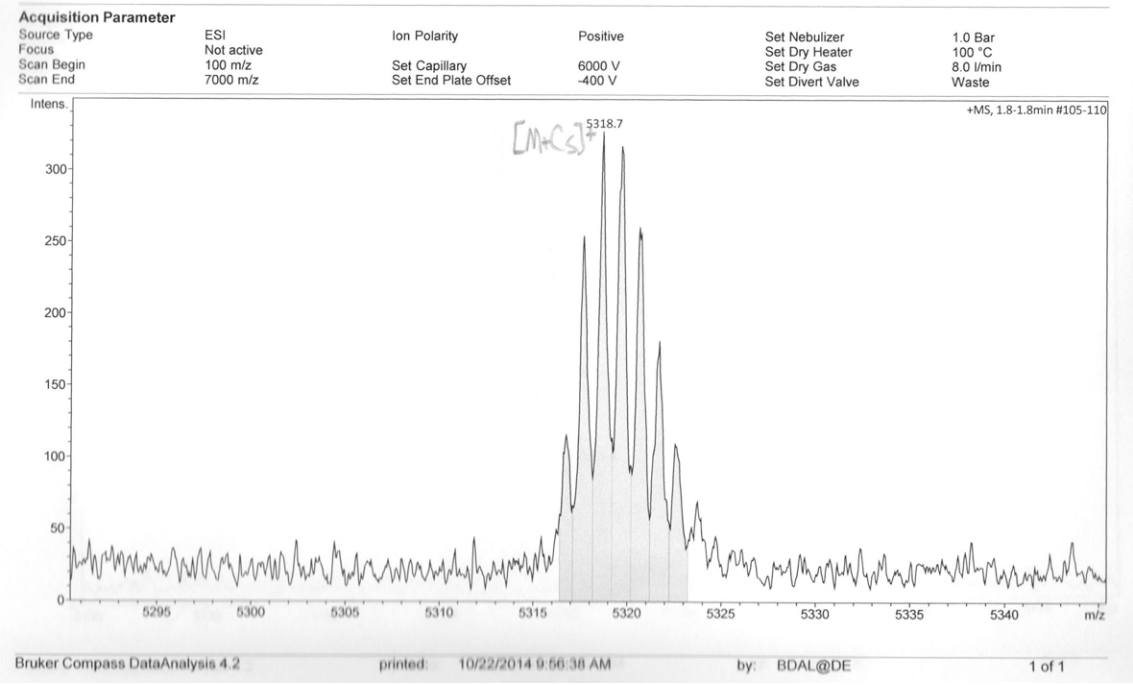


**Figure S48**. Mass spectrum of **L-G4-NHBOC** (ESI, 1:1 $CH_2Cl_2$:MeOH).

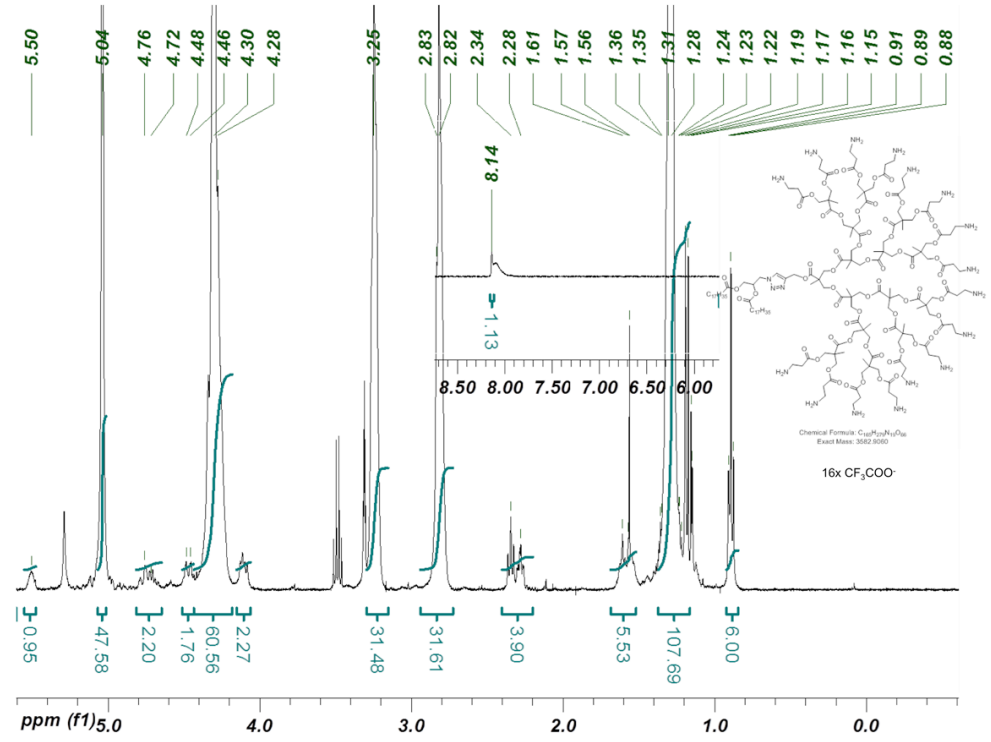


**Figure S49.** $^{1}$H NMR spectrum of **L-G4-NH$_2$** (400 MHz, $CD_3OD$).

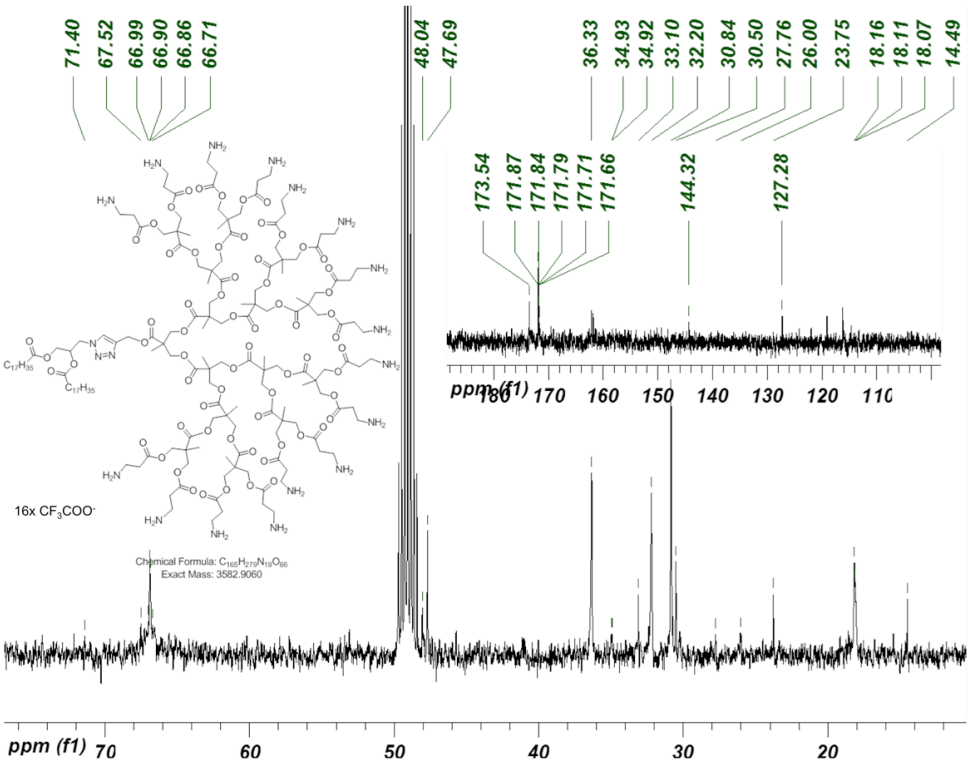


**Figure S50.** $^{13}$C NMR spectrum of **L-G4-NH$_2$** (100 MHz, $CD_3OD$).

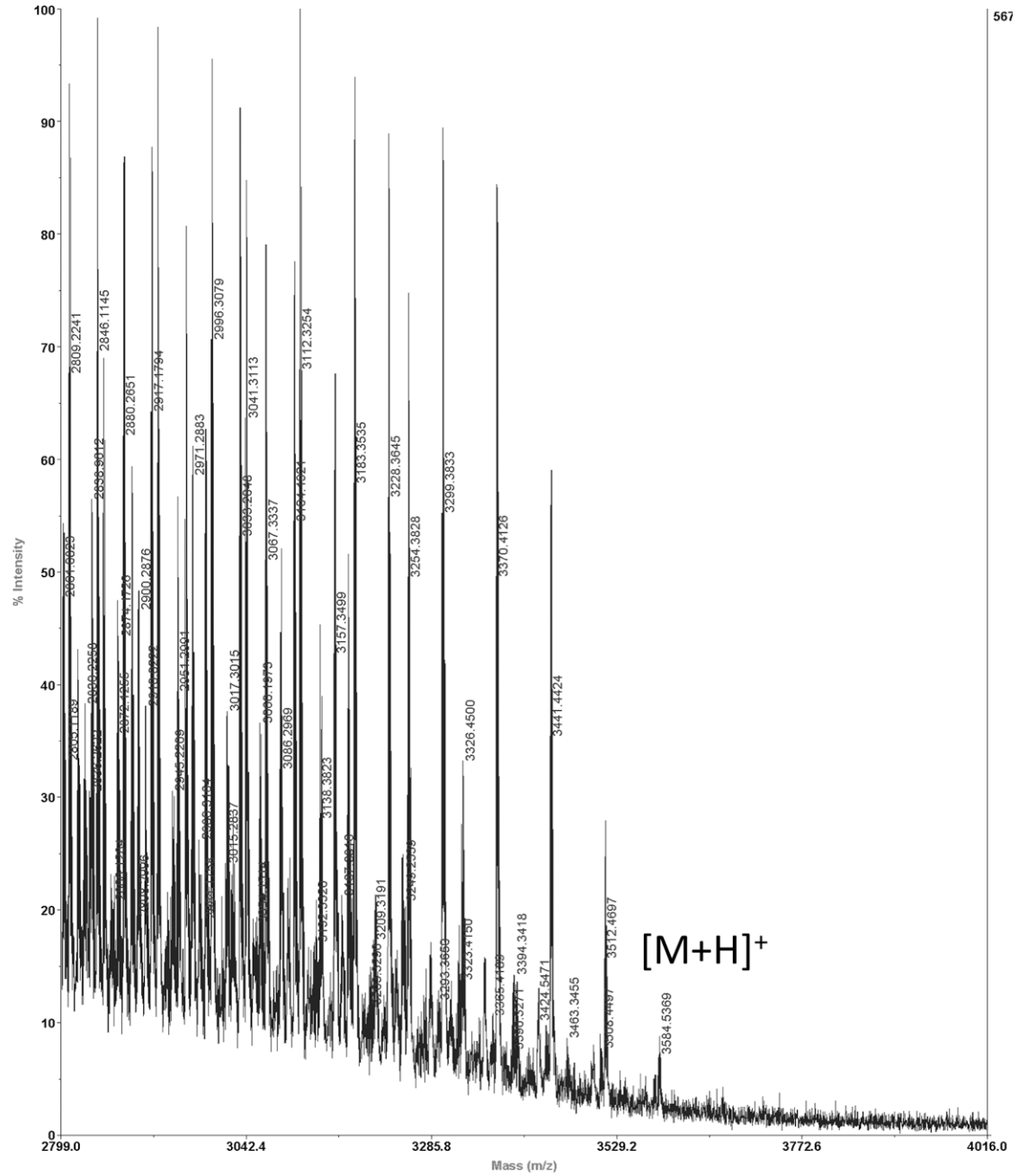


**Figure S51**. Mass spectrum of **L-G4-NH$_2$** (MALDI, 7:3 $CH_3CN$:$H_2O$). Note that fragmentation corresponds to loss of $C(O)CH_2CH_2NH_2$ groups (72 g/mol) from the dendron periphery as these esters are susceptible to cyclization and other cleavage mechanisms. No signals are observed at lower laser power, while higher laser power leads to more fragmentation.

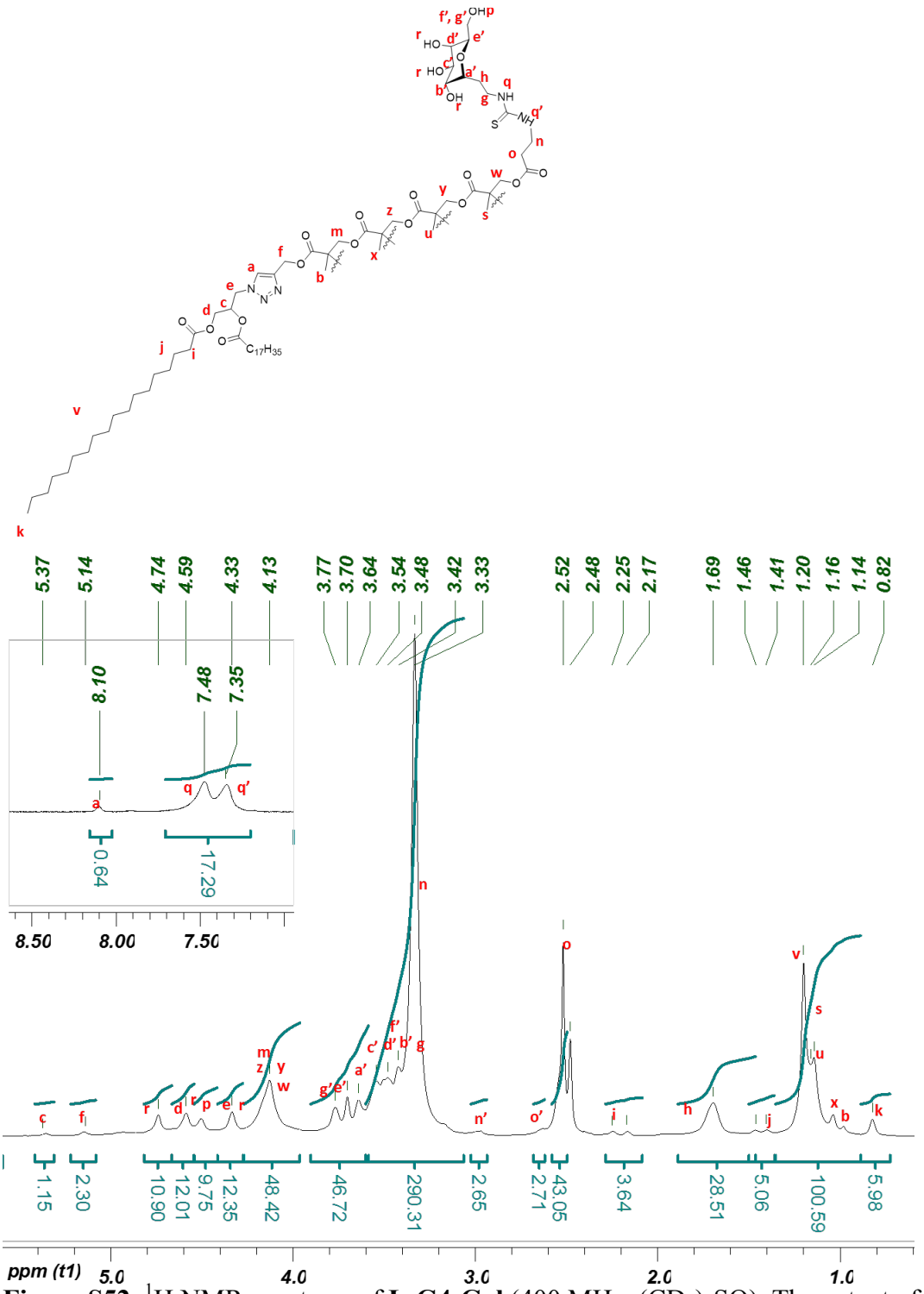


**Figure S52.** $^{1}$H NMR spectrum of **L-G4-Gal** (400 MHz, $(CD_3)_2SO$). The extent of functionalization of the amines with α-Gal was calculated to be 92% based on the ratio of the integrations of the peaks labelled o and o', where o' corresponds to protons on an unfunctionalized β-alanine moiety (with the amine in its protonated form). Although some overlap with the residual DMSO peak is observed, this analysis is also quite consistent with the analysis based on the ratio of the integrals of peaks h to k (89%).

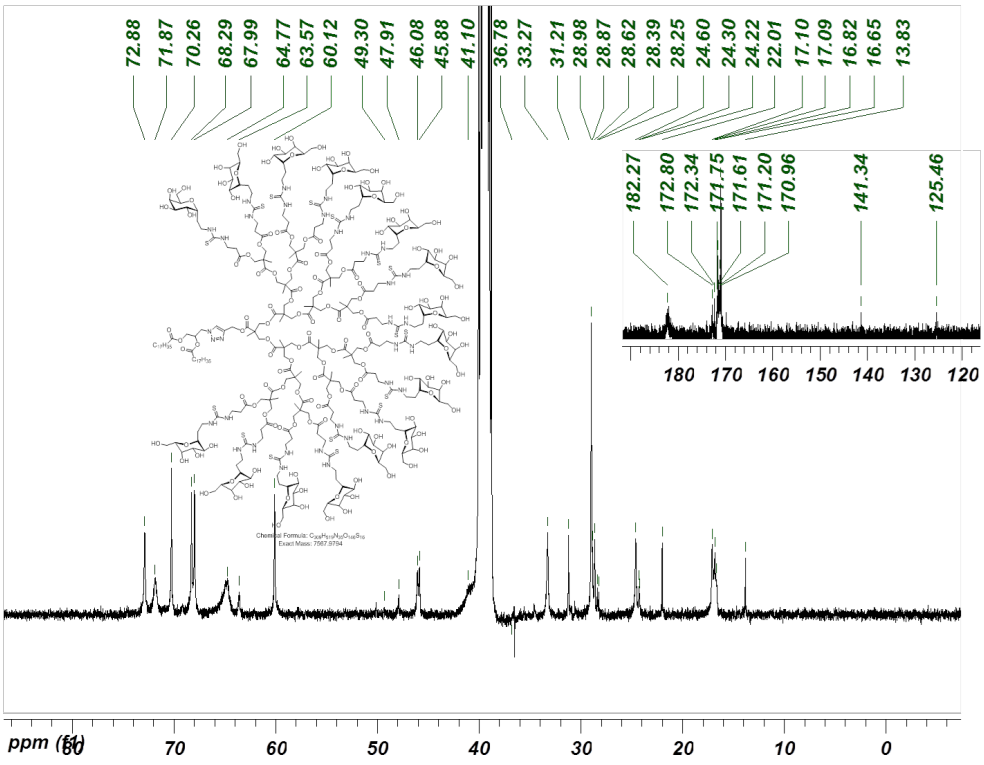


**Figure S53.** $^{13}$C NMR spectrum of **L-G4-Gal** (100 MHz, $(CD_3)_2SO$).

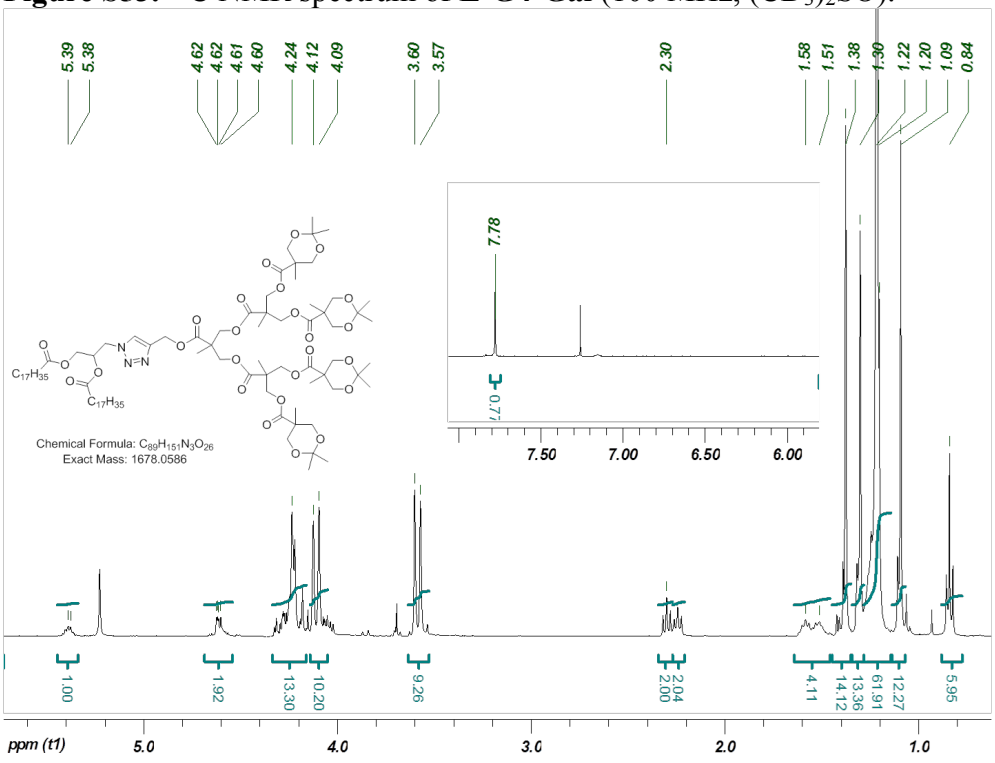


**Figure S54.** $^{1}$H NMR spectrum of **L-G3-Acet** (400 MHz, $CDCl_3$).

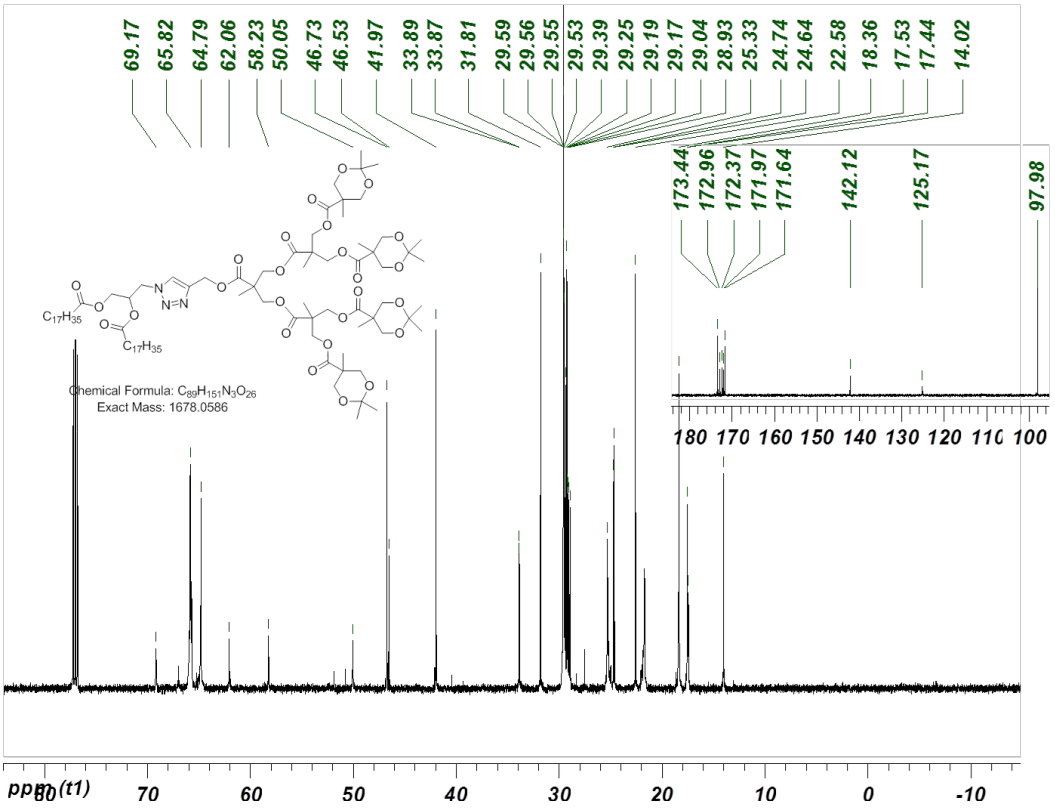


**Figure S55.** $^{13}C$ NMR spectrum of **L-G3-Acet** (150 MHz, $CDCl_3$).

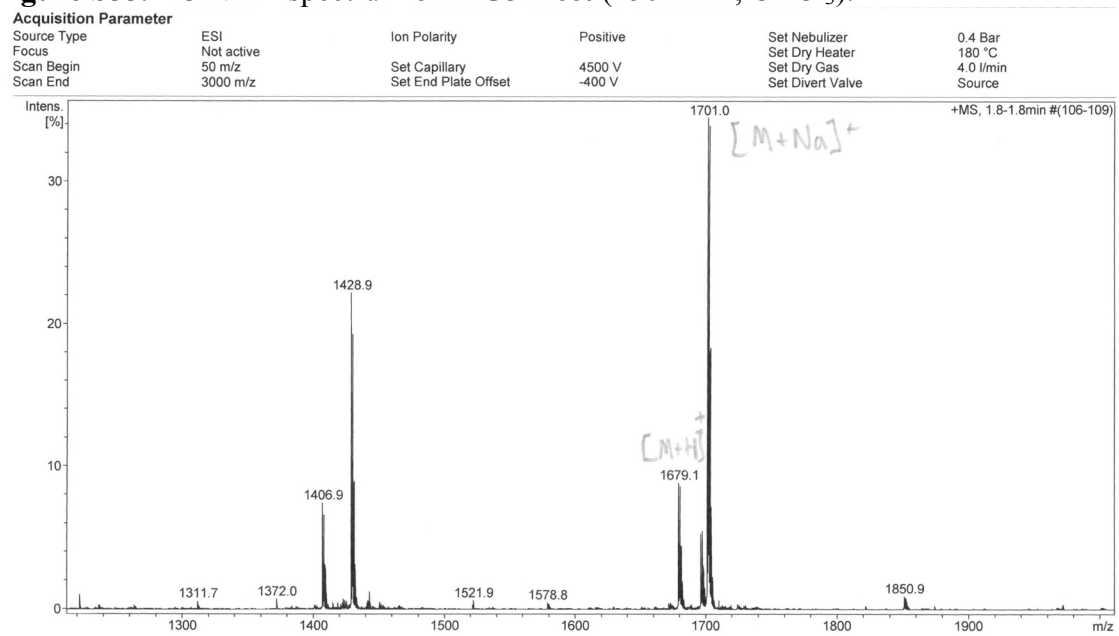


**Figure S56**. Mass spectrum of **L-G3-Acet** (ESI, $CH_2Cl_2$).

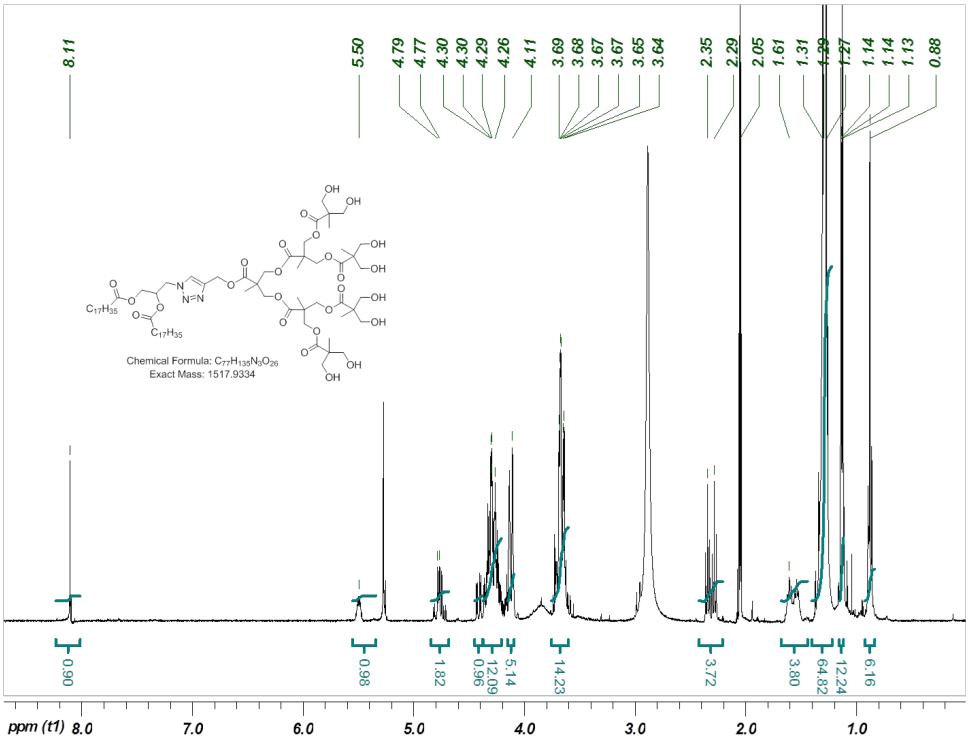


**Figure S57.** $^{1}$H NMR spectrum of **L-G3-OH** (400 MHz, $CDCl_3$).

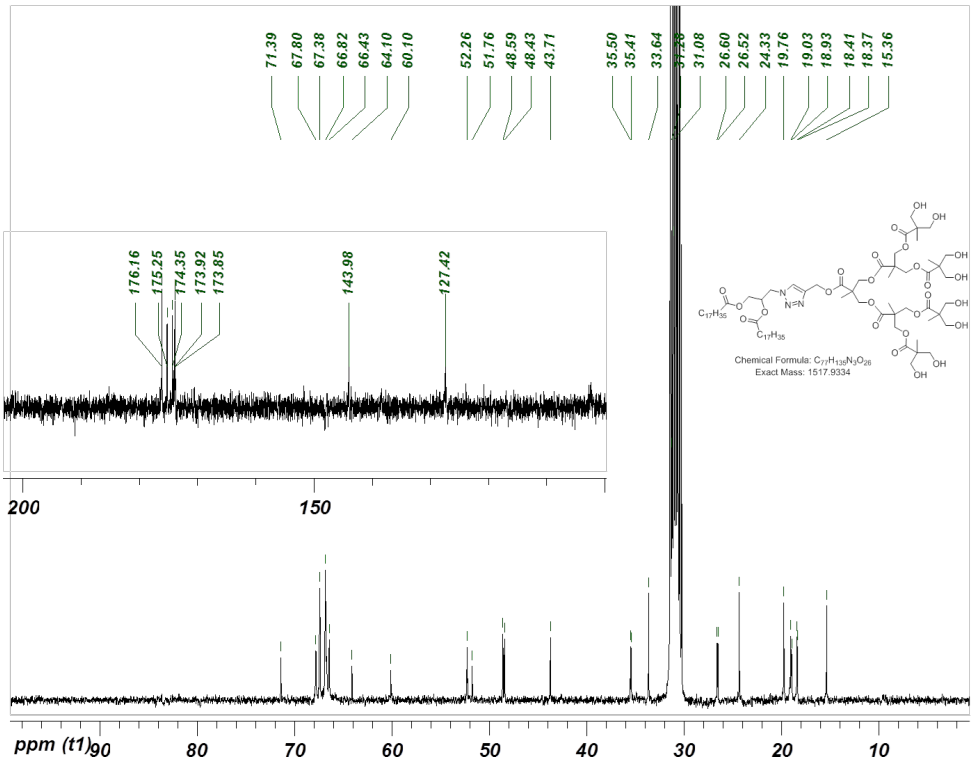


**Figure S58.** $^{13}$C NMR spectrum of **L-G3-OH** (100 MHz, $(CD_3)_2CO$).

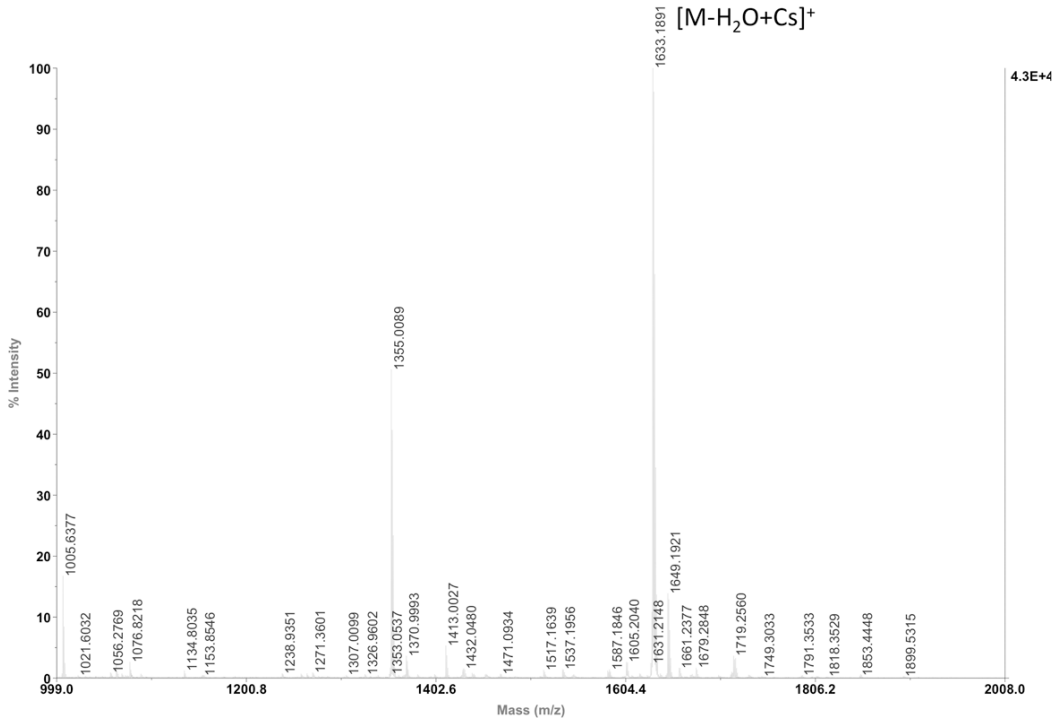


**Figure S59**. Mass spectrum of **L-G3-OH** (MALDI, 1:1 THF:$H_2O$).

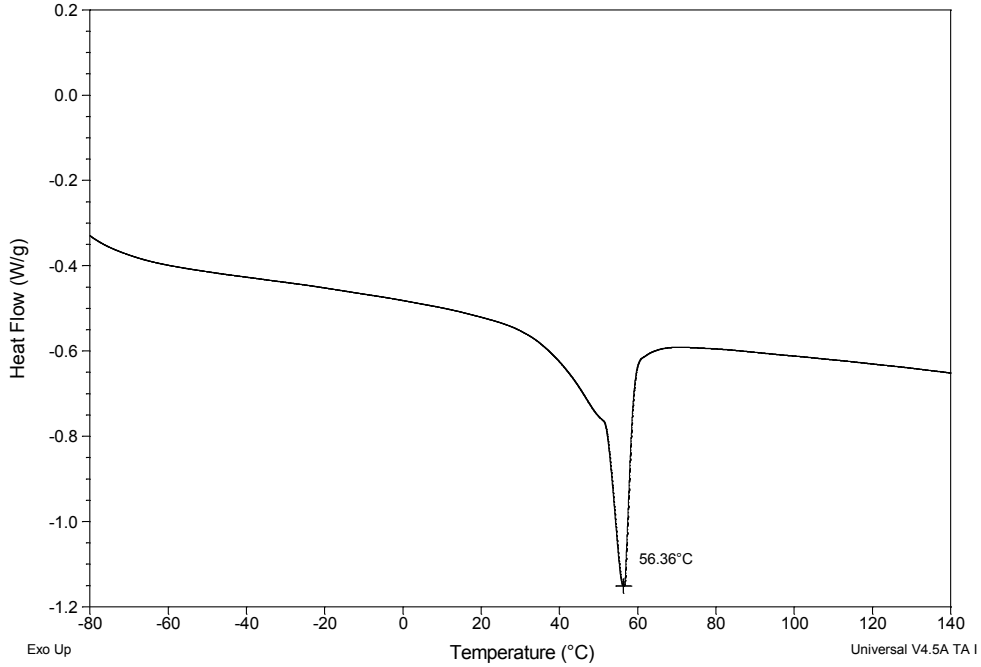


**Figure S60.** DSC thermograph of **L-G0-Gal** (second heating cycle).

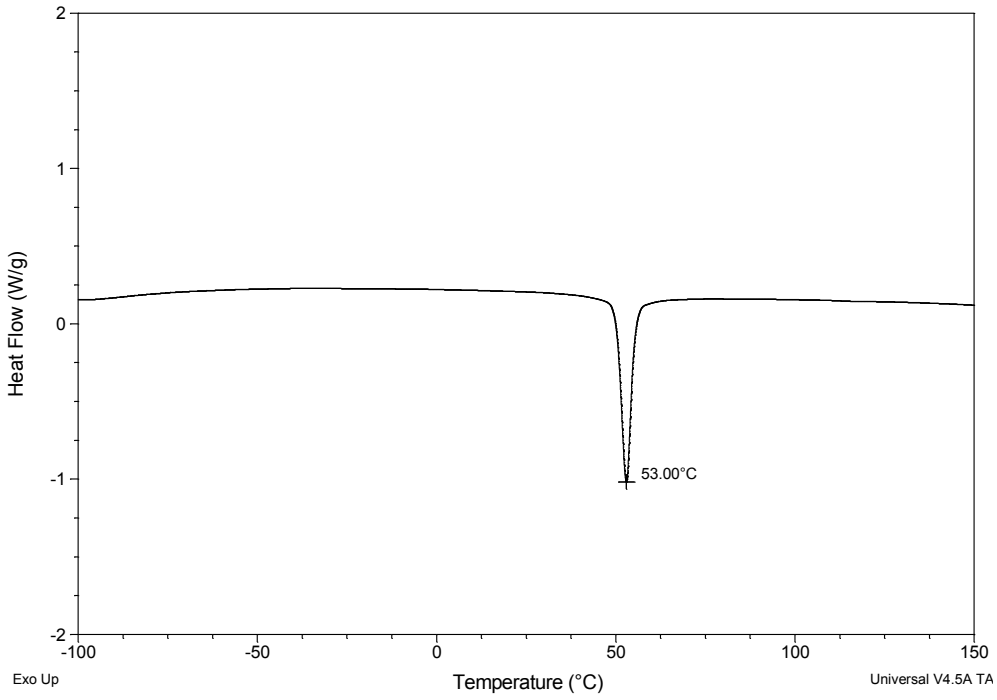


**Figure S61.** DSC thermograph of **L-G1-Gal** (second heating cycle).

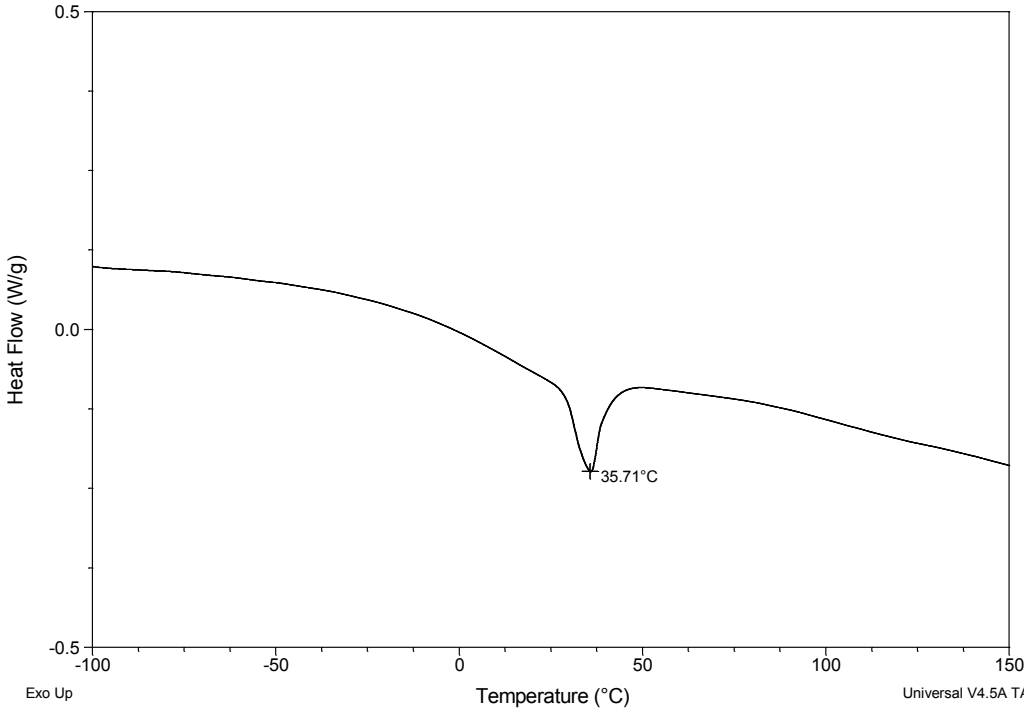


**Figure S62.** DSC thermograph of **L-G2-Gal** (second heating cycle).

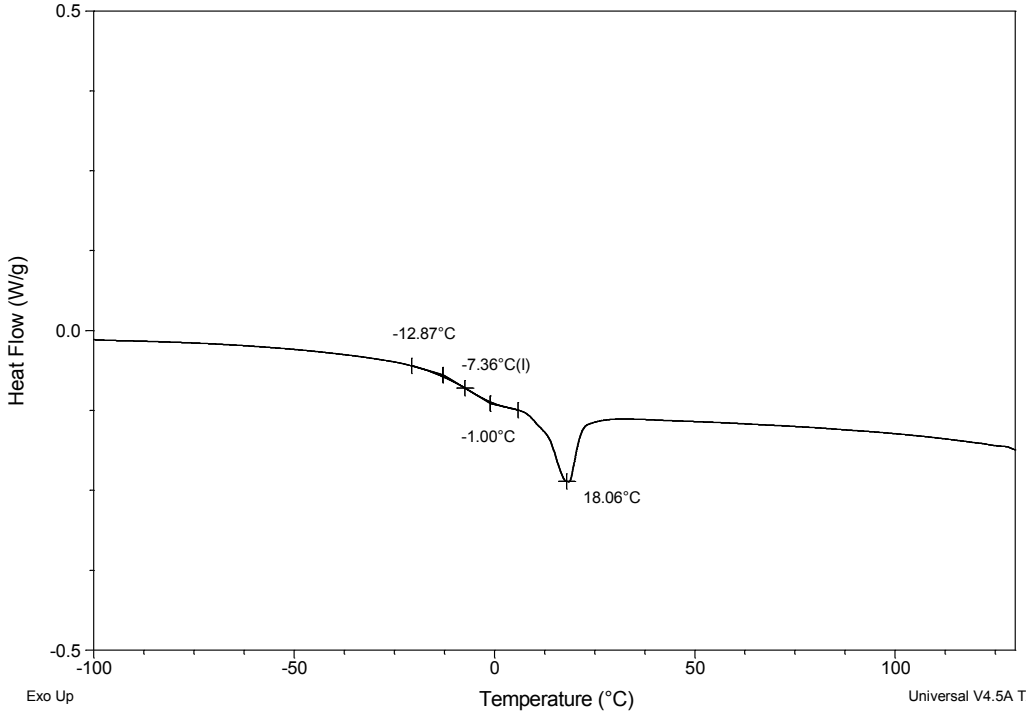


**Figure S63.** DSC thermograph of **L-G3-Gal** (second heating cycle).

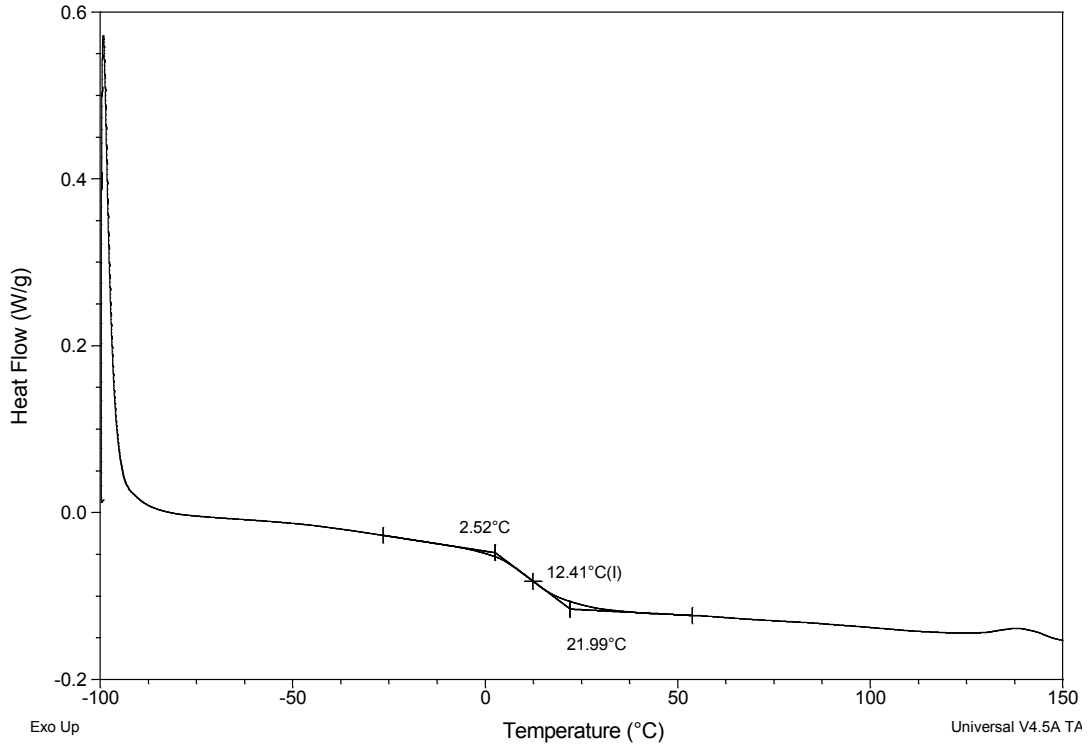


**Figure S64.** DSC thermograph of **L-G4-Gal** (second heating cycle).

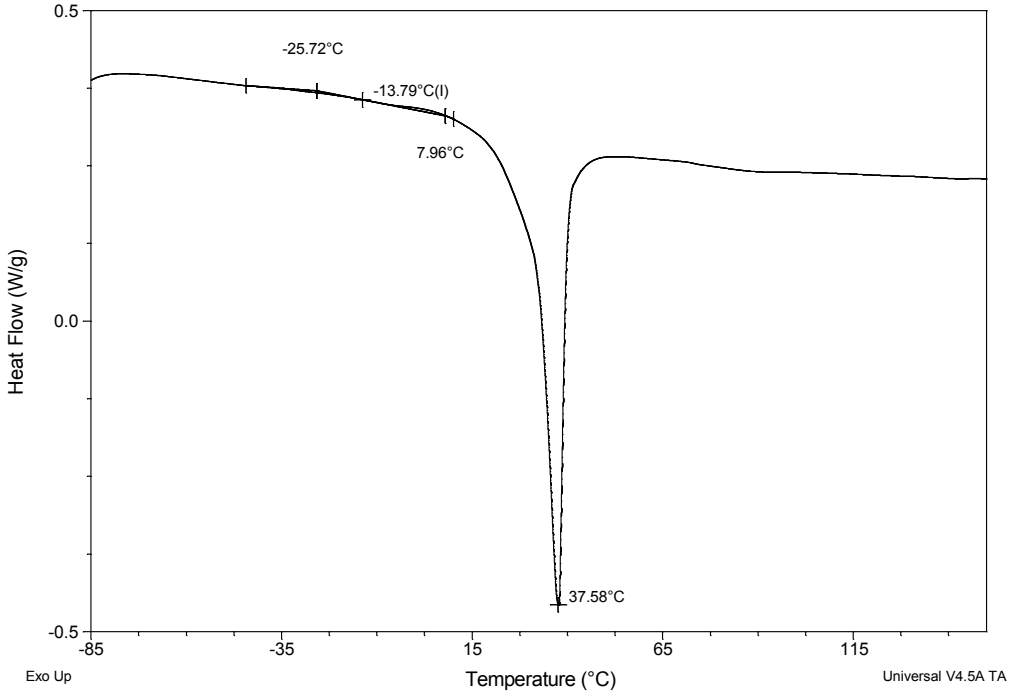


**Figure S65.** DSC thermograph of **L-G3-OH** (second heating cycle).

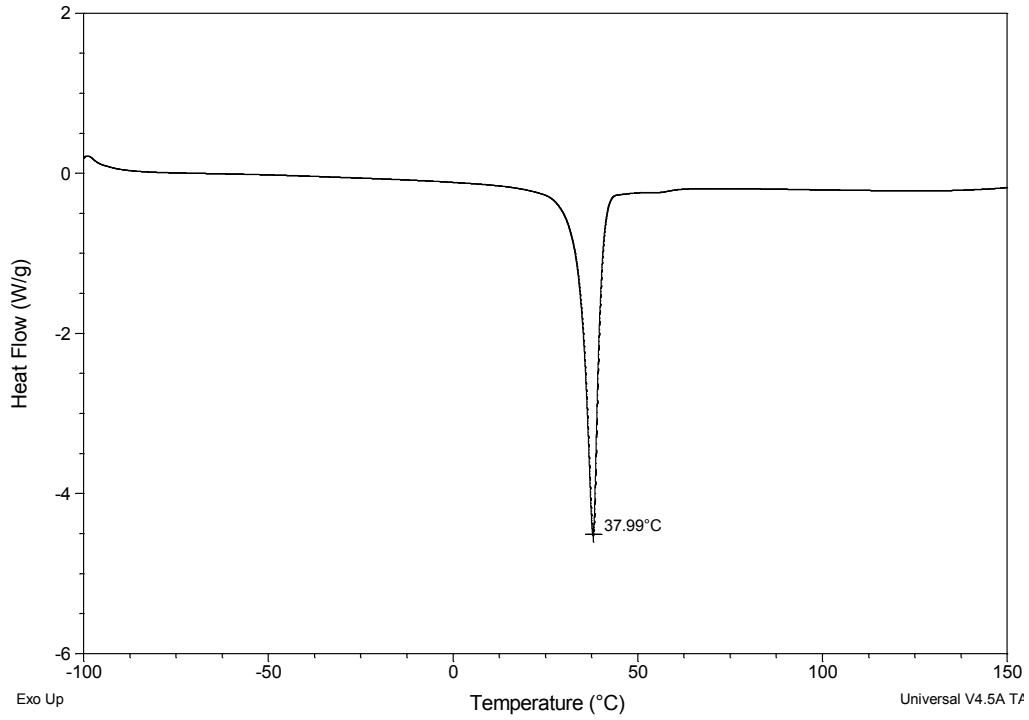


**Figure S66.** DSC thermograph of lipid derivative **2** (second heating cycle).

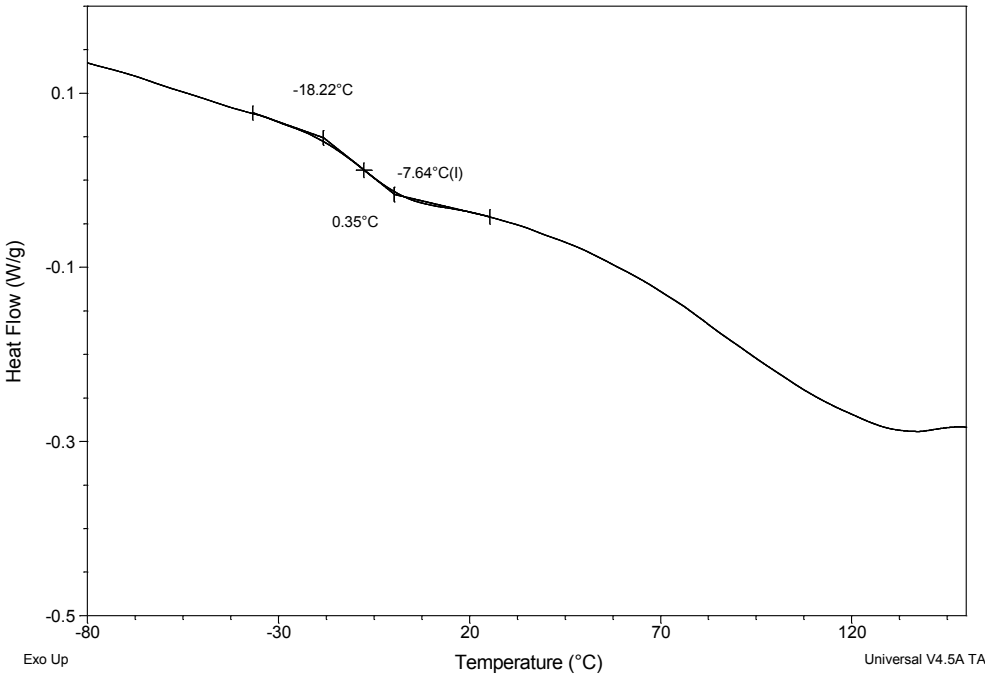


**Figure S67.** DSC thermograph of **Propargyl-G3-Gal** (second heating cycle)**,** the dendron without a lipid attached (synthesis previously published[3]).

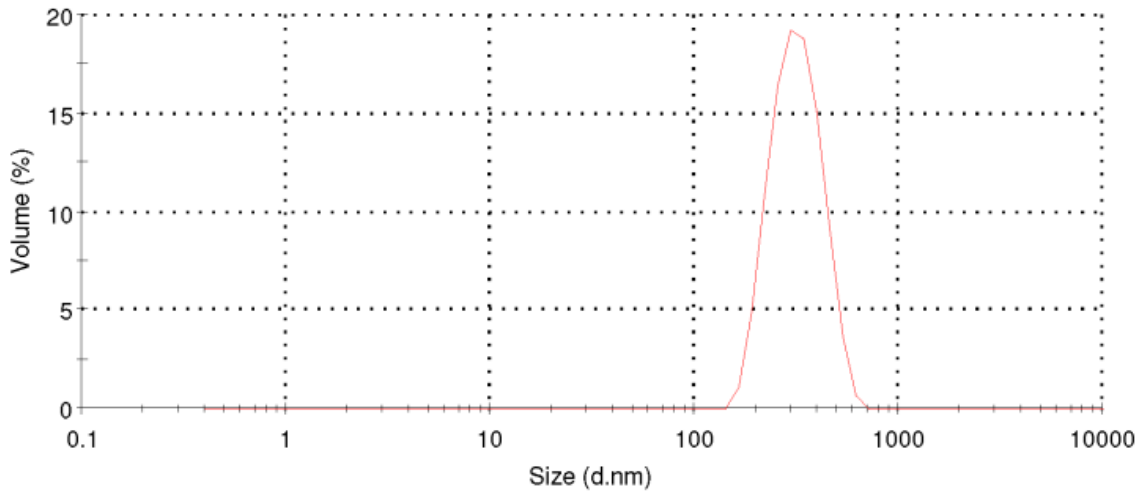


**Figure S68.** Representative volume distribution of assembly diameters formed from **L-G0-Gal**, as measured by DLS.

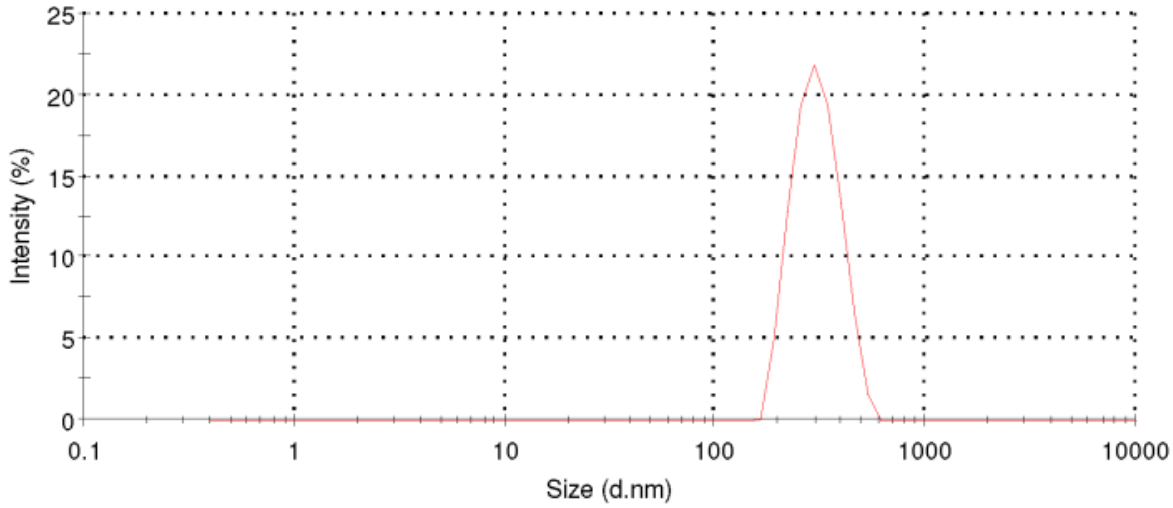


**Figure S69.** Representative intensity distribution of assembly diameters formed from **L-G0-Gal**, as measured by DLS.

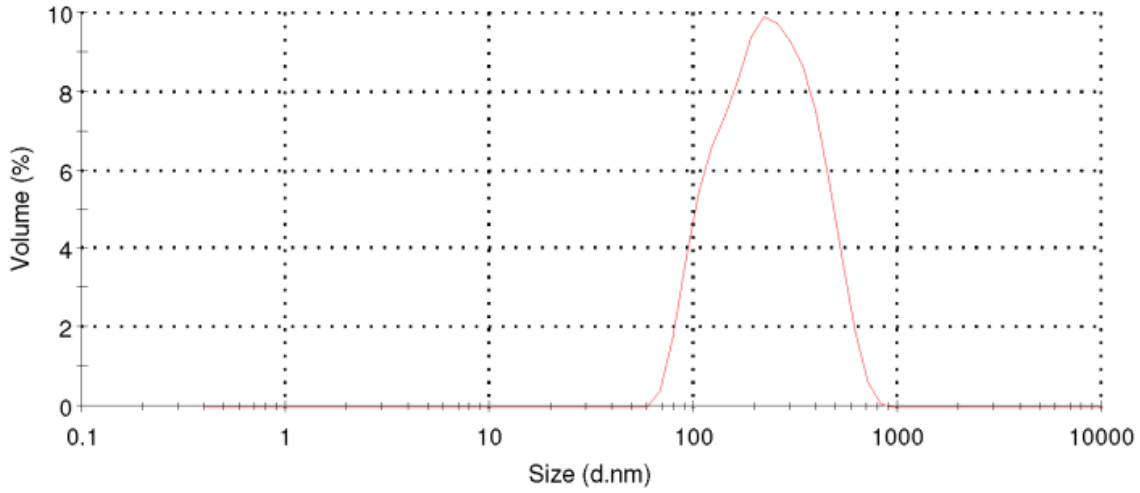


**Figure S70.** Representative volume distribution of assembly diameters formed from **L-G1-Gal**, as measured by DLS.

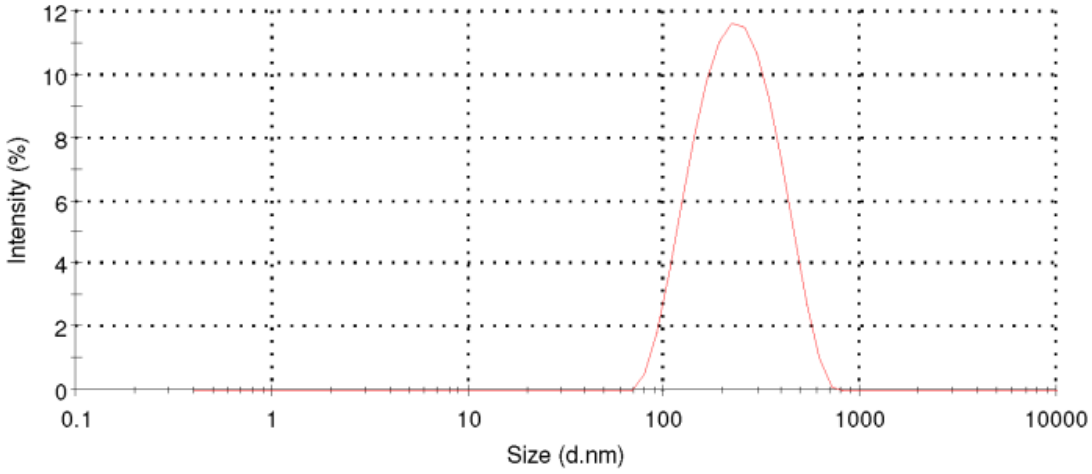


**Figure S71.** Representative intensity distribution of assembly diameters formed from **L-G1-Gal**, as measured by DLS.

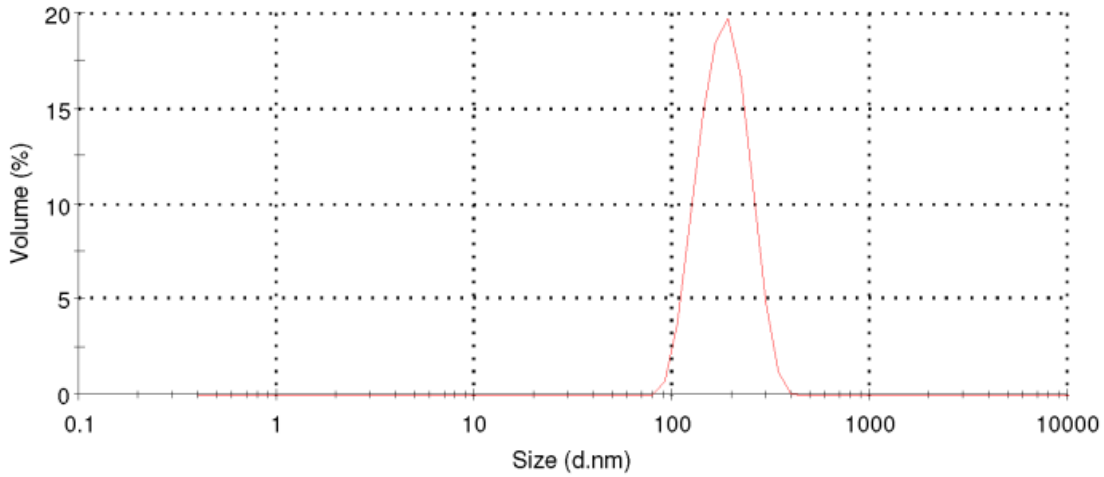


**Figure S72.** Representative volume distribution of assembly diameters formed from **L-G2-Gal**, as measured by DLS.

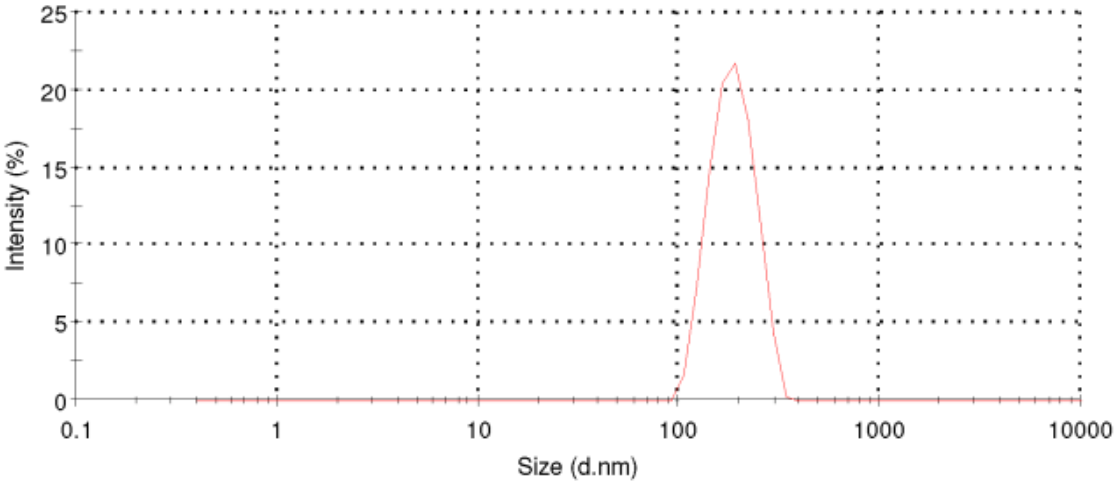


**Figure S73.** Representative intensity distribution of assembly diameters formed from **L-G2-Gal**, as measured by DLS.

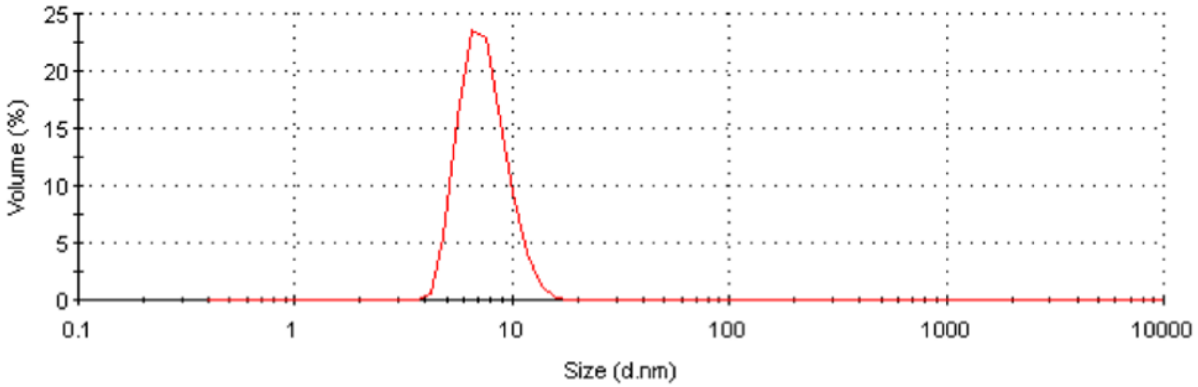


**Figure S74.** Representative volume distribution of assembly diameters formed from **L-G3-Gal**, as measured by DLS.

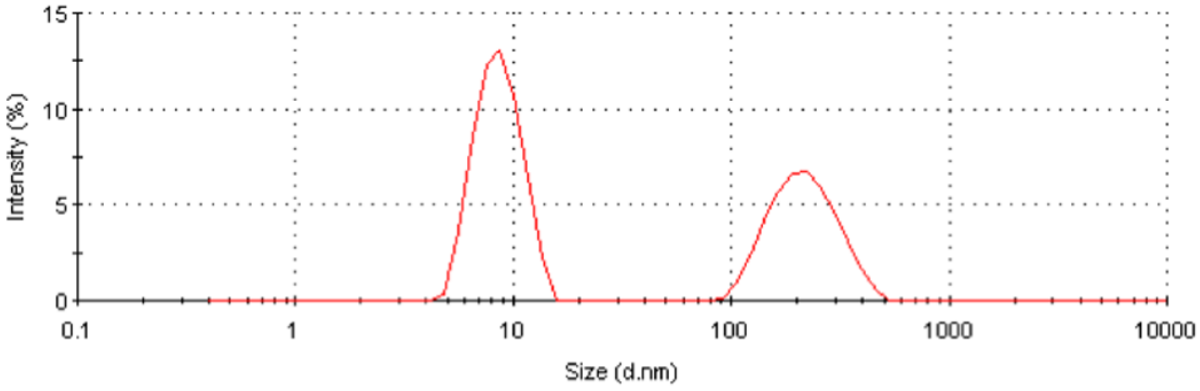


**Figure S75.** Representative intensity distribution of assembly diameters formed from **L-G3-Gal**, as measured by DLS.

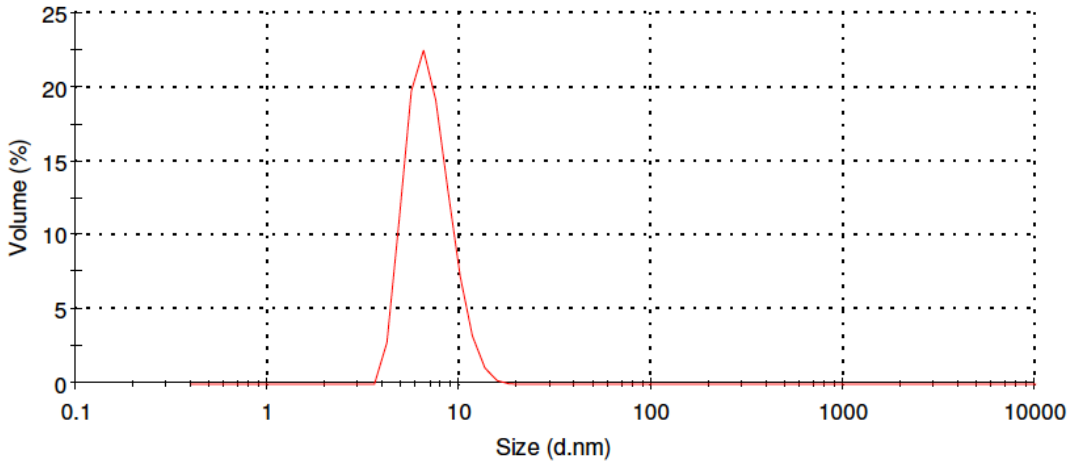


**Figure S76.** Representative volume distribution of assembly diameters formed from **L-G4-Gal**, as measured by DLS.

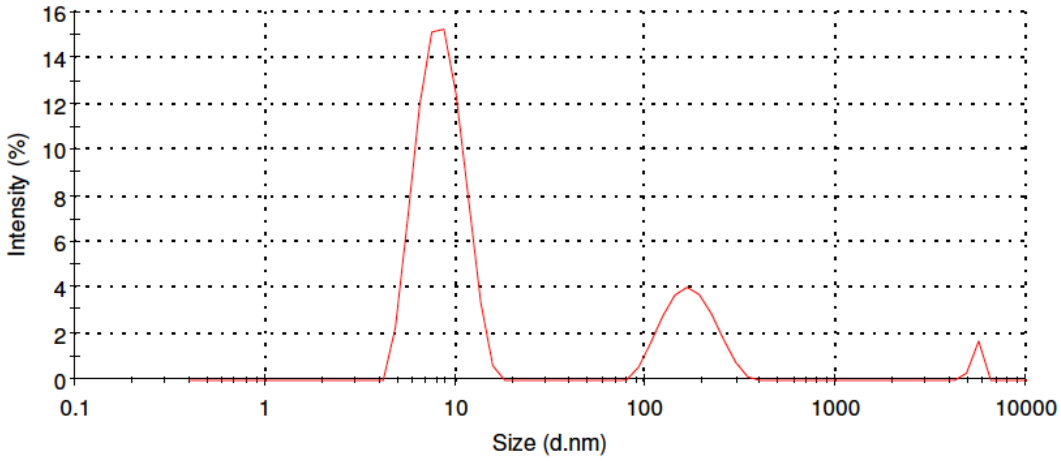


**Figure S77.** Representative intensity distribution of assembly diameters formed from **L-G4-Gal**, as measured by DLS.

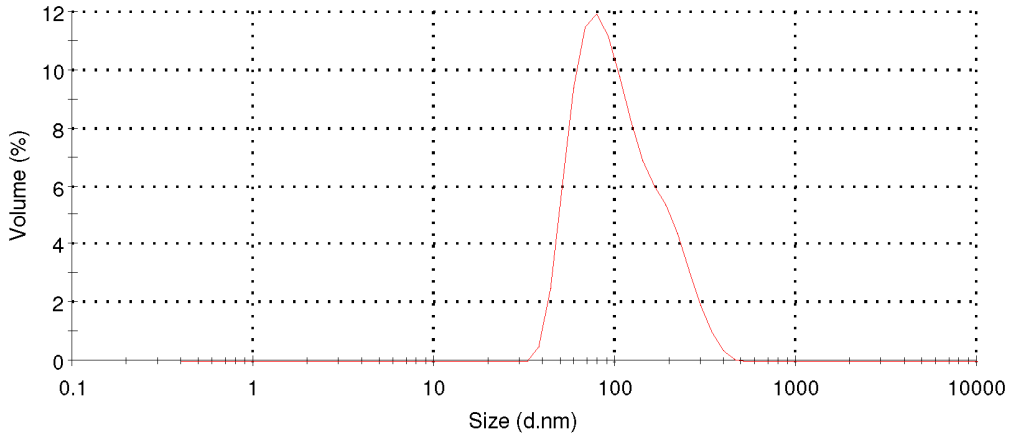


**Figure S78.** Representative volume distribution of assembly diameters formed from **L-G3-OH**, as measured by DLS.

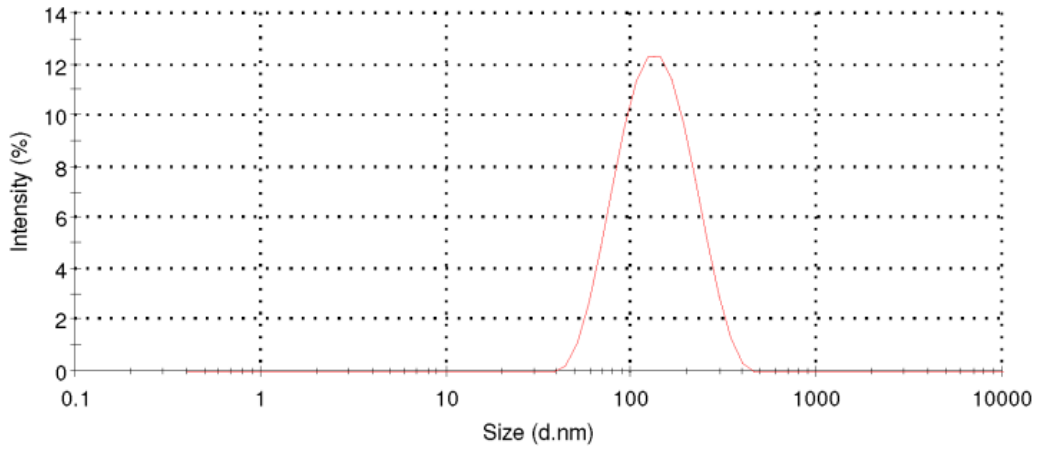


**Figure S79.** Representative intensity distribution of assemblies formed from **L-G3-OH**, as measured by DLS.

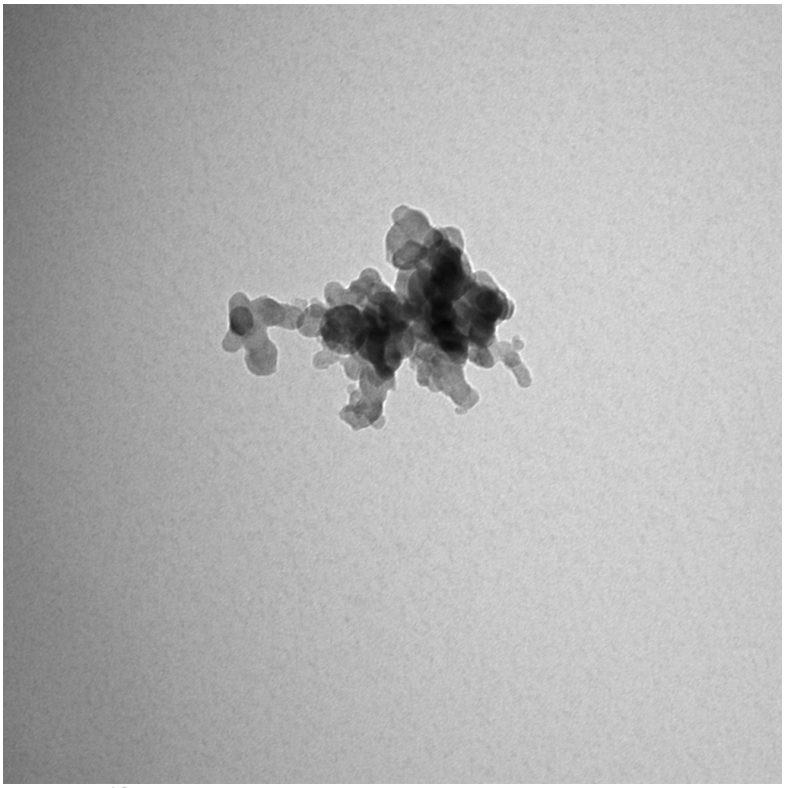


**Figure S80**. Additional TEM image of assemblies formed from **L-G3-Gal** showing aggregates composed of smaller micelles, consistent with the DLS results shown in Figure S75.

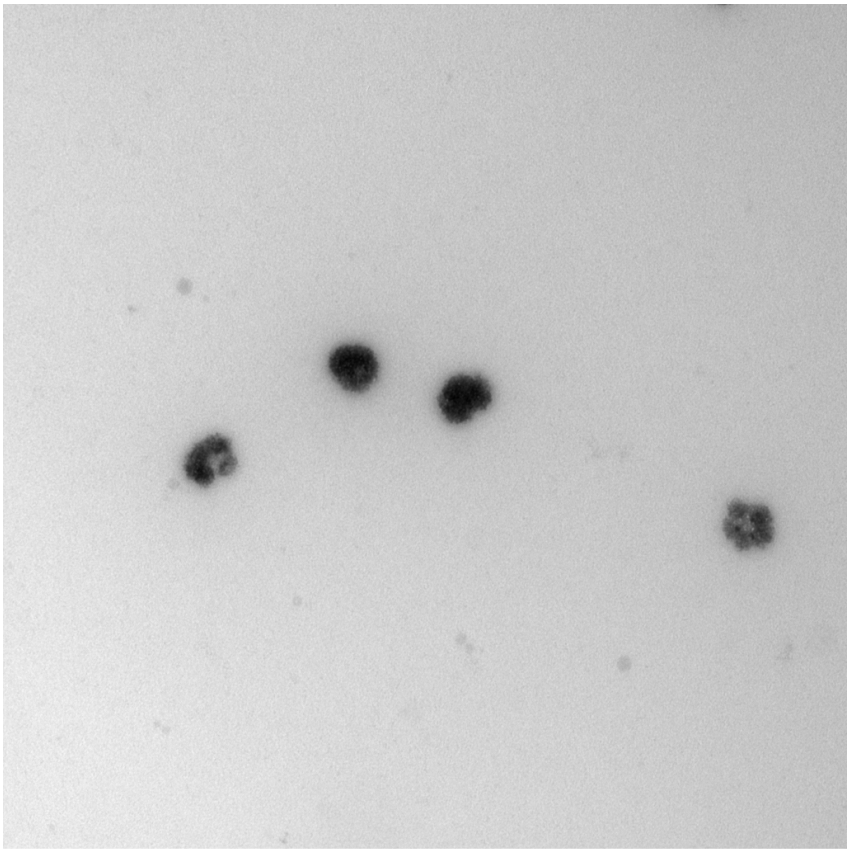


**Figure S81**. Additional TEM image of assemblies formed from **L-G4-Gal** showing aggregates composed of smaller micelles, consistent with the DLS results shown in Figure S77.

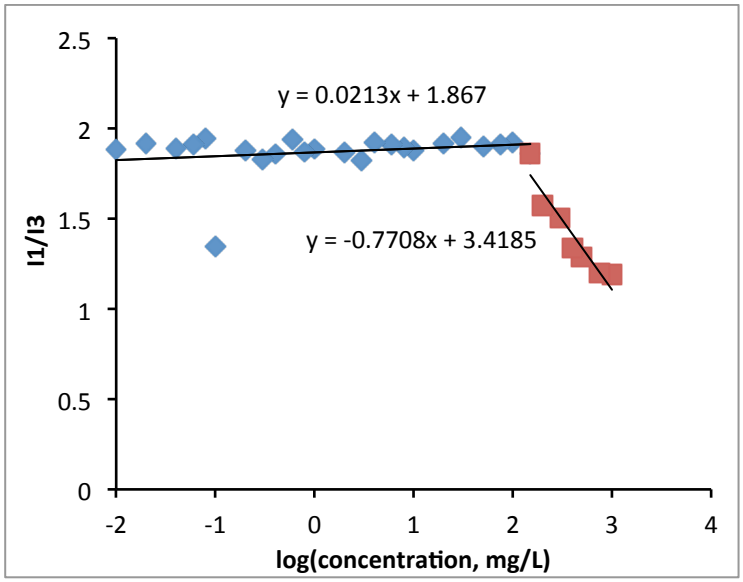


**Figure S82.** Ratio of the emission intensities ($I_1/I_3$) versus log of the amphiphile concentration in mg/mL for **L-G0-Gal**. The CAC is determined to be the point of intersection between the lines defined by the nearly horizontal region at low concentration (blue) and the region of negative slope (red).

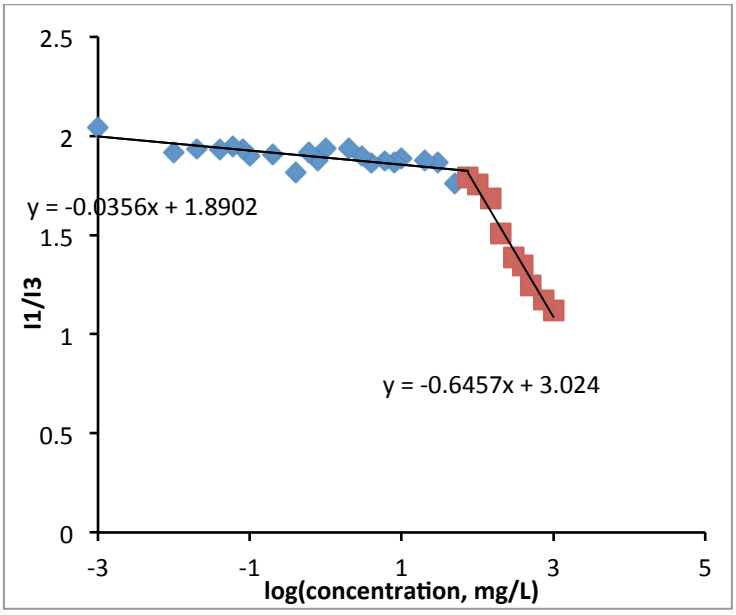


**Figure S83.** Ratio of the emission intensities ($I_1/I_3$) versus log of the amphiphile concentration in mg/mL for **L-G1-Gal**. The CAC is determined to be the point of intersection between the lines defined by the nearly horizontal region at low concentration (blue) and the region of negative slope (red).

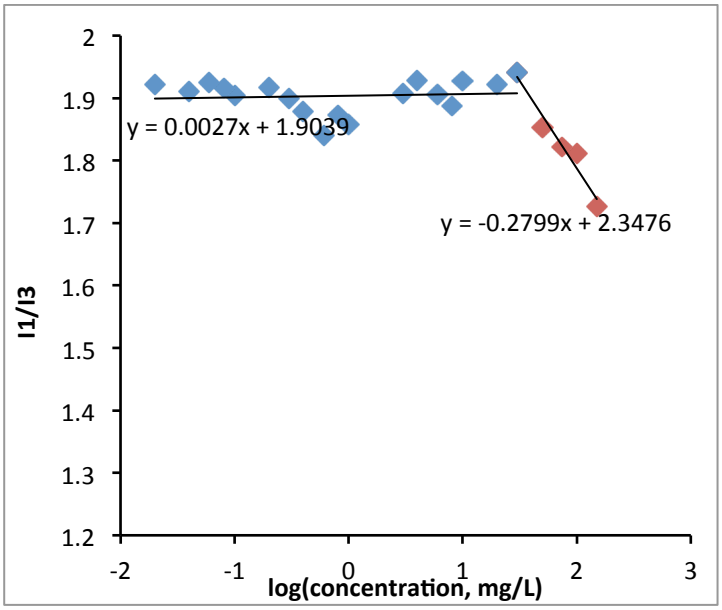


**Figure S84.** Ratio of the emission intensities ($I_1/I_3$) versus log of the amphiphile concentration in mg/mL for **L-G2-Gal**. The CAC is determined to be the point of intersection between the lines defined by the nearly horizontal region at low concentration (blue) and the region of negative slope (red).

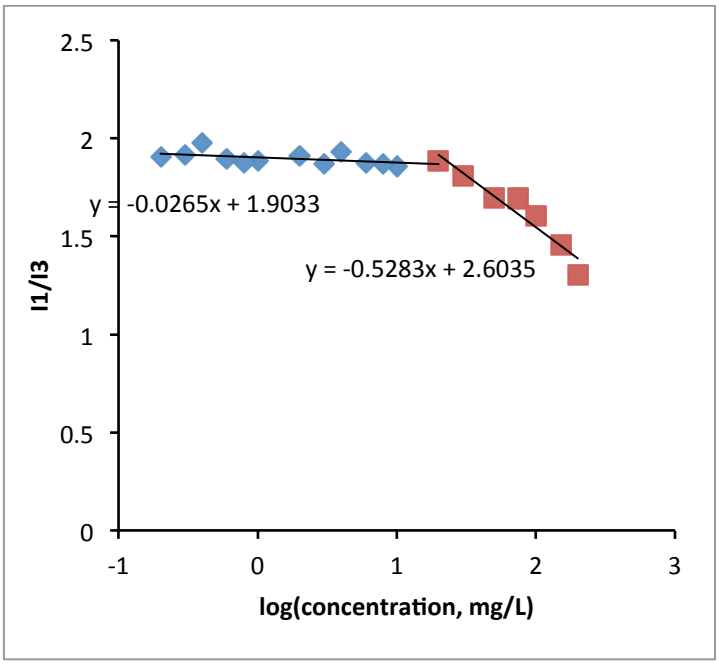


**Figure S85.** Ratio of the emission intensities ($I_1/I_3$) versus log of the amphiphile concentration in mg/mL for **L-G3-Gal**. The CAC is determined to be the point of intersection between the lines defined by the nearly horizontal region at low concentration (blue) and the region of negative slope (red).

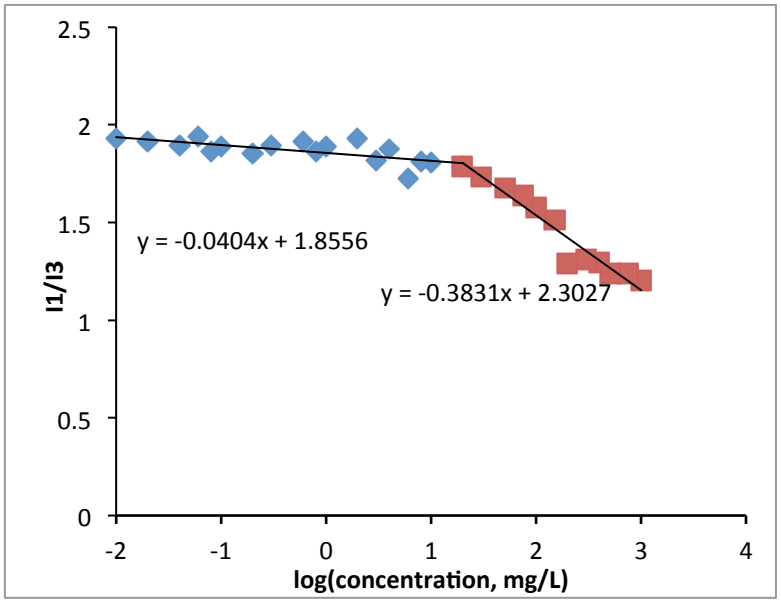


**Figure S86.** Ratio of the emission intensities ($I_1/I_3$) versus log of the amphiphile concentration in mg/mL for **L-G4-Gal**. The CAC is determined to be the point of intersection between the lines defined by the nearly horizontal region at low concentration (blue) and the region of negative slope (red).

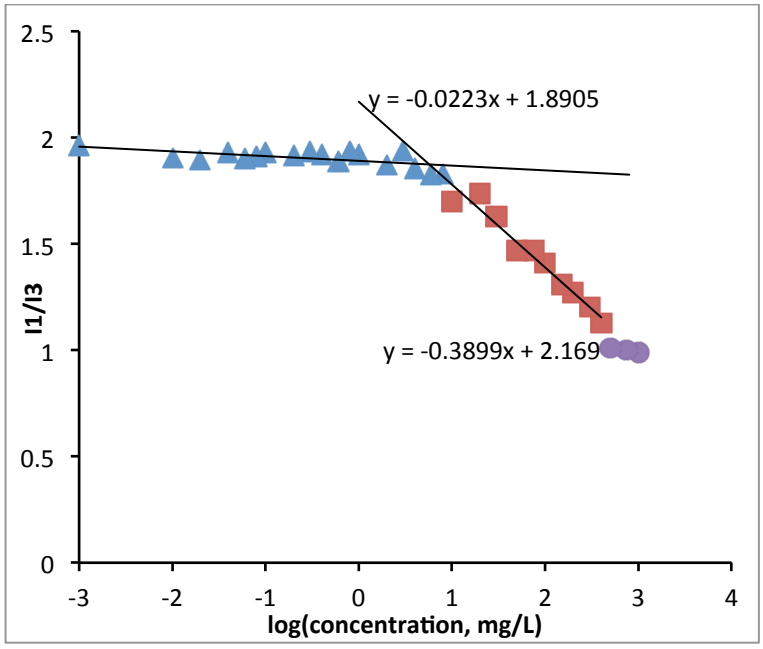


**Figure S87.** Ratio of the emission intensities ($I_1/I_3$) versus log of the amphiphile concentration in mg/mL for **L-G3-OH**. The CAC is determined to be the point of intersection between the lines defined by the nearly horizontal region at low concentration (blue) and the region of negative slope (red).

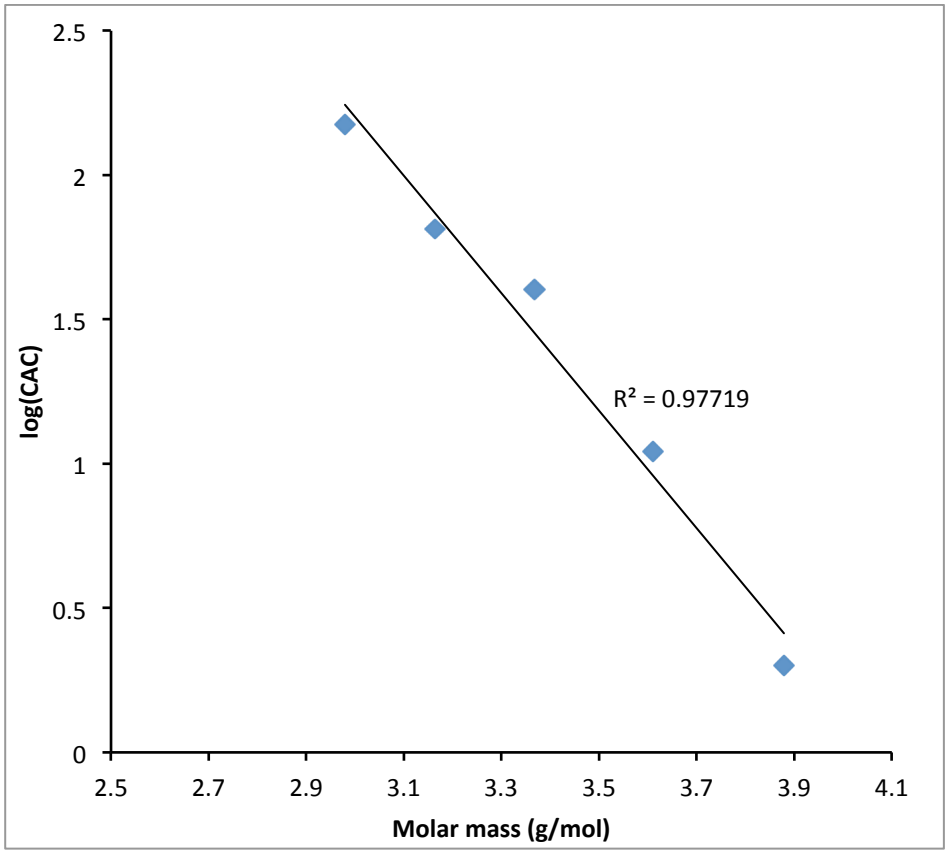


**Figure S88.** Plot showing the linear dependence of log(CAC) versus log(molar mass) for G0 through G4 carbohydrate-dendron-lipid hybrids.

**Table S1.** Relative fluorescence of nile red encapsulated in assemblies used for the lectin binding assay.

| | $\lambda_{max}$ | Relative fluorescent intensity |
|---|---|---|
| **G3-OH** | 603 | 29.5 |
| **G0-Gal** | 587 | 2.0 |
| **G1-Gal** | 611 | 9.1 |
| **G2-Gal** | 610 | 15.0 |
| **G3-Gal** | 601 | 13.2 |
| **G4-Gal** | 608 | 9.6 |

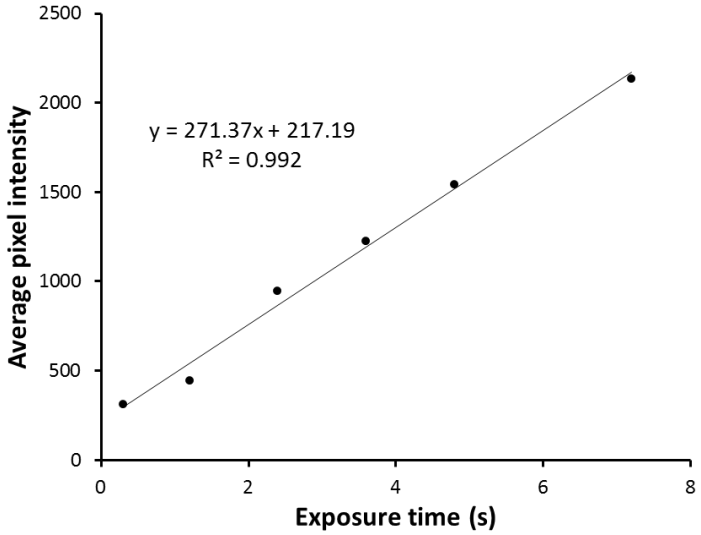


**Figure S89.** Calibration curve used to confirm the linear relationship between exposure time and fluorescence intensity over the exposure time range used in this study (0.3 to 7.2 s).

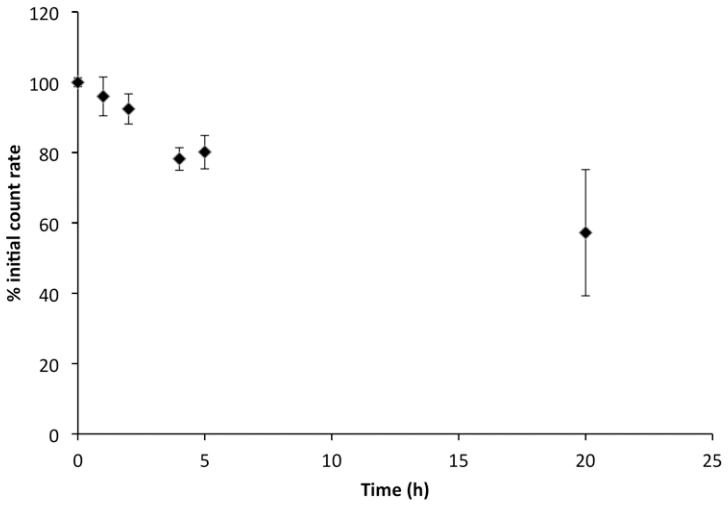


**Figure S90.** Change in DLS count rate over time for assemblies formed from **L-G0-Gal** following dilution from above the CAC (0.5 mg/mL) to below the CAC (0.075 mg/mL).

**Table S2**. Data corresponding to manuscript Figure 5. Levels of murine IL-2 following exposure to α-Gal-dendron-lipid hybrids and controls, prepared as diluted assemblies or via direct dissolution and dilution, at either 20 ng/mL or 1 μg/mL.

| Sample | mean | STDEV | | mean | STDEV |
|---|---|---|---|---|---|
| | | | | | |
| KRN-7000 | 2176.0 | 61.2 | | | |
| media | 12.9 | 17.9 | | | |
| L-G3-OH [1 μg/mL] | 6.4 | 9.1 | | | |
| | | | | | |
| | 1 μg/mL | | | 20 ng/mL | |
| Dissolution at 10 ug/mL | | | | | |
| L-G0-Gal | 19.2 | 19.0 | | 31.8 | 6.3 |
| L-G1-Gal | 46.6 | 26.4 | | 31.8 | 11.0 |
| L-G2-Gal | 40.3 | 7.3 | | 55.0 | 3.7 |
| L-G3-Gal | 93.0 | 24.0 | | 80.4 | 9.7 |
| L-G4-Gal | 143.8 | 40.8 | | 241.2 | 79.7 |
| | | | | | |
| | 1 μg/mL | | | 20 ng/mL | |
| Assemblies made at 1 mg/mL | | | | | |
| L-G0-Gal | 2.2 | 3.8 | | 2.1 | 0.1 |
| L-G1-Gal | 21.2 | 26.4 | | 12.8 | 12.8 |
| L-G2-Gal | 23.4 | 22.2 | | 44.5 | 27.6 |
| L-G3-Gal | 23.3 | 34.9 | | 48.7 | 42.2 |
| L-G4-Gal | 135.3 | 48.0 | | 137.5 | 101.2 |

**References**

(1) Kazemi, F.; Kiasat, A. R.; Ebrahimi, S. *Synth. Commun.* **2003**, *33*, 999.
(2) Losey, E. A.; Smith, M. D.; Meng, M.; Best, M. D. *Bioconjugate Chem.* **2009**, *20*, 376-383.
(3) Peyret, A.; Trant, J. F.; Bonduelle, C. V.; Ferji, K.; Jain, N.; Lecommandoux, S.; Gillies, E. R. *Polym. Chem.* **2015**, *6*, 7902-7912.
(4) Wu, P.; Malkoch, M.; Hunt, J. N.; Vestberg, R.; Kaltgrad, E.; Finn, M. G.; Fokin, V. V.; Sharpless, K. B.; Hawker, C. J. *Chem. Commun.* **2005**, 5775-5777.
(5) Frindi, M.; Michels, B.; Zana, R. *J. Phys. Chem.* **1992**, *96*, 8137-8141.
(6) Regev, O.; Zana, R. *J. Colloid Interface Sci.* **1999**, *210*, 8-17.
(7) Rodríguez-Hernández, J.; Chécot, F.; Gnanou, Y.; Lecommandoux, S. *Prog. Polym. Sci.* **2005**, *30*, 691-724.
(8) Aguiar, J.; Carpena, P.; Molina-Bolívar, J. A.; Carnero Ruiz, C. *J. Colloid Interface Sci.* **2003**, *258*, 116-122.
(9) Zana, R.; Lévy, H.; Kwetkat, K. *J. Colloid Interface Sci.* **1998**, *197*, 370-376.
(10) Torigoe, K.; Tasaki, A.; Yoshimura, T.; Sakai, K.; Esumi, K.; Takamatsu, Y.; Sharma, S. C.; Sakai, H.; Abe, M. *Colloids Surf., A* **2008**, *326*, 184-190.
(11) Yoshimura, T.; Saito, M.; Esumi, K. *J. Oleo Sci.* **2013**, *62*, 213-221.
(12) Pang, Z.; Laplante, N. E.; Filkins, R. J. *J. Microsc.* **2012**, *246*, 1-10.
(13) Lantz, O.; Bendelac, A. *J. Exp. Med.* **1994**, *180*, 1097-1106.